Brain-wide cell assembly patterns for memory-guided behaviour

Roman Rothaermel

Thesis submitted for the degree of Doctor of Philosophy

Balliol College

University of Oxford

Trinity Term 2021

Abstract

Brain-wide cell assembly patterns for memory-guided behaviour

Roman Rothaermel, Balliol College

Thesis submitted for the degree of Doctor of Philosophy, Trinity Term 2021

The brain uses functionally specialized regions to represent information in the sensory, motor, and cognitive domains. How does the brain integrate discrete representations spread across the brain to drive effective behaviour?

I trained male mice to approach or avoid a dispenser delivering either rewarding or aversive outcomes contingent on sets of visual and auditory cues. I found that groups of neurons scattered across the hippocampus, amygdala, prefrontal cortex, nucleus accumbens and ventral tegmental area cooperate to form cross-regional firing patterns of millisecond-timescale coactivity. These distributed assembly patterns report multimodal task-cue contingencies and require a common input from glutamatergic VTA neurons to support the expression of appropriate behaviour in our task relying on the integration of multiple external cues. Our findings uncover a diverging glutamatergic VTA pathway for organizing multiple local representations into brain-wide cell assemblies, dynamically adapting behaviour to environmental contingencies.

Acknowledgements

Firstly, I would like to thank Professor David Dupret not only for his never ending academic, technical, and creative abilities, but also for his mentorship. His supervision profoundly enabled my development, both in personal and professional fronts, and set a world-class example for me to strive towards.

Additionally, the lab has supported me in many different ways. I would like to thank Dr. Pavel Perestenko for his impressive technical support by designing and building all necessary behavioural lab equipment from scratch. Furthermore, I thank Dr. Laura Lefèvre for her viral injections, immunohistochemistry, and histology in the optogenetic experiments. I also wish to thank Dr. Alexander Morley, whose data went into single-cell analysis, and Charlie Clarke-Williams for his help with EMD. Moreover, many thanks to Dr. Vitor Lopes dos Santos for always providing helpful tips with coding and for his implementation of assembly analysis in the lab. Lastly, I would like to acknowledge Natalia Campo-Urriza for building the recording drives and Ben Micklem for fluorescence microscopy. My studies have been funded by the Wellcome Trust.

On a more personal note, I would like to express my deepest thanks to my closest friends Dr. Michael Ben-Yehuda, Dr. Sean Heelan, Dr. Glenn Cahilly-Bretzin, Dr. Adam Steel and Dr. Vadim Koren who made my time in Oxford the most amazing time of my life. I will always be grateful for having met them here.

A very special thanks goes to my partner and soon to be Dr. Laura Fritsch for her loving support (literally) every hour of the day for the last 445 days. I could not imagine the last year without her and I look forward to many more years filled with her inspiration, wisdom, and happy nature.

Table of contents

Figures

Tables

Abbreviations

ANOVA	analysis of variance
ArchT	archaerhodopsin
BLA	basolateral amygdala
CA1	cornu ammonis 1
ChRh2	channelrhodopsin 2
CPP	conditioned place preference
CS	conditioned stimulus
DABEST	data analysis with bootstrap coupled estimation
DAT	dopamine transporter
DP	decision point
EMD	empirical mode decomposition
GFP	green fluerescent protein
ICA	independent component analysis
IMF	intrinsic mode function
ISI	inter-spike interval
LDA	linear discriminant analysis
LED	light emitting diode
LFP	local field potential
mRNA	messenger ribonucleic acid
NAc	nucleus accumbens
PBS	phosphate buffered saline
PCA	principal component analysis
PD	Parkinson’s disease
PDP	parallel distributed processing
PFC	prefrontal cortex
SEM	standard error of the mean
TCA	tensor component analysis
TH	tyrosine hydroxylase
US	unconditioned stimulus
VGlut2	vesicular glutamate transporter 2
VTA	ventral tegmental area

1 CHAPTER 1: GENERAL INTRODUCTION

1.1. Evolution of concepts in memory research

Memory research dates back to Ancient Greece. For Plato (estimated 428–347 B.C.), memories were bridges between perceptions and the idealised world of abstractions (Plato's Meno). His pupil Aristotle (384–322 B.C.) elaborated on his ideas, which resulted in the definition of the four laws of associativity (contiguity, similarity, contrast) (Aristotle's De Sensu and De Memoria), implying that memories are formed through linkages of different mental items. This idea has influenced many western philosophers including John Locke (Locke 1847) and David Hume (Hume 1874). Derivatives reverberated all the way into modern day neuroscience, when empirical evidence started to underpin the associative nature of memories starting with Ivan Pavlov's conditioning experiments (Pavlov Ivan 1927). In the early 20th century, a key discussion in memory research concerned the degree to which individual memories were isolated from each other (Howard Eichenbaum 2017). Proponents of detailed stimulus-response studies (Spence 1950) favoured the idea that individual associations corresponding to one given memory are strongly separated, whereas proponents of more cognitive theories of learning and memory such as (spatial and multimodal) cognitive maps (Tolman 1948; H. Eichenbaum et al. 1999) highlighted the interrelations of individual memory items. In the second half of the 20th century (Bartlett and Burt 1933) cognitive theories of learning became more elaborate and different structures of mnemonic organisation have been proposed. The term mnemonic is used to refer to processes related to the acquisition, storage and retrieval of memories in this thesis. For instance, behavioural experiments suggested that memory items could be related using different organisational principles: for instance,

in an associative, sequential or hierarchical manner (Mandler 1979, 2011). The predominant opinion today is that memory items are stored in an overlapping fashion in which new memories are embedded into a pre-existing network of associations (Mayford, Siegelbaum, and Kandel 2012; Zeithamova, Dominick, and Preston 2012; Milivojevic, Vicente-Grabovetsky, and Doeller 2015).

1.2. Regional specialisations for mnemonic processing?

Previous studies focused on characterising the involvement of isolated brain regions in specialised tasks and behaviours. Whilst acknowledging that other brain systems are crucially involved in learning and memory, such as the basal ganglia (Packard and Knowlton 2002), I will focus on reviewing key insights derived from five of the more extensively studied brain regions in this context: the dorsal cornu ammonis 1 (CA1) area of the hippocampus, amygdala (Amy), nucleus accumbens (NAc), prefrontal cortex (PFC) and ventral tegmental area (VTA). For the purpose of this work, I will narrow the review down to the mnemonic representations (i.e. different stimuli/modalities) ascribed to those brain regions and where relevant, I will point towards important roles in learning and memory.

1.2.1. Hippocampal CA1 region

Anatomy: CA1 is part of the hippocampal formation which encompasses the dentate gyrus (DG), CA3, CA2 and CA1. A coronal dissection of the dorsal CA1 in mice reveals 4 distinct layers, namely stratum (str.) oriens, str. pyramidale (containing the pyramidal cell bodies), str. radiatum and str. lacunosum moleculare (Andersen et al. 2007). The main input into the hippocampus arrives through a trisynaptic pathway, which starts with the perforant path. Its axons originate from in the entorhinal cortex and terminate

in the dentate gyrus and CA3. DG neurons synapse onto CA3 neurons, which in turn project through the Schaffer collaterals (located in the str. radiatum) to CA1 neurons. Another pathway originating in the entorhinal cortex synapses directly onto CA1 neurons in the str. lacunosum moleculare. Furthermore, CA1 also receives inputs from other regions such as Amy (Pikkarainen et al. 1999) and VTA (Loy et al. 1980).

Role in mnemonic stimulus representation: since the discovery of place cells, which are pyramidal neurons which fire when the animal is in certain locations in space (O'Keefe and Dostrovsky 1971a), hippocampal memory research has been strongly dominated by a focus on spatial representation. Consistently, some forms of spatial learning are impaired following hippocampal lesions in mice (O'keefe and Nadel 1978). However, accumulating evidence indicates that the hippocampus also engages in mnemonic processing of different stimulus modalities. An early study showed that CA1 units responded to both an auditory conditioned stimulus (CS) as well as haptic unconditioned stimuli (US), i.e. a corneal airpuff in rabbits (Berger, Alger, and Thompson 1976; McEchron and Disterhoft 1997)). Furthermore, CA1 neurons can carry temporal information about the stimuli (McEchron and Disterhoft 1997) and respond to a number of different stimulus modalities including olfactory (H. Eichenbaum et al. 1987), auditory (Sakurai 1990) and visual cues (Wible et al. 1986). Moreover, pyramidal neurons of the CA1 region go beyond simple stimulus representation. They are also involved in conjunctive coding of two different stimulus modalities such as odour-place (Manns and Eichenbaum 2009) and place-reward (Komorowski and Manns 2009) associations. Finally, for such associations to be formed, memory items do not need to be experienced simultaneously during learning. A more recent research showed that the CA1 region is crucially involved in associating

cross-modal stimuli that had not been directly paired with each other in an inference-learning based paradigm (Barron et al. 2020).

1.2.2. Amygdala

Anatomy: The amygdala is divided into three nuclei groups: (i) basolateral amygdala (BLA), which consists of the lateral nucleus (LA), the basal nucleus (BA) and the basomedial nucleus (BM), (ii) the cortical like groups and the (iii) centromedial nuclei (Sah et al. 2003). The amygdala receives inputs from all sensory modalities originating in numerous cortical areas including PFC (McGarry and Carter 2017), visual, somatosensory and gustatory cortices (equipping the amygdala with the capacity for the formation of cross-modal associations) (Sah et al. 2003), the ventral hippocampus (Bazelot et al. 2015) as well as subcortical regions (Sah et al. 2003) such as the VTA (Wei Tang et al. 2020).

Role in mnemonic stimulus representation: Early cues towards the involvement of the Amy in attaching emotional meaning to sensory stimuli were obtained in primate lesion studies in the late 19th (S. Brown and Sharpey-Schafer 1888) and early 20th (Klüver and Bucy 1937) century. Subsequent lesion work in rodents (Blanchard, Caroline Blanchard, and Blanchard 1972) demonstrated the involvement of the amygdala in pavlovian fear conditioning, which set the trajectory for the main focus of subsequent studies. For instance, associations between noxious and auditory (Maren et al. 1996) as well as noxious and visual contextual (Bauer, Schafe, and LeDoux 2002) cues is dependent on N-methyl-D-aspartate receptor (NMDAR) mediated synaptic plasticity in the BLA. Consistently, in fear conditioning paradigms Amy neurons respond to auditory (Quirk, Armony, and LeDoux 1997), spatio-contextual (Hobin, Goosens, and Maren 2003) and olfactory (Sevelinges et al. 2004) conditioned stimuli. Other studies

demonstrated that the amygdala is involved in social behaviour (Wellman et al. 2016), the acquisition and expression of reward related associations in operant conditioning experiments with water-deprived animals (Cador, Robbins, and Everitt 1989), and sexual reinforcement (Everitt, Cador, and Robbins 1989). The representation of rewarding versus aversive stimuli appears to be separated at the single cell level although the location of neurons preferentially responding to aversive or appetitive CS and US within the amygdala seems to be intermingled (Paton et al. 2006; Belova, Paton, and Salzman 2008). Although some authors have argued that reward-related first order pavlovian conditioning is not BLA-dependent while second order conditioning is (Hatfield et al. 1996; Parkinson, Robbins, and Everitt 2000), evidence to the contrary exists (Murray and Mishkin 1984; Spiegler and Mishkin 1981; Gaffan and Harrison 1987). It is now generally thought that the amygdala is important in associating stimuli with their reward value (Wassum and Izquierdo 2015; Baxter and Murray 2002).

1.2.3. Nucleus accumbens

Anatomy: Efferent inputs into the NAc originate from the hippocampal formation including (to a minor extent) from CA1 (Kelley and Domesick 1982; Trouche et al. 2019), BLA (Wright, Beijer, and Groenewegen 1996; Groenewegen et al. 1999), PFC (Beckstead 1979; Phillipson and Griffiths 1985; Montaron et al. 1996) and VTA (Fallon and Moore 1978; Phillipson and Griffiths 1985). The NAc is subdivided into two anatomically distinct regions, the core and the shell (Brog et al. 1993). While there is a general overlap in the input to the core and shell (Zahm 1999, 2000), there are some differences. For instance more dorsal CA1 fibers project to the shell than to the core (Trouche et al. 2019) and while the core receives inputs from the parahippocampal

regions the shell receives input from the ventral subiculum (Voorn et al. 2004; Berendse and Groenewegen 1990). Interestingly, these anatomical projections appear to correspond to a functional gradient. While projections from the ventral subiculum to the NAc shell are related to context-dependent reinstatement of memories (Bossert et al. 2016), the projection from CA1 supports appetitive spatial memory (Trouche et al. 2019)

Role in mnemonic stimulus representation: the NAc is thought to act as a limbic-motor interface (Mogenson 1985; Mogenson, Jones, and Yim 1980). Numerous studies have established that the NAc is necessary to learn pavlovian associations (Ciano et al. 2001; Parkinson et al. 2002) and to initiate appetitive approach behaviour (Maldonado-Irizarry and Kelley 1994; Michael Wu, Brudzynski, and Mogenson 1993; M. Wu, Brudzynski, and Mogenson 1993). However, it is not required for instrumental learning (Cardinal and Cheung 2005; Corbit and Balleine 2011; Parkinson et al. 1999b; J. Taylor and Robbins 1986) and to perform discriminations between cues to obtain a reward (Castañé, Theobald, and Robbins 2010; Floresco et al. 2006). NAc cells are capable of acquiring firing rate responses to sensory stimuli as a function of continued pavlovian training: for instance, olfactory cues associated with reward produced firing rate changes in more NAc neurons in proficient mice compared to naive animals (Setlow, Schoenbaum, and Gallagher 2003). Similar results were obtained using audiovisual stimuli (Roitman, Wheeler, and Carelli 2005). Notably, the NAc also processes aversive mnemonic information. Previous studies have shown that the NAc is involved in the acquisition and to a lesser degree in the expression of conditioned responses when using contextual but not discrete cues (Haralambous and Westbrook 1999; Levita, Dalley, and Robbins 2002; Parkinson et al. 1999b). Furthermore, another study demonstrated that NAc neurons exhibit different temporal dynamics of firing rate

changes in response to rewards (sucrose) and aversive tastes (quinine) and encode their predicting audiovisual CS (Roitman, Wheeler, and Carelli 2005). These findings show that the NAc holds both, appetitive and aversive mnemonic representations. It has been argued that the NAc core and shell play different roles in translating such associations into behaviour: while the shell promotes the locomotor response in conditioning paradigms, the core controls the expression or potentiation of pavlovian conditioned responses (Parkinson et al. 1999a).

1.2.4. PFC

Anatomy: The rodent PFC contains the orbital, agranular insular regions, and medial PFC (Van De Werd and Uylings 2008). The medial PFC is further subdivided in the infralimbic cortex, prelimbic cortex and anterior cingulate cortex (Giustino and Maren 2015). The prefrontal cortex is heavily interconnected with the rest of the brain and as such receives input from several regions including, but not limited to, the Amy (Little and Carter 2012; Krettek and Price 1977), CA1 (Jay and Witter 1991), and VTA (Lammel et al. 2008; Chaudhury et al. 2013).

Role in mnemonic stimulus representation: Previous studies have shown that the PFC is engaged in recent (1-2 days) (Kevin A. Corcoran and Quirk 2007) as well as remote (weeks) memory storage, which is accompanied by PFC network restructuring (Bontempi et al. 1999). Cells in the rodent PFC respond to multiple stimulus modalities in memory tasks, such as auditory CS in fear conditioning paradigms (Milad and Quirk 2002), visual stimuli (Xiang and Brown 2004), social representations and olfactory cues (Levy et al. 2019). Moreover, in analogy to primate studies (Wallis, Anderson, and Miller 2001), the rodent PFC neurons can learn to respond to multiple visual stimuli belonging to the same behaviourally meaningful category (Reinert et al. 2021) and

hence, providing a platform for more complex, abstract forms of learning (Miller, Freedman, and Wallis 2002). Lesioning studies indicated the requirement of PFC for space-object associations (Kesner and Ragozzino 2003) and neurons with mixed selectivity for different task variables (Rigotti et al. 2013) have been reported in the PFC using a memory task (Dang et al. 2020). Ultimately, the involvement of the PFC in mnemonic representations as well as decision-making (Domenech and Koechlin 2015) has led to the idea that the PFC 'predicts the most adaptive response based on previous experience' (Euston, Gruber, and McNaughton 2012), meaning that past experiences are synthesised in a way that produce the most effective behaviour during the situation at hand.

1.2.5. VTA

Substantial work has been conducted on the role of the VTA in learning, memory and ongoing behaviour as well as the involvement of different cell types and neurotransmitters in those aspects. I will review these in more detail below in section 1.5 and focus on mnemonic representations in the VTA itself here.

Anatomy: The VTA is divided into medial and lateral VTA with the former consisting of the caudal linear nucleus and interfascicular nucleus and the latter being composed of the parabrachial pigmented nucleus and the paranigral nucleus. The VTA receives input from the NAc (Zahm and Heimer 1993; Usuda, Tanaka, and Chiba 1998), PFC (Carr and Sesack 2000), lateral habenula (Omelchenko, Bell, and Sesack 2009), anterior cortex, the bed nucleus of the stria terminalis (D. Takahashi et al. 2019) and dorsal raphe nuclei (A. J. Chang et al. 2021).

Role in mnemonic stimulus representation: Early work on pavlovian conditioning in the VTA revealed that putative dopaminergic neurons acquire learned responses to

conditioned stimuli from various modalities including visual (Schultz, Dayan, and Montague 1997), auditory (Pan et al. 2005) and spatio-contextual cues (Puryear, Kim, and Mizumori 2010). Notably some VTA neurons exhibited conjunctive coding between the context and movement, the latter of which may be indicative of the motivational state (Puryear, Kim, and Mizumori 2010). More recently, it has been shown that the motivational state can be dissociated from learning signals on the basis of dopamine release in the NAc: reward prediction errors (RPE) but not the motivational state were encoded in dopamine VTA cell activity spiking activity. However, the motivational state had no effect on dopamine release in the NAc, but RPEs did (Mohebi et al. 2019). Anticipatory signals may also extend to cues signaling the onset of a trial in which a motor action can be taken in order to obtain a reward (Ljungberg, Apicella, and Schultz 1992) and reflect mnemonic signatures of learned probabilities of obtaining a reward (Fiorillo, Tobler, and Schultz 2003). The observation that dopaminergic neurons respond to the experience of unexpected rewards and conditioned cues associated with rewards but are inhibited when an expected reward is omitted (Schultz and Dickinson 2000) gave rise to the idea that these VTA neurons may signal an error in the prediction of reward (Schultz, Dayan, and Montague 1997) relying on fast transient responses. Interestingly, dopaminergic VTA neurons also encode deviations from predicted features of rewards, even if their reward value remains the same (Stalnaker et al. 2019; Y. K. Takahashi et al. 2017) and may even have a role in sensory preconditioning (Gardner, Schoenbaum, and Gershman, 2018). The multidimensional sensory content of such a mispredicted event is encoded in the population activity of dopaminergic VTA neurons (Stalnaker et al. 2019). More recent research has uncovered that ramping activity of dopamine neurons also encodes temporal difference errors related to an expected sequence of events leading to a

reward (Kim et al. 2020). Such dynamics have been shown to underlie a gradual backwards shift (from the reward delivery) of conditioned stimulus (Amo et al. 2020). Moreover, uncertainty about the sensory state predicting a future reward modulates reward prediction errors encoded by dopamine neuron activity (Babayan, Uchida, and Gershman 2018). Notably, dopaminergic VTA neurons have been shown to respond to multiple sensory variables and neurons encoding similar combinations of variables are clustered anatomically (Engelhard et al. 2019). Beyond reward, other work has indicated that VTA neurons also acquire responses to CSs in aversive conditioning paradigms using auditory (Guarraci and Kapp 1999) and visual cues (Gore, Soden, and Zweifel 2014). Consistently, dopaminergic VTA neurons reinforce the avoidance of aversive stimuli (Menegas et al. 2018).

1.2.6. Interactions between regions in processing mnemonic stimuli

While neurons appear to respond to mnemonically relevant behavioural parameters in different brain regions, thus holding different parts of whole memories, it is thought that the communication and cooperation of different brain areas allows for the integration of such mnemonic fragments (Schlichting and Preston 2015). While I acknowledge that a plethora of examples involving other brain regions exists, in this paragraph I will focus on reviewing evidence for the communication betIen CA1, BLA, NAc, PFC and VTA (Fig. 1).

The classical understanding of the roles ascribed to the regions is the following: individual neurons in the dorsal CA1 represent spatio-visual surroundings (Wilson and McNaughton 1993; Leutgeb et al. 2005; O'Keefe and Dostrovsky 1971b); Amy and VTA area neurons process negative and positive stimuli (e.g., conditioned auditory cues) (Ambroggi et al. 2008; Beyeler et al. 2016; Herry et al. 2008; Cohen et al. 2012;

Kyriazi, Headley, and Paré 2020; Root, Estrin, and Morales 2018; Engelhard et al., 2019); medial PFC neurons underpin decision-making (Sul et al. 2010; Narayanan and Laubach 2006; Passecker et al. 2019) and NAc neurons process cue-predicted reward outcomes (Lansink et al. 2012; van der Meer and Redish 2009; Lavoie and Mizumori 1994). As a result, anatomical connectivity between these five regions could support the joint processing of aversive and appetitive stimuli while incorporating contextual information and decision making.

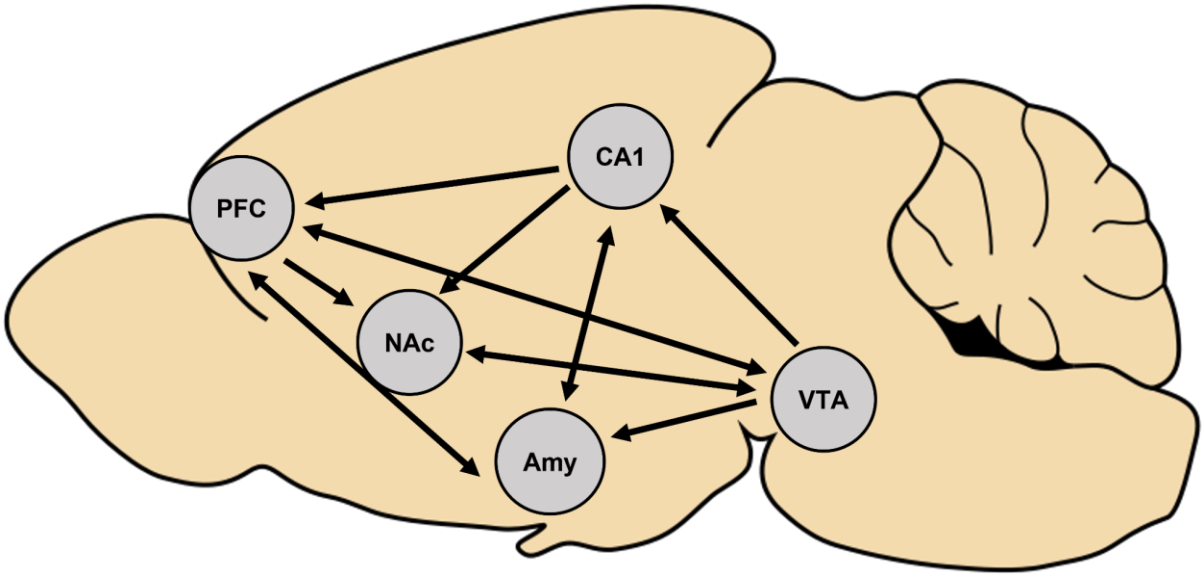

Fig. 1 Schematic of the anatomical connectivity of regions investigated in this thesis.

The anatomical connectivity between CA1, Amy, NAc, PFC and VTA is thought to support behaviour relying on aversive and appetitive stimuli, contextual information, decision making and outcomes.

For instance, CA1 directly projects to the medial PFC (Hoover and Vertes 2007). The PFC is thought to be crucially involved in memory retrieval (Hoover and Vertes 2007) and single neurons in CA1 have been shown to encode contextual information (Daumas et al. 2005). Hence, the *CA1-PFC* projection is thought to support memory retrieval that depends on contextual information (Schacter, Harbluk, and McLachlan 1984; K. A. Corcoran and Maren 2001). CA1, alongside with the PFC and Amy also projects to the NAc (Groenewegen et al. 1999). It has been shown that CA1 provides

contextual information *(CA1-NAc)* (Goto and Grace 2005; Trouche et al. 2019) while PFC inputs facilitate set-shifting behaviour, and hence support executive control via the *PFC-NAc* connection (Goto and Grace 2005). The amygdala sends projections to the NAc (Brog et al. 1993). Consistent with the amygdala's role in processing behaviour relying on cues predicting aversive outcomes (LeDoux 2003) as well as appetitive conditioned stimuli (Uwano et al. 1995), the *Amy-NAc* pathway has been shown to drive responses to reward predicting cues in the NAc and to ultimately promote reward seeking behaviour (Ambroggi et al. 2008). Dopaminergic *VTA-NAc* inputs have been shown to play a key role in regulating glutamatergic transmission from other regions to the NAc and hence, has been suggested to participate in the modulation of goal directed behaviors (Yu et al. 2019). For instance, reward seeking behaviour driven by Amy inputs into the NAc depends on simultaneous D1-receptor activation (Ambroggi et al. 2008) and hippocampal and prefrontal inputs are modulated via D1 and D2 receptor input, respectively (Goto and Grace 2005). Glutamatergic *VTA-NAc* inputs have been shown to drive aversive behaviour by acting on NAc GABAergic neurons (Qi et al. 2016), suggesting a possible dichotomy in the roles for dopaminergic versus glutamatergic inputs for the NAc with the former being related to goal/reward-related behaviour (Ambroggi et al. 2008; Goto and Grace 2005) and the latter regulating aversive behaviours (Qi et al. 2016). The VTA and CA1 are suggested to form a functional loop governing the entry of novel information into long-term memory (John E. Lisman and Grace 2005): in this model of a *VTA-CA1* loop, the hippocampus detects novel information, and sends an indirect signal via the subiculum, NAc and ventral pallidum to the VTA, which in turn activate dopaminergic neurons projecting back to CA1 supporting local synaptic plasticity. Activation of dopaminergic *VTA-PFC* has been shown to have different effects on the PFC's role

in executive control. While tonic excitation of dopaminergic inputs resulted in the maintenance of previously learned behavioural choices associated with reward, phasic excitation produced a deviation from previously learned rules (Ellwood et al. 2017). Furthermore, the PFC also projects to the VTA (Carr and Sesack 2000), where inputs terminate on dopaminergic neurons, potentially providing means for top down modulation by the PFC of VTA neurons. The PFC and Amy are strongly reciprocally connected (Little and Carter 2013). It is generally thought that the *PFC-Amy* projection is involved in regulating fear responses and gates extinction learning (Giustino and Maren 2015; Sotres-Bayon, Bush, and LeDoux 2004). Conversely, inhibitory connections from the Amy to PFC drive reward seeking (but not consumption) behaviour suggesting a role in controlling response inhibition in the PFC (Seo et al. 2016). The Amy projects directly to the ventral hippocampal CA3 and CA1 areas (Pikkarainen et al. 1999). These *Amy-CA1* inputs drive associations between space and emotional content (Yang and Wang 2017) and projections from the posterior BLA to CA1 have an anxiolytic effect, while inputs from the anterior BLA reduce approach behaviour (Pi et al. 2020).

In summary, these five interconnected brain regions are thought to exchange and integrate contextual (CA1) (Schacter, Harbluk, and McLachlan 1984; K. A. Corcoran and Maren 2001) and conditioned cues (Amy) (Ambroggi et al. 2008) in appetitive and aversive behaviours. The PFC integrates those inputs and exerts top-down modulation of its downstream target areas (Ellwood et al. 2017; Goto and Grace 2005; Giustino and Maren 2015; Sotres-Bayon, Bush, and LeDoux 2004). The NAc receives direct input from all the other four regions and appears to regulate balance, and hence the behavioural impact of the inputs on the basis of the dopaminergic transmission levels arriving from the VTA (Goto and Grace 2005; Ambroggi et al. 2011). As such,

dopaminergic transmission from the VTA acts not only as a teaching signal in its target areas but also as a regulator between different behavioural responses, while glutamatergic inputs into the NAc produce aversive behaviour (Qi et al. 2016).

1.3. The assembly hypothesis

In 1949, Donald Hebb suggested that memories are represented in the combined activity of individual neurons forming groups, which he termed ‘cell assemblies’ (Hebb 1949a). He postulated that the mechanism giving rise to such cell assemblies is repeated co-activity leading to strengthened synaptic connectivity between the cells firing together. In his own words: “When an axon of cell A is near enough to excite a cell B and repeatedly or persistently takes part in firing it, some growth process or metabolic change takes place in one or both cells such that A’s efficiency, as one of the cells firing B, is increased.” (Hebb, 1949; p.62). He postulated that strengthened connectivity would then enable neurons to fire together and reinstate the complete representation of a memory even if initially only a subset of the assembly member neurons were activated. He based his argumentation on the at the time recent discovery that in the cortex (i) input from multiple presynaptic neurons is required to trigger action potentials in the postsynaptic cells and (ii) neurons are heavily reciprocally connected (De No 1938). The initial input would be provided by primary sensory areas, which Hebb assumed to be excluded from participation in memory assemblies. More recent research, however, has shown that even lower sensory cortices do indeed participate in memory retrieval (Wheeler, Petersen, and Buckner 2000). Importantly, Hebb recognised that such assemblies could be widely distributed across the brain and exhibit a degree of representational redundancy and, thus, provide resilience to perturbation of the system (Hebb, 1949, p. 74).

More recently, György Buzsáki proposed an argument about why it makes physiological sense for the brain to create groups of co-active neurons (Buzsáki 2010). He argues that an assembly can be defined from a downstream 'reader' neuron point of view, which integrates multiple presynaptic inputs arriving closely in time allowing the reader neuron to reach the depolarisation threshold required to initiate an action potential. Since multiple presynaptic neurons are required to initiate action potentials in downstream reader neurons (De No 1938), the relevant unit in the brain is such a co-firing assembly. This also means that presynaptic inputs need to arrive within the integration time window of the downstream reader neuron, which in the case of cortical and hippocampal cells is between 10-30 ms (Spruston and Johnston 1992; Koch, Rapp, and Segev 1996).

Much of recent work has been conducted on pinpointing the nature of hippocampal assemblies (Kudrimoti, Barnes, and McNaughton 1999; Kenneth D. Harris et al. 2003; Malvache et al. 2016) and linking it to behaviourally relevant representations such as place-selective assemblies of CA1 pyramidal neurons (Van de Ven et al. 2016). However, empirical work on brain-wide distributed assemblies as initially postulated by Hebb (Hebb, 1949, p. 74) has lagged behind. Eichenbaum suggested that distributed assemblies are responsible for the representation of complex percepts and could emerge from local assemblies operating at lower sensory levels (H. Eichenbaum 1993). Building on this, Mesulam proposed that multimodal areas could allow crosstalk between different brain regions by containing directories for binding distributed and modality-specific fragments into coherent concepts (Mesulam 1998). In other words, Mesulam suggests that more interconnected or multimodal areas (e.g. associatives) contain information about how to retrieve fragments of memories in more specialised brain areas (e.g. visual cortical areas). With the help of such multimodal areas,

elements represented in different specialised brain areas could be bound together to one coherent memory. According to him, multimodality serves to create content-addressable associative memories. Wickelgren proposed that neural webs act as neural representations of concepts. Such neural webs could consist of neurons from different brain areas that are connected by long-range projections resulting in the formation of distributed assemblies. The important addition in this concept is that neurons involved in such distributed assemblies could then in turn trigger the formation of local assemblies within the participating brain areas. Such 'locally nested' assemblies in different brain areas could then be recruited to give rise to other new distributed assemblies (Wickelgren 1999). The retrieval of memory fragments could then happen simultaneously in different brain regions and cause the formation of more complex associations and representations as suggested by Sommer and Wennekers (Sommer and Wennekers 2003). Consistently, a study comparing decoding performance of neurons grouped into co-firing assemblies detected in four different brain regions (separately) found that the same behavioural task information could be decoded above chance level in each of the brain areas separately (Deolindo et al. 2017). However, this study did not investigate neuronal co-firing activity between regions. In fact, few studies show co-activation of brain wide distributed neurons at the single cell level and rather focus on pairwise interrogations. For example, firing-sequence replays by single neurons at millisecond timescales are coordinated between CA1 and PFC in a decision-making paradigm reliant on spatial learning (Shin, Tang, and Jadhav 2019) and CA1-PFC co-firing activity is increased during CA1 sharp-wave ripple (SWR) events (Wenbo Tang et al. 2017). Similar results were obtained for CA1-amygdala cell pairs (Girardeau, Inema, and Buzsáki 2017) during SWRs. Furthermore, NAc single unit activity correlates with pyramidal cell firing in CA1

in a CPP task (Trouche et al. 2019) and VTA neurons that were active during the receipt of a reward later co-ordinated with hippocampal cells activity during spatial replay events in SWRs (Gomperts, Kloosterman, and Wilson 2015).

The formation of cell assemblies has been argued to be organised by oscillatory activity, in particular by gamma oscillations (Buzsáki 2010). According to Buzsáki, cycles of excitation and inhibition determine the lifetime of an assembly, which depends on the time constant of ionotropic GABA receptors, AMPARs, and the time-window of spike-time dependent plasticity of participating neurons. He further argues that interneurons play a crucial role in this process by supporting the selection of participating neurons for the assembly. This selection depends on the initial input into the system. Indeed, optogenetic silencing of CA1 inputs prevented the expression of local NAc assembly formation (Trouche et al. 2019) demonstrating the importance of interregional input for local assembly formation. One key unanswered question is how the initial selection of local neurons distributed across the brain works. One possibility is that a divergent pathway innervating multiple brain regions provides this first input for subsequent computation of local and distributed co-activity in a coordinated manner. Such a source would require widespread and far-reaching axonal projections. The VTA (Björklund and Dunnett 2007), raphe nuclei (Xu et al. 2020) and locus coeruleus (Foote, Bloom, and Aston-Jones 1983) could be a prime candidate for the provision of the required anatomical infrastructure.

1.4. Cell types in the VTA and their behavioural relevance

The VTA is involved in a number of different behaviours and exhibits cellular heterogeneity. In this section, I will review anatomical, physiological and behavioural findings relating to different cell types of the VTA.

1.4.1. VTA and dopamine signalling

Physiology and anatomy: dopaminergic neurons are characterised by the expression of tyrosine hydroxylase (TH), an enzyme in the synthetic pathway of dopamine converting L-tyrosine to L-Dopa, a precursor of dopamine (Elsworth and Roth 1997). After dopamine is released, dopamine is taken back up into the cell by the dopamine transporter (DAT). Both molecules are used to identify and tag dopaminergic neurons (Pickel et al. 1975; Ciliax et al. 1995). Dopamine acts on presynaptic as well as postsynaptic dopamine receptors, which can be divided into D1-like (D1, D5) and D2 (D2, D3, D4) - like receptors based similarities in molecular structure and associated signaling cascades (Neve, Seamans, and Trantham-Davidson 2004). All dopamine receptors are metabotropic (G protein coupled receptors i.e. GPCRs) and can exert changes to the membrane potential, albeit at slower timescales than receptors that are ligand gated ion channels. They can also exert longer-lasting plastic changes by modifying gene expression and metabolic processes leading to altered synaptic connectivity. Furthermore, while D1-like receptors mediate predominantly excitatory transmission, D2-like receptors generally have inhibitory effects (Tritsch and Sabatini 2012).

TH expression is relatively uniformly distributed across the entire VTA, while DAT neurons appear to be slightly more prevalent in lateral areas of the VTA (Li et al. 2013; Yamaguchi et al. 2011). A study has shown that dopaminergic neurons projecting to different brain areas receive input from quantitatively different presynaptic sources (Beier et al. 2015). Dopaminergic VTA neurons innervate a vast proportion of the brain via two main pathways, the mesolimbic and the mesocortical pathway (Björklund and Dunnett 2007). The mesolimbic DA pathway projects primarily to the ventral striatum

(which includes the NAc) and other limbic areas such as the amygdala, olfactory tubercle and the septum while mesocortical pathway innervates several cortical areas (Björklund and Dunnett 2007).

Behaviour: It is now well established that dopaminergic neurons increase their firing rate in response to surprising rewards. If a consistent cue precedes the delivery of a reward, this response shifts to the CS instead and the firing rate is decreased if a predicted reward is omitted (Bromberg-Martin, Matsumoto, and Hikosaka 2010; Cohen et al. 2012; Schultz, Dayan, and Montague 1997). Consistently, activation of dopaminergic VTA neurons produces appetitive behaviour (H.-C. Tsai et al. 2009; Witten et al. 2011). It is generally thought that activation of dopaminergic VTA neurons precedes the formation of successful memories (Adcock et al. 2006) and is sufficient to strengthen persistent mnemonic assemblies (McNamara et al. 2014). Furthermore, dopaminergic VTA neurons are thought to encode incentive salience (Berridge 2007) and hence, are involved in motivational control (Bromberg-Martin, Matsumoto, and Hikosaka 2010; Salamone and Correa 2012). Beyond reward, dopaminergic VTA cells also respond to aversive US and CS (Aston-Jones and Moorman 2009; Schultz 2007).

1.4.2. VTA and GABA signalling

Physiology and anatomy: Gamma aminobutyric acid (GABA) is synthesized from glutamate by glutamate decarboxylase 1 (GAD1) or GAD2 (Brady et al. 2005) , which are used as markers for GABAergic neurons. GAD-expressing neurons are evenly spread across the VTA in a similar fashion to TH-expressing neurons (Margolis et al. 2012; Olson and Nestler 2007). GABA ergic neurons in the VTA project to cholinergic interneurons in the NAc (M. T. C. Brown et al. 2012), to the habenula (Root, Mejias-Aponte, Zhang, et al. 2014), to PFC (R. E. Brown and McKenna 2015), brainstem

including the ventral pallidum, lateral and magnocellular preoptic nuclei, lateral hypothalamus, amygdala and thalamus (S. R. Taylor et al. 2014). It is very likely that the VTA GABA population is highly diverse (Root, Mejias-Aponte, Zhang, et al. 2014; Olson and Nestler 2007), which could possibly explain the heterogeneity of behaviours GABAergic VTA signalling is involved in.

Behaviour: GABAergic VTA neurons increase their firing rate in response to reward predicting CS. This increased firing rate remains high throughout the receipt of the reward (Cohen et al. 2012; Tan et al. 2012) indicating a role in appetitive conditioning. On the other hand, optogenetic activation of VTA GABA neurons causes conditioned place aversion (Tan et al. 2012), likely through the inhibition of neighbouring dopamine neurons (van Zessen et al. 2012). Reward consumption is inhibited by optogenetic stimulation of GABAergic neurons in the VTA (van Zessen et al. 2012) and activation of VTA GABA cells mediate defensive behaviour likely through projections to the central Amy (Z. Zhou et al., 2018). Consistently, pathway specific optogenetic activation of GABAergic VTA-NAc projections promotes the animal's ability to discriminate aversive CS (M. T. C. Brown et al. 2012).

1.4.3. VTA and glutamate signalling

Physiology and anatomy: glutamatergic VTA neurons were first demonstrated in 2006 using the vesicular glutamate transporter (VGlut2) as a marker (Kawano et al. 2006). Glutamate acts on pre-and postsynaptic ligand gated in channels (N-methyl-D-Aspartate receptors i.e NMDAR, α-amino-3-hydroxy-5-methyl-4-isoxazolepropionic acid receptor i.e. AMPARs and Kainate receptors) allowing for fast neurotransmission at millisecond timescales as well as the induction of synaptic plasticity (Y. Zhou and Danbolt 2014). Glutamate also acts on GPRCs (mGluR 1-8) causing prolonged

modulation of the membrane potential for hundreds of milliseconds and the induction of plastic changes (Y. Zhou and Danbolt 2014).

Cell bodies of glutamatergic VTA neurons predominantly concentrate in the midline nuclei of the VTA and become progressively less dense towards the lateral areas (Yamaguchi et al. 2011; Yamaguchi, Sheen, and Morales 2007) and receive proportionally different inputs from presynaptic sources compared to GABAergic and dopaminergic neurons (Faget et al. 2016). Glutamatergic VTA neurons have previously been shown to project to a number of target regions spread across the brain. Early evidence demonstrated that electrical stimulation in the VTA elicits fast responses indicative of monosynaptic connections in the rat frontal cortex (Mercuri et al. 1985). Two decades later, it has been shown that GABAergic neurons in the PFC are innervated by glutamatergic VTA cells and only exert a small excitatory effect on pyramidal neurons (Lavin et al. 2005; Kabanova et al. 2015). PFC innervation was also confirmed anatomically using histological methods (Yamaguchi et al. 2011). This study confirmed that VGlut2-only VTA neurons also innervated the NAc. A later comprehensive anatomical study identified projections to the bed nucleus of stria terminalis (BNST), the preoptic nucleus and confirmed projections of VGlut2-only cells to PFC, Amy, lateral habenula, NAc shell and core (S. R. Taylor et al. 2014). Furthermore, optogenetic activation of glutamatergic fibers from the VTA triggered spiking in NAc-GABAergic interneurons, which inhibited neighbouring medium-spiny neurons cells of the NAc (Qi et al. 2016). Glutamatergic projections from the VTA to the Amy have been demonstrated anatomically (Hnasko et al. 2012). Finally, optogenetic glutamatergic axons projecting from the VTA to CA1 triggered spiking in pyramidal neurons (Adeniyi, Shrestha, and Ogundele 2020). Given such a brain wide

innervation pattern it is not surprising that glutamatergic VTA neurons appear to be involved in a large set of behaviours.

Behaviour: The understanding of the role of glutamatergic VTA neurons in specific types of behaviours has rapidly evolved within in the last five years. Generalised optogenetic activation of glutamatergic VTA cell bodies produces appetitive behaviour (H.-L. Wang et al. 2015). However, this effect appeared to be dependent on dopamine and was suggested to be mediated through the excitation of neighbouring dopaminergic neurons. Other research showed that glutamatergic cells are involved in the processing of aversive conditioning: activation of glutamatergic VTA fibers innervating the NAc and the lateral habenula drives aversive conditioning (Qi et al. 2016; Root, Mejias-Aponte, Qi, et al. 2014; Lammel et al. 2015). Since dopaminergic signalling has been historically implicated in reward processing, these early studies on glutamatergic VTA cells gave rise to the idea that different VTA neuron subtypes as defined by their neurotransmitter may be involved in different types of behaviours (Morales and Margolis 2017). This idea is partially supported by more recent research: cell-type specific permanent ablation of glutamatergic VTA neurons abolishes innate defensive behaviour (Barbano et al. 2020). Consistently, the firing rate of the majority of glutamatergic VTA cells increased during an aversive stimulus (airpuff), while the remaining cells decreased firing rate (Root, Estrin, and Morales 2018). Interestingly however, amongst the neurons which responded to an increase in firing rate there were also neurons that also responded to the receipt of a reward. This led the authors to conclude that glutamatergic VTA cell function is heterogeneous. A part of the glutamatergic cell population responds to aversion while another part responds generally to salient events (Root, Estrin, and Morales 2018). Indeed, subsequent research points towards a more complex role of glutamatergic VTA cells in behaviour.

While chemogenic inactivation of glutamatergic VTA fibers innervating the dorsal hippocampus prevents the acquisition and the recall of context-specific fear memory, also the retrieval of conditioned place-preference memories was impaired in treated animals (Han et al. 2020). Furthermore, one subpopulation of glutamatergic VTA neurons appears to decrease in firing rate while another increases in response to reward delivery (McGovern, Polter, and Root 2021). Similar to dopaminergic neurons, glutamatergic VTA cell activation can act as a positive reinforcer in a dopamine independent manner (Zell et al. 2020). As suggested recently, one way of reconciling these findings is that different behaviours depend on different VTA cell subpopulations as defined by their presynaptic inputs (Montardy et al. 2019).

1.5. Anatomical spread of dopaminergic, glutamatergic and GABAergic VTA neurons

In rats, most TH-expressing neurons are concentrated in the lateral VTA. However, in rats neurons expressing DAT (the dopamine transporter required for dopamine reuptake) and (VMAT2, the vesicular monoamine transporter required for vesicular packaging) are expressed in the lateral aspects of the VTA, a lower number of neurons in the medial VTA lacks the expression of these proteins (Li et al. 2013). Consistently, in the mouse VTA also some TH-positive neurons lack the expression of VMAT and DAT (Stamatakis et al. 2013; Lammel et al. 2008). Dopaminergic only neurons (i.e. expressing the TH protein but not VGlut2 mRNA) are roughly equally spread throughout all regions of the VTA in rats (Yamaguchi et al. 2011). VGlut2-only neurons are concentrated and outnumber TH expressing cells in the medial parts of the VTA (Yamaguchi, Sheen, and Morales 2007; Yamaguchi et al. 2011, 2015). Combinatory dopaminergic-glutamatergic neurons (TH protein and VGlut2 mRNA-positive) are concentrated in the medial VTA (Yamaguchi et al. 2011). Such combinatorial neurons

have been shown to project to areas similar to the targets of the dopaminergic VTA, such as the NAc and PFC (Kabanova et al. 2015; Yamaguchi et al. 2011; Stuber et al. 2010; Tecuapetla et al. 2010). In the NAc these fibers have been shown to contain adjacent but separate synaptic terminals for dopaminergic and glutamatergic release sites along the same axon (Zhang et al. 2015). A large-scale synthesizing review aiming to classify VTA cells based on molecular markers identified 6 clusters containing VGlut2-expressing neurons that are spread throughout the VTA (Poulin et al. 2020). However, findings in this review were generated from animals aged 7 days or younger and cannot be extrapolated to the adult population, as the expression profiles may change as the brain matures. The studies by Yamaguchi et al. however, were conducted in adult mice and show that TH-only and dual TH-VGlut2 neurons occur predominantly in the medial VTA (Yamaguchi, Sheen, and Morales 2007; Yamaguchi et al. 2011, 2015). Furthermore, a small population of VTA neurons expresses VGlut2, GAD and TH (Yamaguchi et al. 2011) and another population projecting to the lateral habenula expresses VGlut2, VGAT, GAD1 and GAD2 (Root, Mejias-Aponte, Zhang, et al. 2014). GABAergic co-transmission with dopamine appears to occur from the same vesicle (Root, Mejias-Aponte, Zhang, et al. 2014) and GABA-glutamate co-release happens from the same terminal with separate vesicles (Zhang et al. 2015).

In summary, the following picture appears: purely glutamatergic neurons are concentrated in the midline nuclei of the VTA accompanied by a smaller subset of glutamate-dopamine co-releasing neurons. Dopaminergic-only neurons are spread across the VTA. By far not all dopaminergic VTA neurons also express glutamatergic neurons. Lastly, a minor proportion of VTA neurons also co-express GABA-glutamate

or GABA-TH-glutamate. A comprehensive review by Marisela Morales summarises these findings (Morales and Margolis 2017).

In summary, the majority of evidence suggests that no one single VTA cell type (as defined by their neurotransmitter) appears to be exclusively dedicated to certain types of behaviour and conversely, the same behaviour appears to be supported by multiple VTA neuron types. In fact, it is unlikely that any neuron type in the brain is responsible for a certain behaviour, but instead a computation that is shared across different behaviours.

1.6. Overview and hypothesis

Based on the reviewed literature, the following picture emerges: mnemonic representations in the brain are distributed across multiple brain regions and exhibit a certain degree of overlap. Such representations scattered across the brain could be tied together in the form of co-firing assemblies. However, it is unclear how the brain computes assemblies distributed across different brain areas.

I hypothesise that a divergent source targeting multiple brain areas could cause co-firing activity across multiple brain areas. Thus, it could support the formation of brain wide distributed assemblies and ultimately mnemonic processes. I hypothesise that the VTA could act as such a divergent source of synchronisation.

The investigation of this hypothesis requires:

a) The identification of a candidate VTA neuronal population. In ***chapter 3***, I investigate the neuronal responses to a behavioural task involving a combination of appetitive and aversive conditioning in a go/nogo paradigm. Using unsupervised clustering, I detect several VTA cell subgroups and map these onto neurotransmitter identities using ground truth obtained from optogenetic tagging (dopamine and glutamate) experiments.
b) Detection of brain-wide distributed assembly patterns. In ***chapter 4***, I show co-firing assemblies detected from simultaneous tetrode recordings from CA1, Amy, NAc, PFC and VTA and their relationship to ongoing behaviour.
c) The establishment of a causal link between the identified VTA cell population and the formation of distributed assembly patterns. In ***chapter 5,*** I show our findings from experiments using optogenetic activation and silencing of the VTA target population with regards to assembly expression and behavioural performance.

Chapter 6 provides overall conclusions based on our results and suggestions for further research.

2. CHAPTER 2: EXPERIMENTAL PROCEDURES

2.1. Animals

I used adult male mice (3–6 months old) that were heterozygous for the transgene expressing the Cre recombinase under the control of either the Vglut2 or the DAT promoter and maintained on a C57BL/6J background (Jackson Laboratories; Vglut2-Cre RRID: IMSR_JAX:028863; DAT-Cre RRID: IMSR_JAX:006660) or were C57BL/6J wild-type mice (Charles River, UK). Mice were housed with their littermates until the surgical procedure with free access to food and water in a room with a 12/12h light/dark cycle (lights on at 7 a.m.). All experiments were conducted according to the UK Animals (Scientific Procedures) Act 1986 under personal and project licenses issued by the UK Home Office following local ethical review.

Strain	Type of preparation	Mice	Recording days	Of which behaviour only
C57BL/J6 WT	● Quintuple-site recording	5	29	8
VGlut2-Cre	● Quintuple-site recording ● ChRh2 viral injection in VTA ● Bilateral optic fibers above VTA	2	13	-
VGlut2-Cre	● Quintuple-site recording ● ArchT viral injection in VTA ● Bilateral optic fibers above VTA	3	21	-
VGlut2-Cre	● Quintuple-site recording ● GFP viral injection in VTA ● Bilateral optic fibers above VTA	2	18	-
DAT-Cre	● VTA tetrode recording ● ChRh2 viral injection in VTA ● Bilateral optic fibers above VTA	2	10	-

Table 1. Number of mice, recording days by type of preparation.

2.2. Surgical procedure

All surgical procedures were performed under deep anaesthesia using isoflurane (0.5–2%) and oxygen (2 l/min), with analgesia provided before (0.1 mg/kg vetergesic) and after (5 mg/kg metacam) surgery. To generate expression of either ArchT-GFP, GFP-only or ChR2-eYFP in VTA neurons, I used a Cre-loxP approach by injecting the Cre-inducible recombinant adeno-associated viral vector rAAV2-CAG-FLEX-ArchT-GFP (from E.S. Boyden at UNC Vector Core), rAAV2-CAG-FLEX-GFP (from E.S. Boyden at UNC Vector Core) or rAAV2-EF1a-DIO-hChR2(H134R)-eYFP-WPRE (from K. Deisseroth at UNC Vector Core), respectively. Viral injections were targeted bilaterally to the VTA using stereotaxic coordinates (-3.25mm anteroposterior from bregma, ±0.4 mm lateral from bregma, and -3.85 mm ventral from the brain surface; 150 nl per site)

at a rate of 100 nl/min using a glass micropipette lowered to the target site and held in place for 5 min after virus delivery before being withdrawn (McNamara et al. 2014). For electrophysiological recordings, mice were implanted with a microdrive containing 12–14 independently movable tetrodes (Fig. 2).

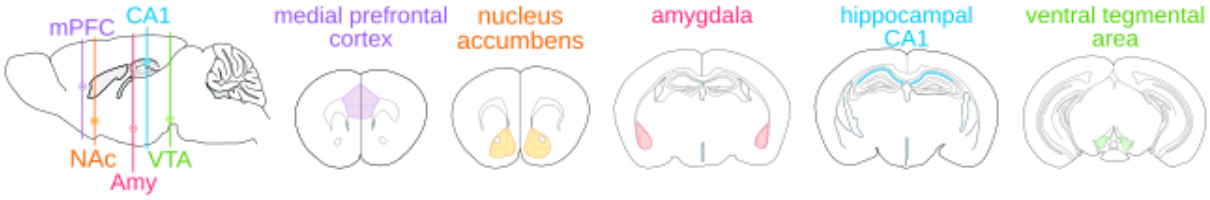

Fig. 2 Multisite recording.

Tetrodes were implanted in the right hemisphere above CA1, Amy, NAc, PFC and VTA and slowly lowered into the target regions.

Tetrodes were constructed by twisting together four insulated tungsten wires (12 µm diameter, California Fine Wire) which were briefly heated to bind them together into a single bundle. Each tetrode was attached to a 6 mm long M1.0 screw to enable independent manipulation of depth. The microdrive was implanted under stereotaxic control with reference to bregma. For dorsal hippocampal CA1, tetrodes were implanted by first identifying central coordinates -2.0 mm anteroposterior from bregma, ±1.7 mm lateral from bregma as a reference to position each individual tetrode contained in the microdrive, initially implanting tetrodes above the pyramidal layer (-1.1 mm ventral from brain surface). A similar approach was used for tetrodes aimed at the medial prefrontal cortex using central coordinates +1.7 mm anteroposterior from bregma, ±0.3 mm lateral from bregma, and an initial -1.5 mm ventral from brain surface; at the ventral tegmental area using central coordinates -3.25 anteroposterior from bregma, ±0.4 mm lateral from bregma, and an initial -3.85 mm ventral from brain

surface; at the nucleus accumbens using central coordinates +1.4 anteroposterior from bregma, ±1.0 mm lateral from bregma, and an initial -3.5 mm ventral from brain surface; and at the amygdala using central coordinates -1.65 anteroposterior from bregma, ±2.75 mm lateral from bregma, and an initial -3.8 mm ventral from brain surface. The distance between neighboring tetrodes inserted in each brain region was 0.4 mm. Following the implantation, the exposed parts of the tetrodes were covered with paraffin wax, after which the drive was secured to the skull using dental cement. For extra stability, four stainless-steel anchor screws were inserted into the skull before the drive was implanted. Two of the anchor screws, inserted above the cerebellum, were attached to 50 µm tungsten wires (California Fine Wire) and further served as a ground and reference electrodes during the recordings. For optogenetic manipulations, two optic fibers (230 µm diameter, Doric Lenses, Canada) were incorporated into the microdrive designed to bilaterally deliver light to VTA and implanted 2 weeks after viral injections.

2.3. Behaviour and recording procedure

Following the post-operative recovery, mice were handled for 3-4 days and daily familiarized to the experimental paradigm, including connection to the recording system equipped with a multichannel rotary commutator with motorized movement compensator (Imetronic, Pessac, France) and exploration of a control (task-unrelated), circular-walled open-field arena (42 cm diameter). Simultaneous to the behavioural training procedure, tetrodes were slowly lowered into their final positions (never more than 250 µm per hour and 1 mm per day). Electrodes were moved by 50-100 µm at the end of each recording day to ensure that new cells were recorded the next day. The electrode placement was guided by the LFP shape and reproducibility

of placement across animals was confirmed using masked empirical mode decomposition (mEMD) (Deering and Kaiser 2005). This was done in collaboration with Charles Clarke-Williams, a DPhil student who implemented the method in the lab. In short, EMD iteratively splits the signal into frequency components called intrinsic mode functions (IMFs). The masking process further allows for separation of components with similar frequencies by adding a sinusoidal masking signal to the extraction process which can be subsequently subtracted to obtain the true component. The advantage of EMD over other methods, such as the Fourier transform is that non-stationarity is better preserved because the iterative IMF extraction process is informed by the signal itself as opposed to by externally imposed sinusoids. IMFs were extracted from sessions in which the animal was performing the behavioural task. Visual inspection of the extracted IMFs confirms inter-regional differences as well as consistency across animals within regions (Fig. 3).

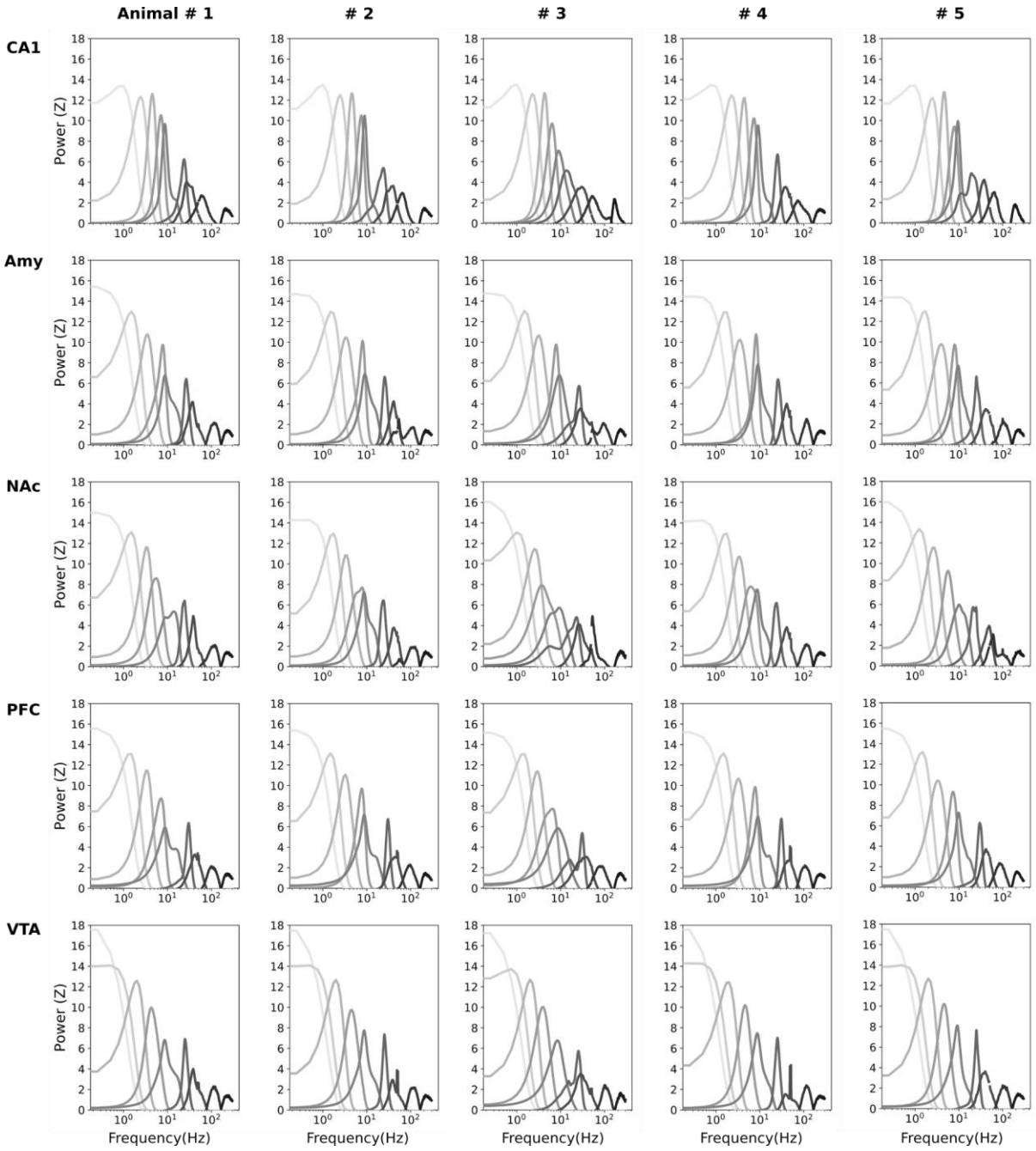

Fig. 3 IMFs for different regions across different example mice.

IMFs were extracted using mEMD from the five mice without optogenetic intervention. Spectral components differ across regions but are consistent within any given region across different animals. This analysis was conducted with the help of Charlie Clarke-Williams.

For behavioural training, mice were food restricted (to ~90% body weight) and underwent a two-step procedure to learn the task (Fig. 4). During the entire training procedure, mice were already implanted with the microdrive device. Mice were first

trained to associate the tone (5 sec, 5 kHz, 70 dB SPL) presentation with the delivery of a drop of sucrose solution at the outcome dispenser in a task-unrelated environment (5-7 training days). Once animals approached and consumed the sucrose drop in 70% of the trials, animals were transferred to the task arena (45 x 45 cm square-walled enclosure, with 12 cm high walls), where they were trained on the LED-tone-outcome task contingencies (5-7 training days). Animals were subjected to recordings once mice reached a 70% accuracy for the first time, but where necessary, mice with approx. 60% performance after 7 days of training were also admitted for recordings in order to avoid progressive deterioration of the tissue around the implanted tetrodes. Mice were put off food deprivation every 4-5 days for 2 days for recovery purposes. Subsequently, the recording was started (5-7 training days). On some days, the same animal underwent two sessions during the same day to avoid progressive deterioration of the tissue over the course of the recording days. The same outcome dispenser, fitted with infra-red beams to detect lick events, was used to deliver either the sucrose or the quinine drops according to the active LED wall-display. Using random intervals ranging from 30-90 secs, the 5-sec tone was presented to signal the availability of a liquid drop (10 µl) at the dispenser. One LED panel was paired with delivery of sucrose (15% solution in water) whereas the other LED panel predicted quinine (0.2 mM solution in water). Each drop solution was available for 5 s from the end of the tone before being automatically withdrawn by reverting the pressure at the spout. The active LED was randomly switched across task sets every 1 to 4 tones (average LED duration: 105.46±4.28 sec). The behavioural response to each tone was quantified in the time window between tone onset and drop removal, with dispenser approaches defined as the animal's position within 3.5 cm from the dispenser in the time interval between the tone onset and the removal of the drop. In experiments with non-

transfected mice, the animals experienced 40 trials per session, whereas transfected mice were exposed to 15-20 trials per session with optogenetic intervention in order to limit potentially more long-term network alterations as a result of prolonged optogenetic silencing of glutamatergic VTA neurons. Behavioural performance during tone trials was quantified using the ratio of dispenser approaches in both LED conditions and computing a preference score as the ratio of tone trials with approach response in set 2 over those in set 1, minus 1. A schematic of the behavioural task setup can be seen in chapter 3 (Fig. 7). Positive scores indicate that mice approached the correct (sucrose-delivering) dispenser in set 2 more frequently.

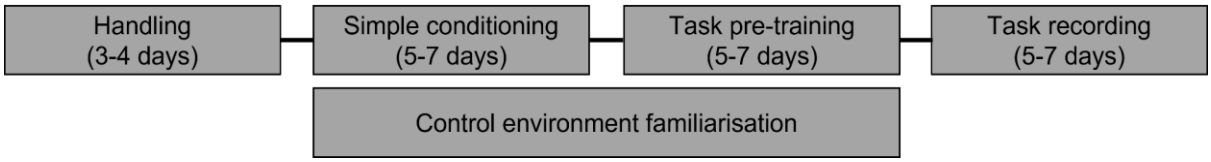

Fig. 4 Training protocol.

Mice were first handled for 3-4 days before undergoing a simple conditioning paradigm. Subsequently, mice were trained for 5-7 days on the behavioural task, before proceeding to the recording stage (5-7) days. During the entirety of the pre-training phase, animals would also be familiarised with the control enclosure.

2.4. Multichannel data acquisition and position tracking

The extracellular signals from the electrodes were amplified, multiplexed, and digitized using a single integrated circuit located on the head of the animal (RHD2164, Intan Technologies; gain x1000). The amplified and filtered (0.09 Hz to 7.60kHz) electrophysiological signals were digitized at 20kHz and saved to disk along with the synchronization signals from the position tracking. To track the location of the animal, three LED clusters were attached to the electrode casing and captured at 25 frames

per second by an overhead color camera using positrack (https://github.com/kevin-allen/positrack).

2.5. Spike detection and unit isolation

For the offline detection of spikes, the recorded signals were first band-pass filtered (800 Hz to 5 kHz). Spikes were then detected based on the power (root-mean-square) of the filtered signal calculated in 0.2-ms sliding windows. Detected spikes of the individual electrodes were combined per tetrode. To isolate spikes belonging to the same neuron, spike waveforms were first up-sampled to 40 kHz and aligned to their maximal trough (Jozsef Csicsvari et al. 1998). Principal component analysis was applied to these waveforms ±0.5-ms from the trough to extract the first three or four principal components per channel, such that each individual spike was represented by 12 waveform parameters. An automatic clustering program (KlustaKwik, http://klusta-team.github.io) was run on this principal component space and the resulting clusters were manually recombined and further isolated based on cloud shape in the principal component space, cross-channels spike waveforms, auto-correlation histograms and cross-correlation histograms (K. D. Harris et al. 2000; Kadir, Goodman, and Harris 2014). All sessions recorded on the same day were concatenated and clustered together. Each cluster used for further analysis showed throughout the entire recording day stable cross-channels spike waveforms, a clear refractory period in its auto-correlation histogram, well-defined cluster boundaries and an absence of refractory period in its cross-correlation histograms with the other clusters. I further used an automated clustering pipeline using Kilosort (https://github.com/cortex-lab/KiloSort) (Pachitariu et al. 2016) via the SpikeForest sorting framework (https://github.com/flatironinstitute/spikeforest) (Magland et al. 2020). To apply

KiloSort to data acquired using tetrodes, the algorithm restricts templates to channels within a given tetrode bundle, while masking all other recording channels. The resulting clusters were manually curated to check all clusters and remove spurious cells using metrics derived from the waveforms and spike times, and then verified by the operator. This procedure was cross-validated using several data sets and verified against manual curation, by computing confusion matrices to validate that clusters obtained automatically were also obtained with the previous method.

2.6. Statistics on recorded neurons

In total, this study includes n=4,364 neurons (169,168 co-firing pairs): 1,191 neurons from 5 mice without optogenetic interventions (71.8±2.7 neurons per mouse per day: 16.9±1.3 PFC; 9.6±0.7 NAc; 8.3±0.8 Amy; 21.6±1.1 CA1; 15.4±1.7 VTA); n=949 neurons from 2 Vglut2^{VTA}::ChR2-eYFP mice with 473-nm VTA light delivery (73.0±3.6 neurons per mouse per day: 18.4±1.5 PFC; 12.4±1.4 NAc; 15.3±1.9 Amy; 21.6±1.9 CA1; 5.2±0.8 VTA); n=945 neurons from 3 Vglut2^{VTA}::ArchT-GFP mice with 561-nm VTA light delivery (mean±SEM neurons per mouse per day: 17.1±3.1 PFC; 5.4±0.8 NAc; 5.6±0.7 Amy; 22.1±1.6 CA1; 12.7±2.3 VTA); n=882 neurons from 2 Vglut2^{VTA}:: GFP-only control mice (mean±SEM neurons per mouse per day: 17.7±1.5 PFC; 12.1±1.6 NAc; 8.5±1.7 Amy; 23.5±1.9 CA1; 11.5±1.7 VTA); n=397 neurons from DAT^{VTA}::ChRh2-eYFP mice (mean±SEM neurons per mouse per day: VTA=39.7±3.9).

2.7. Single-neuron firing modulation by task variables & response score

To determine the firing response to a given task variable (LED, tone, ‘decision point’ or dispenser outcome), the average firing rate of each neuron was calculated in the

100-msec time bins that spanned a ±5 sec window centered on either the onset of a given sensory cue (i.e., the TTL pulses activating a given LED or the tone presentation), the time bin corresponding to the 'decision point' in each tone-initiated trial (evaluated by the sudden change in animal's velocity towards the dispenser), or drop licking (detected using the IR beams at the dispenser spout). The traces were then standardised with respect to the standard deviation and mean of the 5 sec baseline preceding the event onset. From these standardised firing rate traces I obtained a 'response score' to a given behavioural task variable by taking the value of the bin with the largest absolute standardized firing rate (the modulation could be either negative or positive).

2.8. Decision point detection

The decision points were defined as the periods immediately preceding commencement of approach towards the dispenser and were heuristically estimated to be the last point in time at which the animal had zero velocity towards the dispenser before the arrival at that location.

2.9. Coactivity pattern detection and tracking: PCA/ICA method

Firing patterns of co-active neurons were detected using a statistical framework based on Independent Component Analysis (Lopes-dos-Santos, Ribeiro, and Tort 2013; van de Ven et al. 2016) (Fig. 5). Epochs of active exploration (speed above 2 cm/sec) before tone presentation in the task arena (i.e., outside tone-initiated trials, drop delivery and laser activation) or in the control enclosure as appropriate, were divided into 25-ms time-bins and the spikes discharged by every neuron in each bin was

counted. To avoid biasing the identification of coactivity patterns toward spike-trains of neurons with higher firing rates, the binned spike-counts were standardised for each neuron by a *z*-score transformation:

$$z_{i,b} = \frac{x_{i,b} - \mu_{x_i}}{\sigma_{x_i}}$$

where $x_{i,b}$is the spike-count of neuron in bin *i, b* and $\boldsymbol{\sigma}_{\text{xi}}$ and are respectively the mean and standard deviation of neuron *i* 's spike-counts across bins. This allows the normalized activity of each principal neuron to have null mean rate and unitary variance. With the numbers *n* of simultaneously recorded neurons and *B* of time-bins, the neuronal population activity was represented by *Z* as the *n x B* binned and *z*-scored spike-count matrix with element *(i,b)* equal to $Z_{i,b}$. The coactivity patterns embedded within matrix *Z* were then extracted in a two-step procedure (Lopes-dos-Santos, Ribeiro, and Tort 2013; Van de Ven et al. 2016). First, the number of significant patterns was estimated as the number of principal components of the activity matrix with variances above a threshold $\boldsymbol{\lambda}_{max}$ derived from an analytical probability function for uncorrelated data (Marcenko-Pastur distribution). Second, independent component analysis was applied to extract patterns from projection of the data into the subspace spanned by the significant principal components. Each coactivity pattern was thus captured by an independent component. Since the corresponding weight vector was typically asymmetrical, the direction where weights were highest was assigned positive weights. Detected coactivity patterns consisted of a few neurons with high weights and a larger group of neurons with weights around zero. For each pattern, I refer to neurons with weight exceeding the mean weight by two standard deviations (with both mean and standard deviation calculated from only the weights of that pattern) as members of the same “cell assembly” (mean of 5.1±0.1 % member

neurons per pattern from an average of 71.8±2.7 neurons recorded per day). Note that this definition of “cell assembly” is used for an intuitive way of interpreting and discussing the results presented in this study. Importantly, all analyses were performed directly on the patterns themselves (i.e., using the weight-vectors formed by the contribution of all simultaneously recorded neurons defining matrix *Z*, unless stated otherwise. I detected a total of 230 coactivity patterns: 78 in sessions without light-delivery, 81 in sessions with light-delivery in Vglut2^{VTA}::Arch-T mice, and 71 in sessions with light-delivery in Vglut2^{VTA}::GFP-only control mice.

The activation strength *A* of each coactivity pattern at time *t* was computed as:

$$A_t = Z_t^T P Z_t$$

where Z_t is the population vector carrying the z-scored instantaneous firing rate of each neuron at time *t*, *P* is the projection matrix of the corresponding independent component constructed from the outer-product of its weight vector, and *T* is the transpose operator. A_t is therefore the squared projection of Z_t onto the component that represents the coactivity pattern. This projection represents the similarity between the independent component (representing all neurons recorded on that day) and the population rate at a given 25-msec time bin. The main diagonal of *P* was set to zero before calculating A_t, in order to eliminate the contribution of single neurons to the coactivity pattern strength. The resulting value of A_t reflected expression strength of a particular coactivity pattern. With this approach, only co-firing of neurons can contribute towards the expression of a given pattern, which strength at any time point does also not reflect the number of (“member”) neurons with the highest contribution to that pattern but rather the entire weight vector representing all neurons.

In the case of cross-structural assembly patterns, manipulation of *P* offers access to the individual co-firing pairs between different regions. As *P* represents the co-firing between identified pairs of neurons, this allows for analytical selection of a given set of co-firing pairs (i.e., neurons within a given brain region or between two regions) by setting the remaining values of *P* to 0. Using this approach, which I refer to as 'masking', I isolated within-region, between-region and PFC-NAc-CA1-Amy co-activation strength (whilst ignoring all possible co-firing pairs involving VTA). Similarly, this allowed us to extract co-firing activity of all cross-structural co-activity pairs involving any chosen anchor region, such as VTA-PFC, VTA-NAC, VTA-NAc, VTA-CA1 co-activity (in this example with VTA being the anchor region). The mean coactivation rate was: 0.13±0.01 Hz.

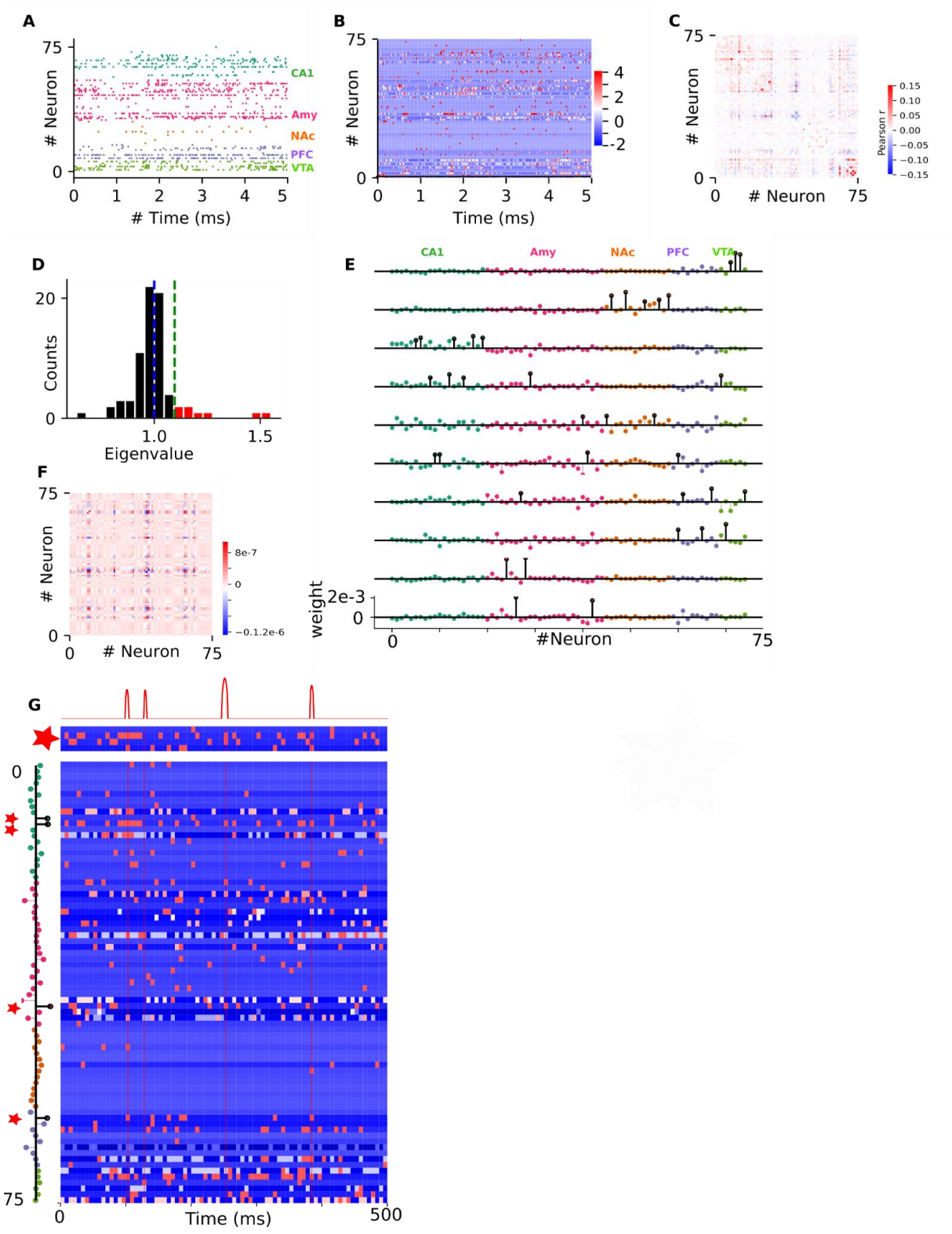

Fig. 5 Detection of co-activation patterns and tracking of expression strength over time.

The different steps to identify neuronal co-activation patterns are illustrated for 75 simultaneously recorded neurons from CA1, Amy, NAc, PFC and VTA (A). After binning (25 ms time bins) and normalizing (z-score) each neuron's spike counts (B), principal component analysis (PCA) is applied to the resulting correlation matrix (C) of the binned (and z-scored)

spike count matrix to find the number of patterns describing statistically significant co-activations between neurons, as estimated by the number *n* of eigenvalues exceeding the Marcenko-Pastur threshold λ_{max} (D; blue dotted line indicates mean, green dotted line indicates λ_{max}). Independent component analysis (ICA) is then used to identify *n* assembly patterns, which are defined as weight vectors indicating the contribution of each neuron to that pattern (E). For each pattern, neurons with a high contribution (i.e., weight exceeding two standard deviations above the mean) are colored black for display purpose. Please note that several assemblies have neurons with high contributions in different brain regions. Tracking of assembly pattern expression strength: For each assembly pattern, a projection matrix *P* is constructed by taking the outer product matrix of its weight vector and setting the diagonal to zero. The latter step ensures that only co-activations but not single neuron activity can contribute to the expression of an assembly pattern (F). (G) The assembly pattern expression strength over time is then calculated by projecting the z-scored spike trains onto the projection matrix (expressed as the quadratic form of the projector matrix with the z-scored spike trains). The magnitude of the expression strength can thus be interpreted as projected z-scores onto the weight vector of the assembly pattern. The red stars indicate neurons that strongly contributed to the assembly pattern (above two standard deviations of the mean of the assembly vector). For visualisation purposes, these neurons are shown again on top of the main matrix. Every time these cells fire together, the assembly strength increases. The assembly strength is shown as the red line in the very top of the panel. Please note, that neurons have been sub-selected for visualisation purposes only. All other calculations are performed on the entire assembly vectors.

2.10. Response properties of assembly neurons

Within one assembly, every neuron was assigned a feature vector describing its firing rate responses to the different task elements based on the response scores obtained for every task element for both task sets ($LED_{sucrose}$, $LED_{quinine}$, $Tone_{sucrose}$, $Tone_{quinine}$, $decision\ point_{sucrose}$, $decision\ point_{quinine}$, $Drop_{sucrose}$, $Drop_{quinine}$) weighted by the neuron's contribution to the assembly weight vector. I then computed the average cosine similarity between all feature vectors corresponding to one assembly (Fig. 6). The cosine similarity is a measure for how similar two vectors of equal length are. The metric is bounded between -1 and 1, whereby negative values signal dissimilarity and positive values similarity. For each pairwise cosine-similarity I compared it to the corresponding null-distribution. To obtain the null-distribution, I applied a shuffling procedure to the feature vectors whilst keeping the assembly weights constant (i.e. the response scores were shuffled across the population). This way it is only the

neuron's response profile that is randomised whilst assembly structure remains the same. Importantly, I noticed that for many neurons the response score during the same task element between the two contingencies can be correlated (e.g. the response to the tone during the sucrose condition may be similar to the response during quinine condition). To preserve this correlation in our shuffling procedure, task elements within the same response category were shuffle together (i.e. quinine and sucrose response scores to a given task element were always taken as a pair together from a randomly selected VTA cell). It is important to note that this method likely inflates cosine similarity between neurons (for both, shuffled and original assemblies), since most weights in assembly vectors are close to zero and hence so are the feature vectors weighed by them.

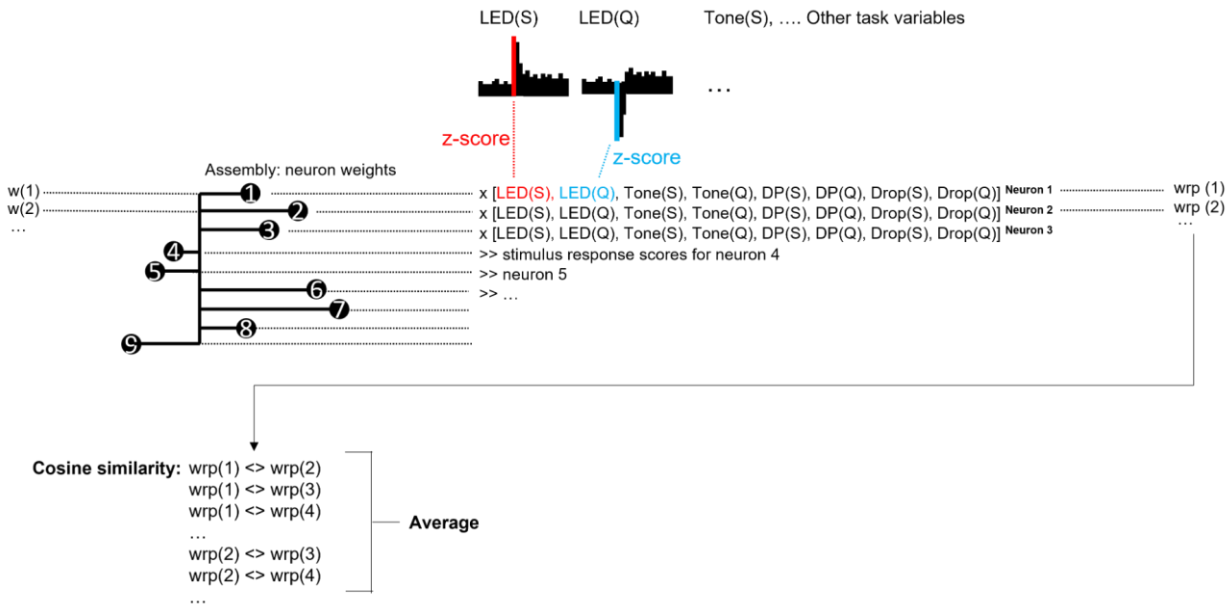

Fig. 6 Computation of assembly modality scores.

For every cell a vector containing the maximum absolute z-scored bin value (in 100 ms bins) of a response PSTH is created. For any given assembly, this vector is multiplied by the same cell's assembly weight. Subsequently, the cosine similarity (a measure of how similar two vectors are) between all possible cell pairs is computed and averaged for a given assembly.

2.11. Task-cue set decoding based on assembly time course or single-unit firing rates

To determine the relationship between the activation strength of co-activity patterns to the task-set animals were currently experiencing I used Gaussian Naive Bayes classifiers as implemented in Python's scikit-learn package (https://scikit-learn.org/stable/modules/naive_bayes.html). During each "on-trial" period, I trained a Naïve Bayes classifier to discriminate between the task-cue set 1 and set 2 on a trial-by-trial basis. I used the first four principal components of the activation time course of coactivity patterns in time windows from tone onset until the drop was removed as input features. As control time-windows, I used equivalent time periods directly prior to the tone. For single-VTA neuron decoding, 100-msec binned spike counts during the tone-initiated trial period were used. For each assembly activation time course (or spike train) a new classifier was trained. Uniform priors were used throughout. The performance of the classifier was assessed using 5-fold cross-validation (Ojala and Garriga 2009). In k-fold cross validation the test and training data are split into k (in our case $k=5$) equally sized parts parts (folds) with $k-1$ training folds and one test fold. The classifier is then sequentially trained on all possible combinations of test/train folds and the average classifier performance is then computed. This way, class imbalances and effects of sampling biases in the training splits are minimised. Classifier performance was assessed using the accuracy score, which is defined as the ratio of correctly classified observations out of all observations.

2.12. VTA neuron clustering based on task-related responses and electrophysiology

Clustering procedure: unsupervised clustering for the detection of groups of VTA neurons responding similarly to behavioural variables as well as for the identification of different cell-types based on electrophysiological signatures was performed using hierarchical agglomerative clustering (Hastie, Tibshirani, and Friedman 2001; Ward 1963). This algorithm seeks to build a hierarchy of clusters using the agglomerative (i.e. bottom up strategy), in which each single observation is initially its own cluster. These are then merged together using a linkage criterion until all clusters form a hierarchical tree, which can be expressed as a dendrogram (Fig. 9 C). Linkage can be stopped based on an externally defined threshold. For linkage, Ward's variance minimisation criterion as a linkage method, which minimises overall within-cluster variance (Ward 1963). Optimal cluster numbers have been estimated using the silhouette score (Rousseeuw 1987), Calinski-Harabasz score (Caliński and Harabasz 1974) and cluster distances obtained from the agglomerative hierarchical clustering process. The silhouette score is defined as the difference between the mean intra-cluster distance *x* and the mean nearest-cluster distance *y* for each sample divided by the overall maximum *x* and *y*. The higher the score, the better the clustering. The Calinski-Harabasz-score is defined as the ratio between the within-cluster variance and the between-cluster variance. A higher score indicates better clustering.

Cross-validation with ground truth: in order to assign a neurotransmitter identity to clusters obtained hierarchical agglomerative clustering, a linear-discriminant analysis classifier (LDA; from Python's scikit-learn implementation) was trained to learn the feature-cluster relationship with the (non-opto-tagged) neurons used for agglomerative hierarchical clustering. Subsequently, ground-truth neurons (i.e. opto-tagged VTA

cells expressing Vglut2 and DAT, please see below) neurons were transformed into the same feature space as non-opto tagged neurons and then assigned a cluster using the already trained LDA classifier. The LDA classifier is based on linear combinations of the features that best separate the different classes and produces a linear decision boundary (Fisher 1936).

Features: for spike wave form clustering I upsampled the raw spike wave form of the tetrode with the largest spike amplitude (peak to trough) to 80 kHz, applied a gaussian kernel for smoothing (sigma = 0.5 standard deviations) and centered the trough on zero. Spikes for the inter-spike interval (ISI) distributions were taken from periods of exploration (> 2cm/sec) of a familiar environment.

2.13. In vivo light delivery for optogenetic interrogations

In order to optogenetically identify glutamatergic and dopaminergic neurons in the VTA, a 473nm diode-pumped solid-state laser (Laser 2000, Ringstead) was used to deliver trains of 20 ms-long blue light (~15 mW) pulses to the VTA of either Vglut2-Cre or DAT-Cre mice injected in the VTA with a AAV vector encoding Channelrhodopsin-2 (ChR2) fused to the enhanced yellow fluorescent protein (eYFP) under the control of a Cre-dependent EF1a promoter (from Karl Deisseroth, AAV2-EF1a-DIO-hChR2(H134R)-eYFP-WPRE, 2.5E12 vg/mL, UNC Vector Core). In VGlut-Cre mice, tetrodes and optic fiber were placed -3.25 anteroposterior from bregma, ±0.4 mm lateral from bregma, and an initial -3.85 mm ventral from the brain surface. For DAT-Cre animals, tetrodes were located within 0.5 mm from the optic fiber. For the VTA targeted optic fiber the implant was positioned at a 40 degree angle from the antero-posterior axis on the horizontal plane and then at an angle of 10 degrees from the

dorso-ventral axis. The optic fiber was positioned at 2.7 mm posterior and 1 mm lateral from bregma and lowered into the brain at the angle described at a distance of 3.9 to 4.2 mm. This way, the tetrode placement was optimised for the respective target population of VTA neurons: for glutamatergic VTA neurons, tetrodes were positioned more medially, whereas for dopaminergic VTA cells, tetrodes were more lateral. A total of 700 laser pulses were delivered with an interval of 8 ± 2.5 s between each pulse. For the identification of opto-tagged cells, I binned spike trains around the laser onset in ±50 ms within 2ms bins to ensure robust PSTHs. I then considered only those cells opto-tagged if any of the first two bins following laser onset exceeded two standard deviations of the mean of the pre-laser period. The laser-response latencies of these neurons were subsequently validated by determining the latency to the first spike following the laser onset. Opto-tagged cells were identified on the basis of a firing rate increase within the first teo In order to evaluate the effect of glutamatergic VTA neuronal spiking on spiking activity in PFC, NAc, Amy, dCA1 and other VTA neurons, the same 473 nm laser was used to deliver blue light pulses (20 ms-long with probabilistic inter-pulse intervals of 6-10 sec) to the VTA of Vglut2-Cre injected with AAV2-EF1a-DIO-hChR2(H134R)-eYFP-WPRE viral vector. In order to optogenetically silence glutamatergic VTA neurons, a diode-pumped solid-state laser (Laser 2000, Ringstead) was used to deliver yellow (561nm) light pulses (~9–11mW) bilaterally to VTA of Vglut2-Cre mice injected in the VTA with an AAV vector encoding Archaerhodopsin-T (ArchT) fused with the green fluorescent protein (GFP) under the control of a Cre-dependent CAG promoter (from E.S. Boyden; AAV2-CAG-flex-ArchT-GFP, 2.0E12 vg/mL, UNC Vector Core). Glutamatergic VTA neurons were silenced for the time of the tone until the drop was removed, using random onsets and offsets to activate the laser 0.5-2.5s prior to tone onset (and avoid possible conditioning

effects to tone onset itself) and inactivating the laser at the end of drop availability plus-minus 0.5-2.5s. In these silencing experiments, coactivity patterns were only detected during the off-trial epochs, as in non-optogenetic experiments, and discarding any windows with active laser just preceding tone.

2.14. Anatomy

To confirm viral transduction, injected mice were deeply anaesthetised with isoflurane/pentobarbital and transcardially perfused with PBS followed by cold 4 % PFA and 0.1 % glutaraldehyde dissolved in PBS. The brains were extracted and sliced into 50 µm thick coronal sections. The sections were rinsed extensively in PBS with 0.25 % Triton X-100 (PBS-T) and blocked for 1 h at room temperature in PBS-T with 10 % normal donkey serum (NDS). Sections were then incubated at 4°C for 48 h with primary antibodies (chicken anti-GFP, 1:1000, Aves Labs, cat# GFP-1020, RRID: AB_10000240; guinea pig anti-TH, 1:2000, Synaptic Systems, cat# 213-104, RRID: AB_2619897; rabbit anti-Vglut2, 1:1000, Synaptic Systems, cat# 135-403, RRID: AB_887883) diluted in PBS-T with 3 % NDS ("blocking solution”). After that, sections were rinsed three times for 10 min in PBS and incubated for 24 h at 4°C in secondary antibodies (donkey anti-chicken Alexa Fluor 488, 1:500, Jackson ImmunoResearch, cat# 703-545-155, RRID: AB_2340375; donkey anti-guinea pig Cy3, 1:1000, Jackson ImmunoResearch, cat# 706-165-148, RRID: AB_2340460; donkey anti-rabbit Alexa Fluor 647, 1:500, Jackson ImmunoResearch, cat# 711-605-152, RRID: AB_2492288) diluted in PBS-T with 1 % NDS. This step was followed by three rinses for 15 min in PBS. Sections were then incubated for 1 min with 4',6-diamidino-2-phenylindole (DAPI; 0.5 µg/ml, Sigma-Aldrich, cat# D8417) diluted in PBS to label cell nuclei, before undergoing three additional rinse steps of 10 min each in PBS. Sections were finally

mounted on slides, cover-slipped with Vectashield mounting medium (Vector Laboratories) and stored at 4 °C. Images were acquired on a laser scanning confocal microscope (LSM 880/Axio Imager, Zeiss).

2.15. Statistical analyses

Data were analysed in Python 3.6 and using the packages DABEST (Ho et al. 2019), scikit-learn, SciPy, NumPy, pandas and tensortools for assembly detection using tensor-component-analysis (Williams et al. 2018). Throughout the manuscript, I use Gardner-Altman plots (to compare 2 groups) and Cumming plots (for more groups) from the *Data Analysis with Bootstrap-coupled ESTimation* (*DABEST*) statistical framework to assess, beyond P values, the significance of changes between groups (Ho et al. 2019). Notably, these DABEST plots allow visualizing the effect size by plotting the data as the mean difference between one of the groups (the left-most condition of each plot, used as group-reference) and the other groups (to the right, along the x-axis of each plot). For each estimation plot: (*i*) the upper panel shows the distribution of raw data points for the entire dataset, superimposed on bar-plots reporting group mean±SEM; and (*ii*) the lower panel displays the difference between a given group and the (left-most) group-reference, computed from 5,000 bootstrapped resamples and with difference-axis origin aligned to the mean of the group-reference distribution, with *black-dot*: mean; *black-ticks*: 95% confidence interval; *filled-curve*: bootstrapped sampling-error distribution. In addition, I used *t-test* and *ANOVA* to compare conditions following a normal distribution with similar dispersion; or *Mann-Whitney U test* and *Kruskal-Wallis* tests otherwise.

3. CHAPTER 3: BEHAVIOURAL RELEVANCE AND DIVERSITY OF SINGLE UNIT ACTIVITY IN VTA

3.1 Introduction

As outlined in the introductory chapter, VTA neurons are thought to be involved in processing positive and negative sensory cues and a broad range of behavioural aspects (Schultz 2002; Brischoux et al. 2009; Berridge 2007). Moreover, in real life situations these processes often rely on the integration of multiple sources of information from different sensory modalities. This consideration motivated the following first goal addressed in this chapter:

(i) Characterisation of the diversity of single unit responses to behavioural and sensory variables in the VTA.

Previous studies have reported that dopaminergic neurons are involved in processing both, appetitive (Bromberg-Martin, Matsumoto, and Hikosaka 2010; Cohen et al. 2012; Schultz, Dayan, and Montague 1997) and aversive stimuli (Aston-Jones and Moorman 2009; Matsumoto and Hikosaka 2009). A landmark study showed that dopaminergic and GABAergic neurons respond with firing rate changes to reward using optogenetic tagging (Cohen et al. 2012). The authors revealed that while dopaminergic neurons show phasic excitation upon conditioned stimuli and the receipt of reward, GABAergic cells show prolonged increases in firing rates during reward. Interestingly, Cohen et. al identified a third class of VTA neurons that responded with a decrease in firing activity during reward outcomes. Similarly, another study reported three distinct VTA cell clusters based on the spike waveform and ascribed neurotransmitter identities to two of those clusters using pharmacological means (dopaminergic and GABAergic)

(Fujisawa and Buzsáki 2011). However, both studies have not characterised the molecular identity of said third cluster.

Several studies investigated whether there is a relationship between molecularly defined VTA cell types and behavioural parameters. For instance, while stimulation of glutamatergic VTA cell somata causes appetitive behaviour via excitation of neighbouring dopamine neurons (H.-L. Wang et al. 2015), strikingly optogenetic activation of glutamatergic VTA fibres to NAc or the lateral habenula appears to be related to aversive behaviour (Qi et al. 2016; Root, Mejias-Aponte, Qi, et al. 2014). While initial studies suggested that possibly both cell types are involved in different aspects of behaviour, recent work paints a more complicated picture in which one subset of the glutamatergic VTA cell population responds to aversive stimuli, but another subset signals salience (Root, Estrin, and Morales 2018). Consistently, glutamatergic VTA neurons signaling does not seem to be restricted to aversive stimuli as silencing glutamatergic VTA axons projecting to CA1 prevent the retrieval of conditioned place preference (Han et al. 2020) and in fact, the role of glutamatergic VTA neurons in approach and aversion may depend on the VTA neuron subpopulation in question (Montardy et al. 2019).

In order to be able to ascribe certain representational correlates to different cell types, one needs to be able to reliably discern them. Traditionally, the average firing rate (2-10 Hz), the spike width (> 2.2 ms) or spike waveform (biphasic positive to negative deflection, wide spike waveform) (Ungless and Grace 2012) have been used to isolate dopaminergic from non-dopaminergic cells in extracellular single unit recordings. However, there has been growing skepticism about the reliability of purely electrophysiological markers to identify dopaminergic neurons in the VTA. Traditional

heuristics to identify dopamine neurons are based on parameters derived from cyto-histochemical, pharmacological and electrophysiological studies in the substantia nigra (Guyenet and Aghajanian 1978; Grace and Bunney 1980; Grace and Onn 1989), which do not appear to be readily applicable to VTA neurons (Margolis, Lock, Hjelmstad, et al. 2006). Furthermore, cytohistological and electrophysiological studies provide evidence for the existence of non-dopaminergic VTA cell types with properties previously assumed to be confined to dopaminergic cells (Johnson and North 1992b; Margolis, Lock, Chefer, et al. 2006). This hints towards a considerable functional as well as phenotypic heterogeneity in VTA cells. With the advent of optogenetics, it has become possible to identify molecularly defined neuronal subpopulations in vivo (Fenno, Yizhar, and Deisseroth 2011) in freely behaving animals. By exploiting this technique, the second question I addressed is:

(ii) Do glutamatergic and dopaminergic VTA neurons respond differently to behavioural and sensory variables?

Lastly, in his cell assembly hypothesis, Donald Hebb suggested that memories are represented in the combined activity of individual neurons forming groups, which he termed ‘cell assemblies’ (Hebb 1949a). He postulated that the mechanism giving rise to such cell assemblies is repeated co-activity leading to strengthened synaptic connectivity between the cells firing together. Given the rich behavioural repertoire which the VTA is involved in, I hypothesised that complex behavioural events could be supported by the combined activity of multiple cells in the VTA. In this light, the last question addressed in this chapter is:

(iii) Are there behaviourally relevant co-firing assembly patterns within the VTA?

3.2 Behavioural results

I selected a behavioural task that would selectively engage different aspects and allow us to probe for those variables in neural recording. To this end, I established a behavioural task where mice experienced two sets of sensory cues that governed the aversive versus appetitive nature of an outcome (task-cue set 1 versus set 2; Fig. 7 A, B). In this task, mice explored an arena where an auditory cue signalled the delivery of a drop-solution at a liquid dispenser at the end of a 5-second tone (Fig. 7 C). The drop was made available immediately following the offset of the tone and was removed using a vacuum pump 5 seconds later (Fig. 7 A). Importantly, however, the identity of each tone-signalled drop was contingent on the concurrently active visual cue (Fig. 7 B). Namely, one of two LED wall-displays was associated with a bitter (quinine; task-set 1) solution, whereas the other LED was associated with a reward (sucrose; task-set 2) solution. The tone remained the same. The active LED was switched across task sets every 1 to 4 tones (average LED duration: 105.46±4.28 sec) at random points in time, with the constraint that the currently active LED was in the visual field of the animal to ensure the presence of the contextual reminder.

This behavioural task allowed us to probe for representations of space and context in CA1 (Wilson and McNaughton 1993; Leutgeb et al. 2005; O'Keefe and Dostrovsky 1971b), positive and negative conditioned stimuli Amy and VTA (e.g., conditioned auditory cues) (Ambroggi et al. 2008; Beyeler et al. 2016; Herry et al. 2008; Cohen et al. 2012; Kyriazi, Headley, and Paré 2020; Root, Estrin, and Morales 2018; Engelhard et al., 2019), decision-making in the PFC (Sul et al. 2010; Narayanan and Laubach 2006; Passecker et al. 2019) and cue-predicted reward outcomes in the NAc (Lansink et al. 2012; van der Meer and Redish 2009; Lavoie and Mizumori 1994).

In order to assess behavioural performance, I computed the probability of approaching the dispenser during one given task set. The animal's choice to approach the dispenser during one task set over the other is then summarised in a preference score defined as the ratio of approach probabilities for sucrose versus quinine minus 1 so that a positive preference score indicates sucrose preference.

Mice successfully learned to approach the dispenser during tone-initiated trials in task-cue set 2 to obtain the sucrose drop solution, avoiding the dispenser in task-cue set 1 trials where quinine was dispensed. I obtained 29 behavioural recording days from 5 mice. The approach ratio was 0.56±0.03 and 0.82±0.03 for task set 1 and 2, respectively. Accordingly, the preference score was 0.6±0.1 (n=5 mice; p=4.8e-3, paired t-test, Fig. 7 D, E, F). I obtained similar results when only considering the first trial of each block (n=5 mice, p=6.5e-3, paired t-test), indicating that animals indeed used LED-contextual cues to solve the task contingencies as opposed to other strategies relying on working memory of preceding trials (Fig. 7 J). Over time (i.e., recording sessions), there was no identifiable trend in the animal's performance (Fig. 7 G). I could not analyse pre-training data of the simple conditioning stage or the task pre-training stages as this data was not recorded. However, I noticed that animals returned to near chance level of performance in the beginning of every recording session, which then rapidly improved throughout the session (Fig. 7 H, I). This improvement was driven by the mouse progressively approaching the dispenser less during the quinine condition (Fig. 7 H). To assess whether neural responses during the task period could be due to speed modulation, I compared the animal running speed during the tone between the two conditions. I found no significant differences in running speed (p=0.16, paired t-test). Our results show that mice solved the task

ambiguity caused by the two overlapping sets of sensory cues, inferring the outcome of each tone presentation from the active LED on a trial-by-trial basis. Furthermore, mice return to a baseline level of performance each session and then rapidly improve throughout the recording session.

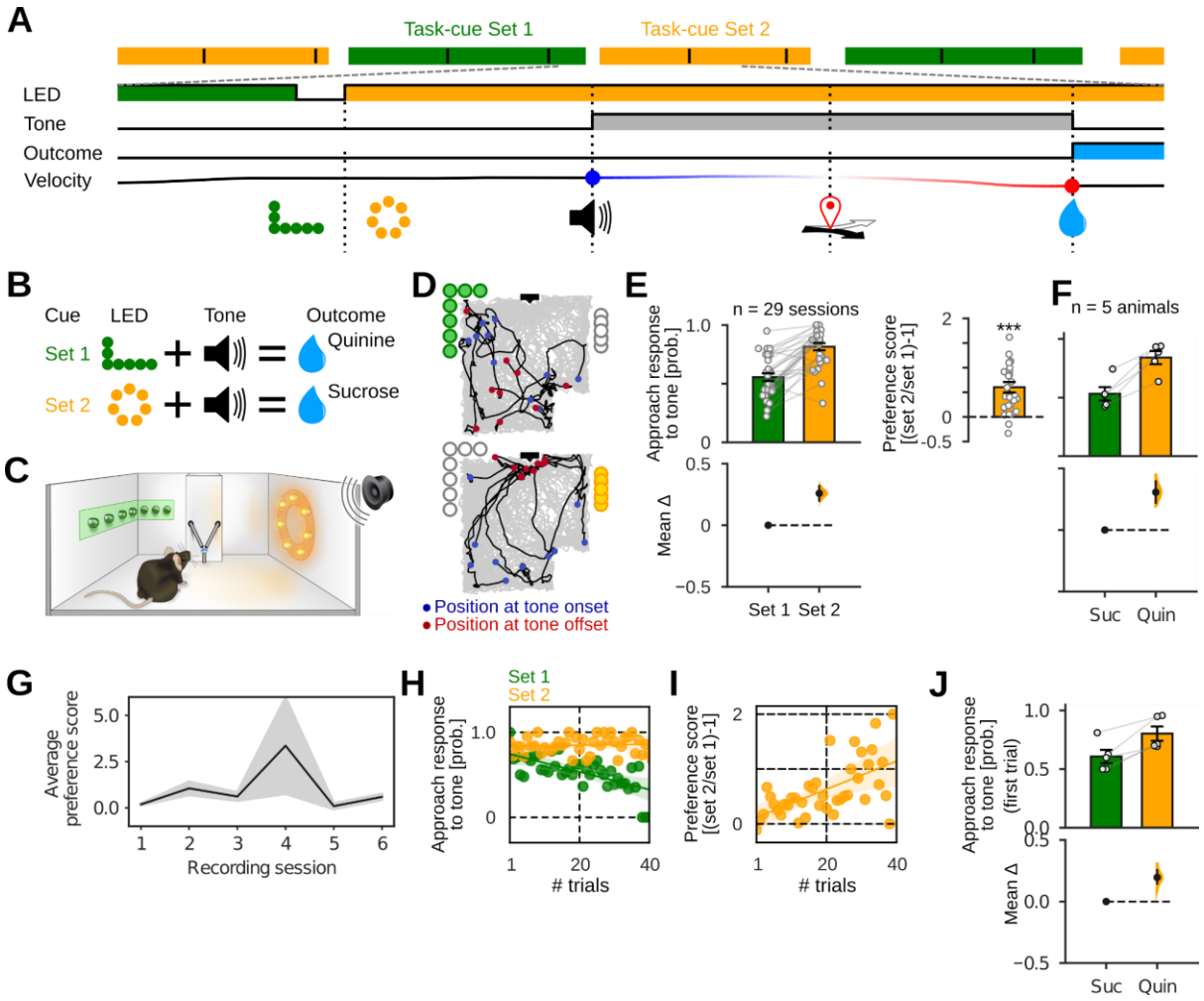

Fig. 7 Neuronal representations of task variables by distributed brain regions.

(A) Schematic illustrating the layout of the TTL pulses governing the presentation of the sensory cues (LED and tone) and the delivery of the outcome during the task. In addition, the animal's velocity was monitored to assess the behavioural "decision-making point" with respect to tone presentation. (B) Sets of sensory cues and outcomes defining multimodal task contingencies. (C) Open field task arena. (D) Example animal paths (black) during tone-initiated trials in task-set 1 (top) and task-set 2 (bottom). Each path is overlaid on the overall path (grey) for one session, with blue and red dots representing the animal's position at tone onset and offset, respectively. (E) Mice approached the dispenser during tone presentation in task-set 2 more than task-set 1. Left: Data Analysis with Bootstrap-coupled ESTimation (DABEST) plots (see methods) to visualize the effect size for behavioural performance across contingencies; top-left panel shows the ratio of trials with an approach response to tone over the total number of trials per set, with each pair of connected points showing tone-initiated

approach across sets on a given session; the bottom-left panel displays the across-set performance difference computed from 5,000 bootstrapped resamples, with difference-axis origin aligned to the mean of set 1 distribution; black-dot, mean difference; black-ticks, 95% confidence interval; orange-filled-curve: sampling-error distribution. Right: summary performance score as the ratio of approach in set 2 over set 1, minus 1; positive scores thus indicate that mice approached the dispenser in set 2 (sucrose) more frequently. Bar charts: mean±SEM. (F) Average behavioural performance for each mouse. The panel shows the ratio of trials with an approach response to the tone. (G) There is no visible trend in behavioural performance change over recording days. Behavioural performance is defined by preference for sucrose is shown as an average over mice from the first to the last recording day. (H) Within-session behavioural performance over time (trials). Each dot is the average over animals. Every day mice improve at not approaching the dispenser during the quinine condition. (I) Within-session improvement expressed as preference for sucrose approach. (J) Average behavioural performance for each mouse. The panel shows the ratio of trials with an approach response to the tone computed only from the first trial of each block.

3.3 Task related representational diversity of VTA single units

I next investigated the representation of task variables (LED, tone, decision point and liquid outcome) in the VTA with regards to firing rate changes. Firing rates were computed in 100-ms bins and z-scored using the mean and standard deviation of the baseline directly preceding the event onset. The decision points were defined as the periods immediately preceding commencement of the dispenser approach in the time interval between tone onset and before the drop was removed for sucrose and quinine trials alike. Visual examination of single-cell examples reveals a strong heterogeneity in responses to the task variables (Fig. 8). VTA cells increased and decreased firing rates in response to all task events and notably, neurons responded to more than one task event, often exhibiting positive, negative, biphasic or a combination of those directionalities of firing rate changes.

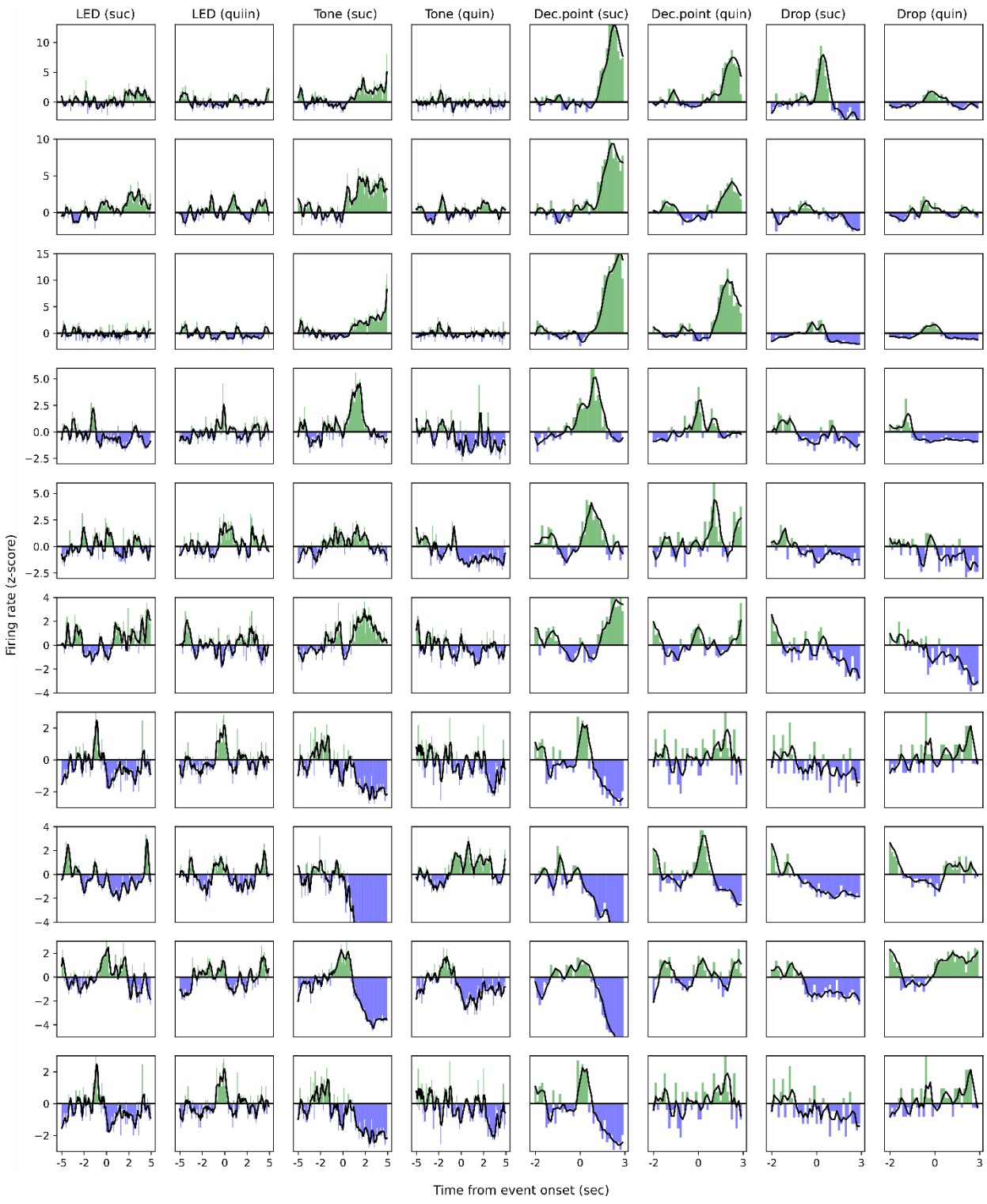

Fig. 8 Single cell responses to task events in the VTA.

Each row corresponds to one cell and contains the responses to the different events of the task split by the different task sets (From left to right: LED-sucrose, LED-quinine, Tone-sucrose, Tone-quinine, decision point-sucrose, decision point-quinine, drop-sucrose, drop-quinine). Blue shading indicates negative and green shading means positive modulation relative to the time period directly preceding the onset of the event.

I next attempted to extract groups of neurons that would exhibit similar response properties by applying an unsupervised clustering framework (hierarchical clustering, see chapter 2.13). For each neuron, the feature vector was constructed containing the first three principal components to each of the z-scored average time courses of the task events described above (Fig. 8). This way, the temporal dynamics of the response are taken into account and each task event is weighted equally in the clustering process. Neurons with zero standard deviation during the baseline period were excluded from the analysis to avoid divisions by zero for the standardisation relative to baseline (total of 30 cells). This means that neurons that were silent before the event and fired only afterwards are excluded. Physiologically speaking these neurons are likely to carry a significant amount of biologically relevant information as spikes after silence can be particularly informative. These cells could possibly have formed a separate cluster in our analysis. I estimated the optimal cluster number to be 5 based on a minimization of inter-cluster variance (Ward 1963) as can be seen in the dendrogram (Fig. 9 C, see chapter 2.13 for methods). However, alternative methods to determine the optimal cluster number such as the silhouette score (Rousseeuw 1987) and the Calinski-Harabasz score (Caliński and Harabasz 1974) suggested an optimal split at two clusters (Fig. 9 A, B). While this may be mathematically true (optimal separation of two data clouds), this does not necessarily reflect biologically meaningful clustering, since several clearly distinct clusters can be identified when splitting the data into more groups, as I did here. In fact, if separating the data in only two clusters, the resulting grouping reflects cells that respond to the task variables in any detectable way versus the ones that do not (Fig. 10). I reasoned that this likely biologically not the most sensible solution, since this would severely limit the repertoire of information that can be transmitted by VTA cell firing. Notably, the dendrogram as

well as Ward's method and the silhouette score indicated a somewhat poor separation of the clusters suggesting that response variability in the VTA may form a continuum (Fig. 9 Hence, I decided to break the data into 5 clusters in order to reveal response properties that would otherwise be hidden in the average. While alternative approaches, such as manifolds or linear models could be considered to model such a potential continuum, a separation into distinct clusters allows for a visual inspection of the response profiles of different clusters. Visual inspection of the obtained clusters confirms that the clustering procedure successfully extracted prominent features in response magnitude, directionality, temporal dynamics, and response conjunctions across multiple different stimuli (Fig. 11). Please note that the assignment of dopaminergic versus glutamatergic cells in the figure below is addressed in section 3.4 of this chapter.

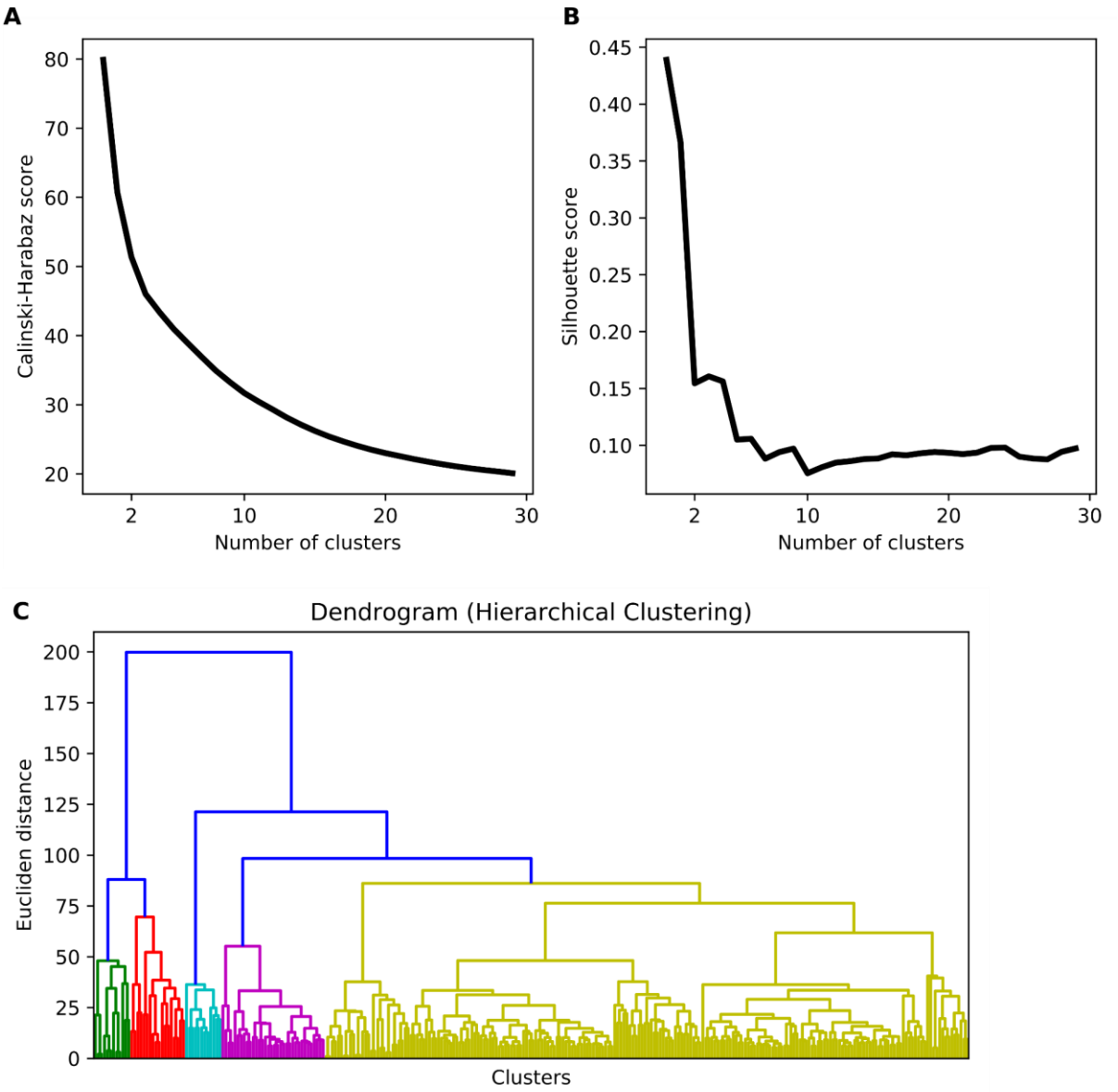

Fig. 9 Determining optimal cluster number for VTA cells based on firing rate responses to behavioural task variables.

(A) Calinski-Harabasz-score: the score is defined as the ratio between the within-cluster dispersion and the between-cluster dispersion. (B) Silhouette score: the score is defined as the difference between the mean intra-cluster distance (x) and the mean nearest-cluster distance (y) for each sample divided by the overall maximum x and y. (A, B). The higher the score, the better defined and further apart the clusters are. Hence, a peak in the score indicates the theoretical optimal cluster number. Beyond the initial peak at two, cluster separability declines rapidly as a function of cluster number indicating poor cluster separability. (C) Dendrogram for agglomerative hierarchical clustering. The tree has been constructed using Ward's variance minimisation criterion.The longer the vertical lines connecting two clusters are before they are joined, the better the cluster separation. All methods clearly indicate an optimal cluster separation at 2 clusters. Please note that the theoretically determined

optimal cluster number does not necessarily coincide with biologically meaningful clustering. The dendrogram indicates reasonable cluster distance at 5 clusters. To use five clusters, the cluster separation threshold (expressed in the Euclidean distance between the clusters) was lowered.

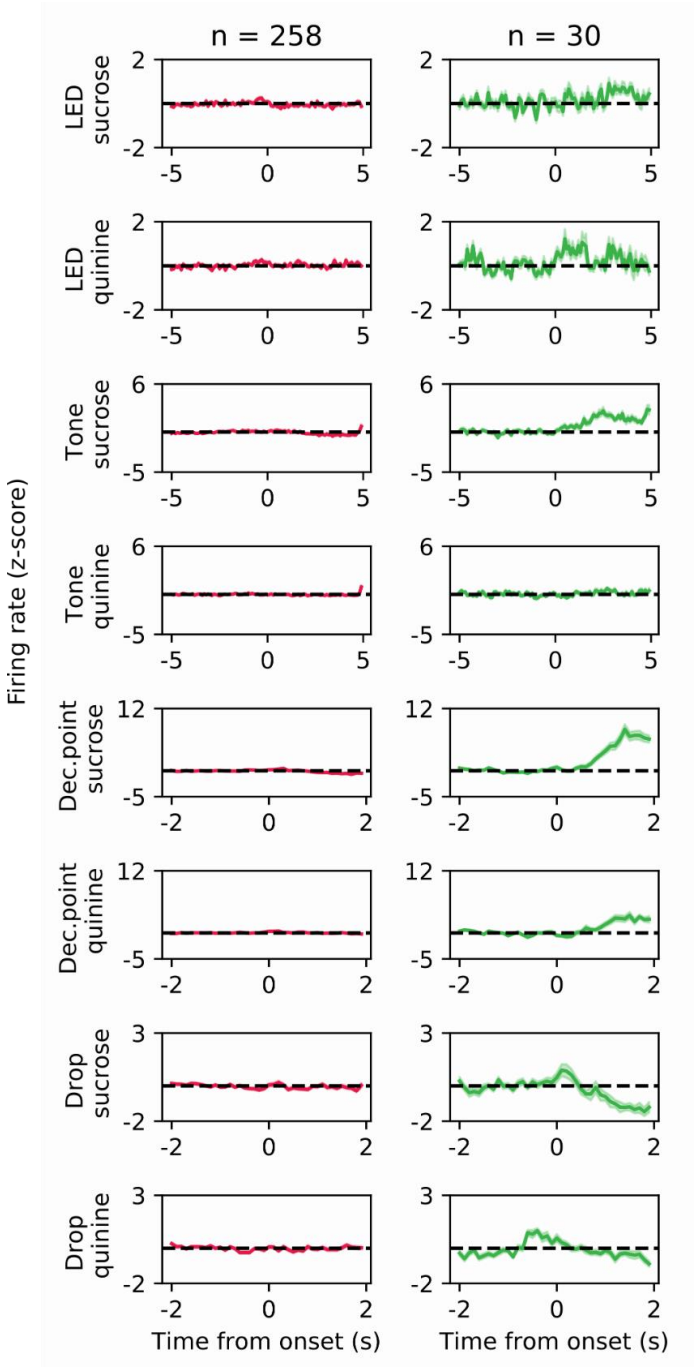

Fig. 10 Average firing rate responses to behavioural task variables of two main clusters.

Splitting VTA single neurons based on their standardised firing rate responses in two clusters, as suggested by mathematical methods to estimate the optimal cluster number (Fig. 9), results in one main cluster of cells that do not respond with firing rate changes to the measured task variables and one cluster that does.The traces are average firing rate responses with shaded areas indicating SEM.

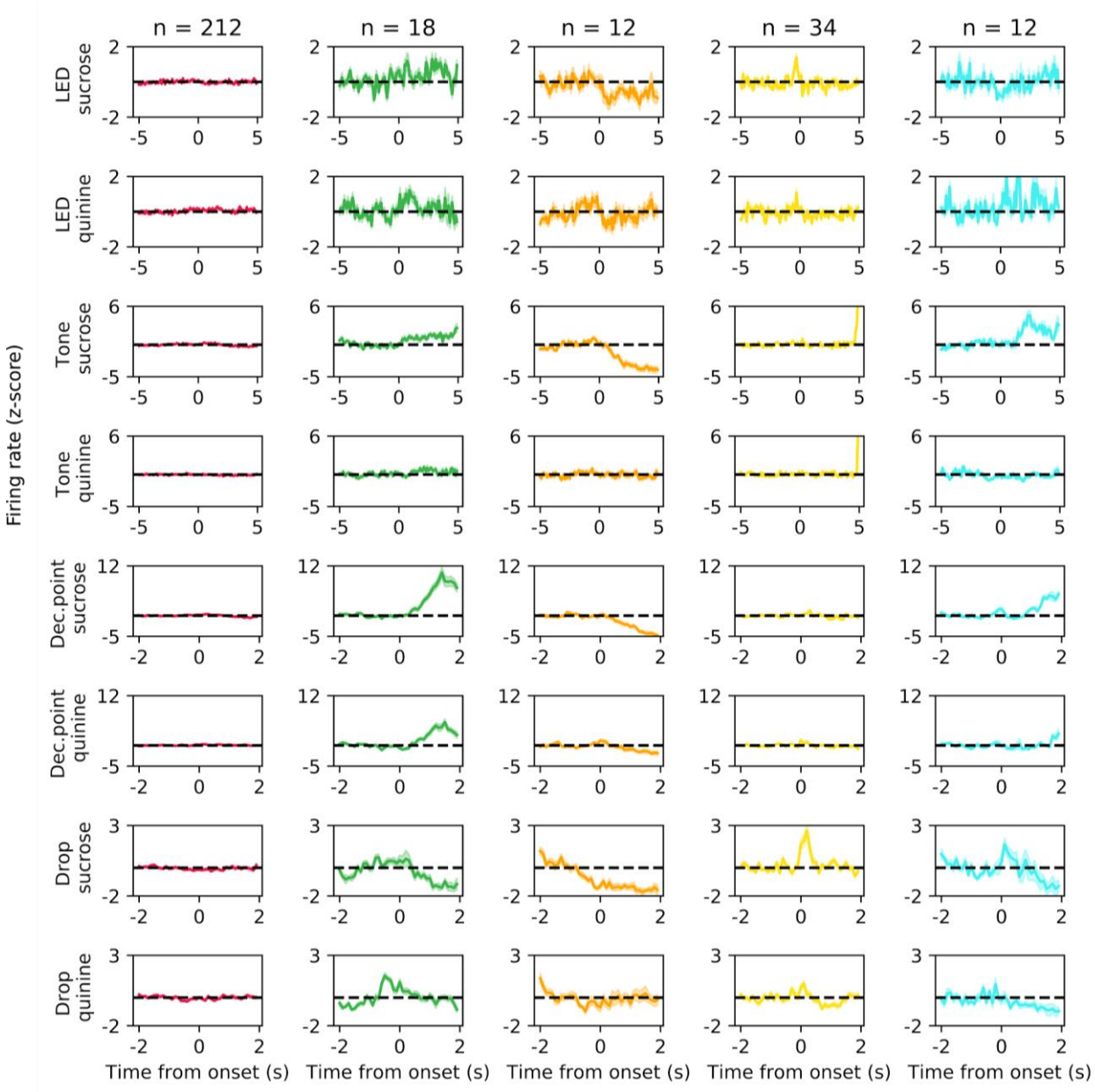

Fig. 11 VTA neuron clusters based on firing rate response to behavioural task variables.

Unsupervised clustering of single VTA neurons based on their firing rate modulation by behavioural task events. Each column corresponds to one cluster and each row one behavioural task event.

Cluster 1: this cluster does not exhibit any responses to the task variables assessed in this analysis. This does not mean that these cells do not encode task relevant information. It is likely that many of these cells respond to other variables, which could include such as place, the level of satiety, fatigue throughout the task etc.

Cluster 2: cells of this cluster show a modest increase in firing rate in response to the tone during the sucrose condition as well as during the decision point. Interestingly, this cluster also responds to the decision point during the quinine condition, but to a lesser degree compared to the sucrose trials. This may indicate that these cells encode the incentive salience driving the animal to start running towards the dispenser. Furthermore, these neurons respond with a transient increase in firing rate to the sucrose drop, but are inhibited following quinine drop consumption, suggesting that these neurons additionally encode the outcome value. This suggests a representational conjunction between incentive salience and outcome value.

Cluster 3: these neurons exhibit a sustained reduction in firing rate following the LED, tone and decision point in the sucrose condition, but not during quinine trials. This may suggest a role in promoting disinhibition of approach behaviour during sucrose trials.

Cluster 4: these cells respond with a transient increase in firing rate to the onset of the sucrose-paired LED and the drop consumption. This signature is strikingly reminiscent of traditional dopaminergic neurons that show a response to the CS as well as to the US. Interestingly, these neurons did not respond with a CS to the tone suggesting a backwards shift of the CS response to the LED.

Cluster 5: neurons in this cluster respond with a sharp and sustained increase in firing rate from 1 sec after the sucrose-predicting tone onset onwards. Furthermore, these neurons exhibit an elevated firing rate approximately 1 sec after the decision point

during sucrose trials. These effects were not seen during the quinine condition. Since the response latencies were slower than in cluster 2, these neurons could inform the animal about ongoing states rather than predicted states. Such ongoing states could either be movement towards a reward, the motivational state or simply the ongoing sensory context (tone).

In summary, VTA single units that respond to the behavioural task variables are typically modulated by more than one task event. Response variability may form a continuum across neurons of the VTA covering differences in response magnitude, polarity and temporal dynamics.

3.4 Electrophysiological classification of VTA single units

Next, I sought to investigate how different single unit responses might map onto molecularly-defined VTA neuron types. To this end, I first used an unsupervised machine learning approach to cluster non-opto-tagged into different groups based on their electrophysiology and I subsequently cross-validated those groups using ground truth data obtained from opto-tagging experiments. This approach allows leveraging the size of the non-optotagged dataset (318 neurons from 5 mice) to obtain a more accurate estimate of electrophysiological clusters whilst using the smaller opto-tagged dataset for validation.

To opto-tag glutamatergic and dopaminergic neurons I delivered light pulses (473 nm) to the VTA of either Vglut2-Cre or DAT-Cre mice injected in the VTA with a AAV vector encoding Channelrhodopsin-2 (ChR2) while performing simultaneous tetrode recordings (Fig. 12 A,B; see chapter 2.14 for methodological details). In order to optimise opto-tagged cell yield for the respective target population of VTA neurons,

tetrodes were positioned more medially for glutamatergic neurons, whereas for dopaminergic VTA cells, tetrodes were more lateral (Fig. 12 A, B, see chapter 2.14 for coordinates). While I did not formally quantify overlap of VGlut2 and TH expression yet, David Dupret reported instances where a low number of medial VTA neurons expressed both markers during preliminary scans of histological sections in the medial VTA. A precise quantification of this overlap will be required in the future to estimate the extent to which dopamine from co-releasing cells drove effects in optogenetic experiments of this study. I identified both opto-tagged glutamatergic and dopaminergic neurons based on the following heuristic: a sudden increase in the firing rate above two standard deviations from the mean of baseline (directly preceding the laser pulse) within 4ms of the onset of the laser-coupled TTL pulse in averaged peri-stimulus time histograms (2ms bins, Fig. 12 C). I chose a total of 4 ms for the detection of a significant increase in firing rate following the laser onset in order to be able to bin spikes across 2ms to obtain robust PSTHs. I did not want to discard neurons that would have fallen outside of the first 2ms bin by fractions of a millisecond and hence, extended the detection window by a second 2 ms bin. However, this approach may also include neurons that were activated via local monosynaptic connections. An experiment to control for this would be to test if the optogenetically entrained spikes are insensitive to pharmacological glutamate blockade. By mapping these neurons onto clusters of non-optotagged neurons, I ascribed a neurotransmitter identity to untagged cells. I only computed electrophysiological measures from spikes of opto-tagged neurons from periods not including a 1s period following laser delivery to avoid contamination of our measures with optogenetic artifacts. The prevalence of optogenetically identified glutamatergic and dopaminergic was 10/68 (14.7 %) and 20/321 (6.2 %), respectively.

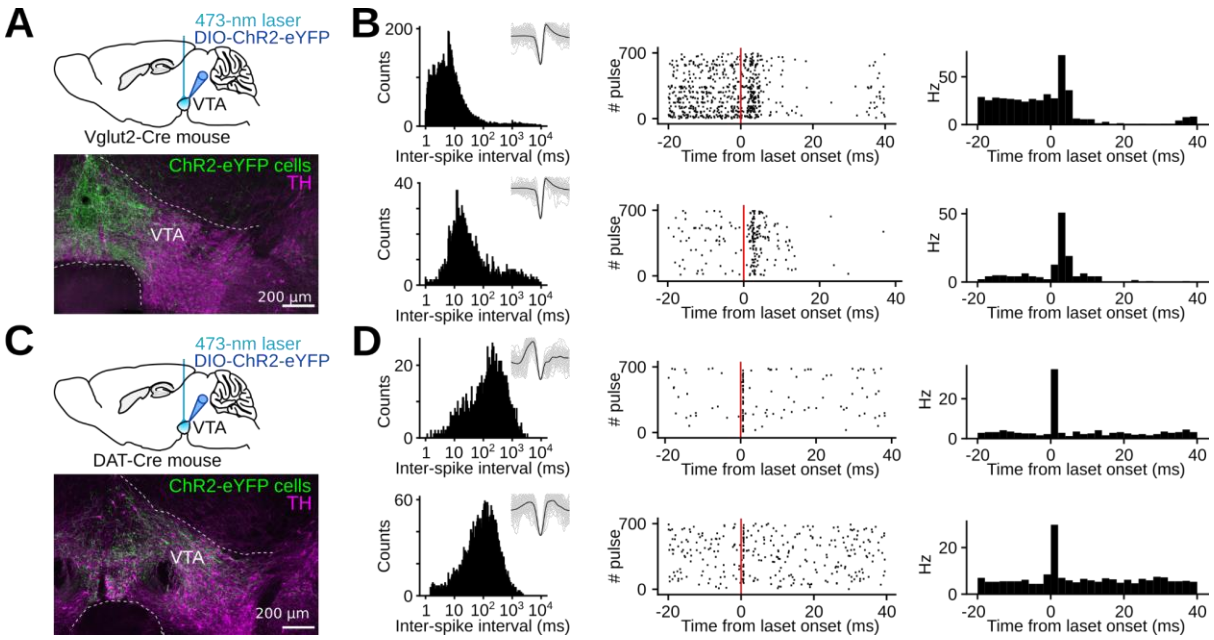

Fig. 12 Opto-tagging of glutamatergic and dopaminergic VTA neurons.

Optogenetic identification of VTA glutamatergic Vglut2-expressing cells and dopaminergic DAT-expressing cells. The schematics in (A) and (B) show the layout for quintuple-brain-region tetrode recording with bilateral optic fibers implanted above the VTA of Vglut2-Cre (A) and DAT-Cre (B) mice injected with the Cre-dependent ChRh2-eYFP viral construct in VTA. Below each brain schematic: wide-field confocal picture showing ChRh2-eYFP expression in VTA cell bodies in one Vglut2-Cre (A) and one DAT-Cre (B) mouse (scale bars are 200 micron). (C) Shown for two example opto-tagged glutamatergic Vglut2 VTA neurons (one cell per row, top two rows) and two example dopaminergic DAT-expressing VTA neurons (one cell per row, bottom two rows), from left to right: ISI distribution and spike waveform, raster plot showing spike times with respect to the onset (red vertical line) of light pulses delivered in the VTA and corresponding firing response histogram.

I sought to decide on an analytical framework to reliably distinguish between glutamatergic and dopaminergic neurons. It is important to note that in this work I deliberately attempted to find a framework that would allow us to impose a categorical distinction between glutamatergic and dopaminergic VTA cells. However, possibly VTA cell subtypes form a continuum. As a result, our classification may capture extreme ends of what is in reality a manifold, but as such not account for neurons that could have characteristics of both, dopaminergic and glutamatergic VTA cells.

I used hierarchical clustering throughout different electrophysiological measures. In order to identify putative dopaminergic neurons, traditionally heuristics based on the spike duration (>1 ms to 4-5 ms) (Aghajanian and Bunney 1974; Johnson and North 1992b), firing frequency (2-10 Hz) and spike shape (wide biphasic waveforms) have been used to identify putative dopaminergic cells from extracellular recordings (Ungless, Magill, and Bolam 2004; Ungless and Grace 2012; Anstrom and Woodward 2005; Dahan et al. 2007; Hyland et al. 2002). I measured the spike duration from the onset of the negative deflection to the return to baseline levels of the waveform. Hierarchical clustering of non-optotagged cells based on a combination of the spike duration and firing rate yielded poor cluster separation (Fig. 13 A). Consistently, mapping opto-tagged neurons on those clusters did not reveal clear separation of glutamatergic from dopaminergic neurons (Fig. 13 A), although I noticed that spike durations for opto-tagged glutamatergic versus dopaminergic neurons were well separated (Fig. 7 I). Furthermore, a heuristic based on the average firing rate alone (2-10 Hz for dopamine neurons) (Satoh et al. 2003; Ungless and Grace 2012) was not sufficient to produce satisfactory discrimination between opto-tagged dopaminergic and glutamatergic VTA-neurons as only 40% of actual dopaminergic VTA neurons are correctly identified as such, whilst the remaining 60% of dopaminergic neurons are pooled together with the 80% of correctly identified non-dopaminergic (glutamatergic) cells (Fig. 13 H). This indicates that a combination of firing rate and spike duration may not be suitable to distinguish between glutamatergic and dopaminergic neurons.

Next I attempted to use the shape of the spike waveform to separate the two cell types, which is typically considered to be biphasic and wide for dopaminergic neurons (Grace and Bunney 1983; Ungless and Grace 2012). To do so, I first normalised the average spike waveform from peak to trough to emphasize the spike shape over its amplitude

for cluster separation. I then extracted the first three principal components as features for hierarchical clustering. I found that although this procedure seemingly produced better cluster separation, half of the opto-tagged glutamatergic neurons were mixed in clusters together with opto-tagged dopaminergic neurons (Fig. 13 B). Hence, the spike shape alone does not appear to be sufficiently informative to establish clear categorical borders.

In the next attempt, I reasoned that the firing pattern might include relevant information of the different neuron types. Similarly to the procedure applied to the spike-waveform, I normalised the inter-spike interval distribution (ISI) and performed hierarchical clustering on its first three principal components of non-optotagged neurons (Fig. 13 G). Visual inspection confirms that this approach yielded the clearest cluster separation. Additionally, optotagged dopaminergic and glutamatergic neurons mapped onto the clusters are well separated from each other. I identified one cluster that contains 8/10 optotagged glutamatergic neurons. Consistently, only one dopaminergic neuron is mapped onto this cluster. Three more clusters map solely onto opto-tagged dopaminergic neurons and one predominantly dopaminergic cluster contains two tagged glutamatergic neurons at the border of the cluster (Fig. 13 C). The proportions of identified glutamatergic and dopaminergic were evenly distributed across mice and recording days with on average 35.7±5.1% of glutamatergic and 64.3±5.01% of dopaminergic cells per recording day. I concluded that the ISI distribution is the most effective measure to establish electrophysiologically defined clusters and to distinguish between dopaminergic and glutamatergic neurons in the mouse VTA. Using this method, I attributed a molecular profile to each recorded cell in non-optogenetically transduced animals. Other attempts at finding the optimal framework showed that a combination of several of these variables, such as ISI-

distribution, waveform and firing rate and autocorrelogram did not yield a better separation of the cell types (data not included in this thesis). Hence, I decided to proceed with the simplest possible model and chose the framework based on the ISI-distribution alone.

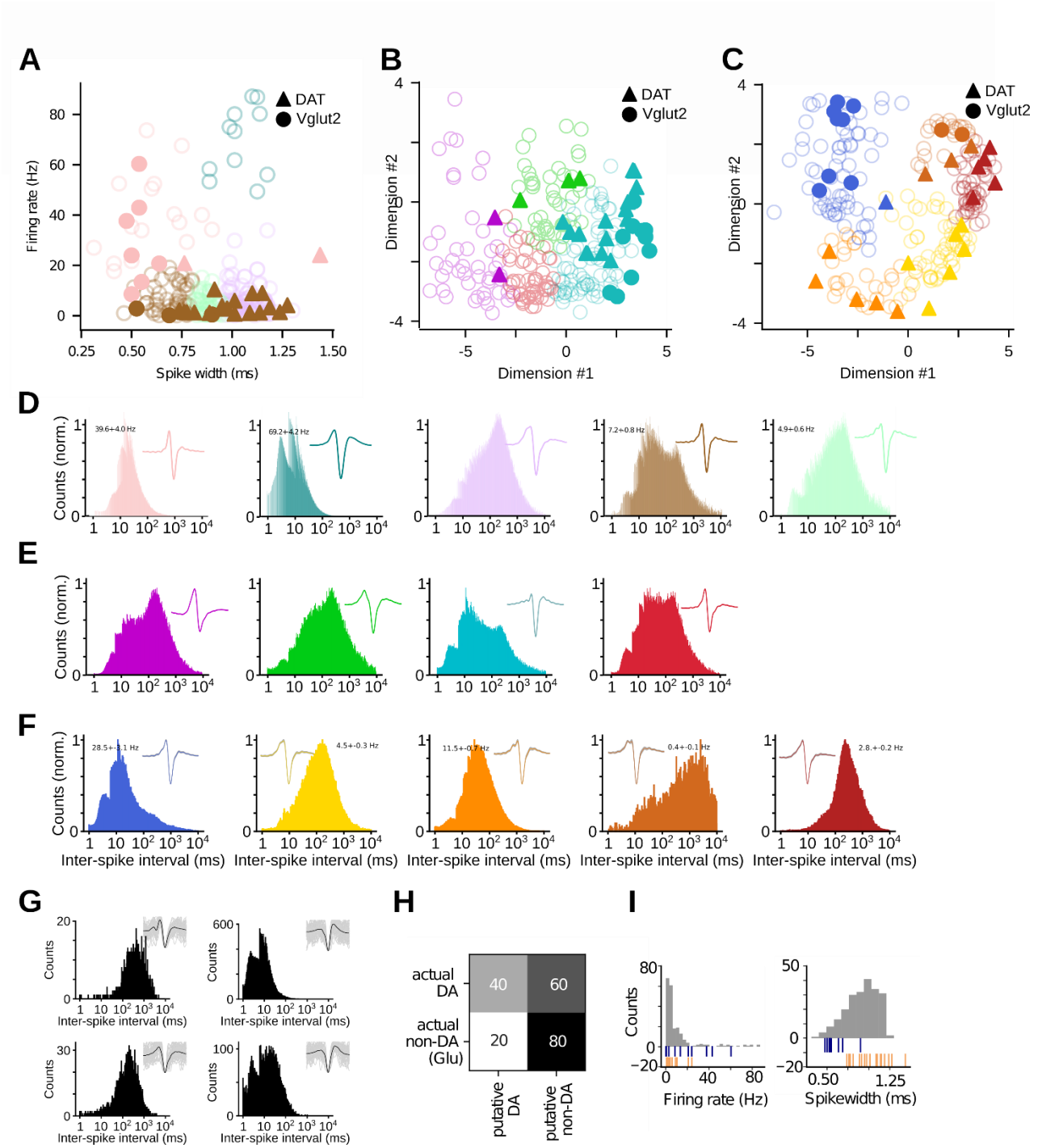

Fig. 13 Optogenetically-validated electrophysiological identification of VTA cell types.

The hierarchical clustering performed using the (A) spike width and firing frequency, (B) the spike waveform and (C) ISI distributions of VTA neurons recorded in non-optogenetically transduced mice (empty circles; each circle representing one neuron) first led to the identification of (color-coded) clusters. Clusters in (B) and (C) are plotted in latent-discriminant analysis space for visualisation purposes. The average ISI distribution and average spike waveform from these VTA neurons of each identified cluster with the different clustering approaches are shown in (D) for spike waveform and firing frequency, (E) for spike-waveform and (F) for ISI-distribution. I noticed that clusters are most clearly separated in (C) and by subsequently mapping the VTA neurons recorded and opto-tagged in Vglut2VTA::ChR2 and DATVTA::ChR2 optogenetically-transduced mice, I observed that identified glutamatergic Vglut2 VTA neurons (filled circles) mainly concentrate in one cluster (blue) whilst opto-tagged dopaminergic DAT VTA neurons (filled triangles) were allocated to the other four clusters. (G) Example inter-spike interval (ISI) distributions from four VTA neurons recorded in a non-optogenetically transduced mouse. Such ISI distributions were used as inputs to a hierarchical clustering. Note the longer ISIs of the two (left-column) example neurons that were subsequently identified to belong to optogenetically-identified dopaminergic cluster in (C). In contrast, note the shorter ISIs of the other two (right-column) example neurons that were clustered with optogenetically-identified glutamatergic cluster. (H) The matrix visualising success for clustering based on a firing-rate heuristic to identify dopaminergic neurons (2-10 Hz) shows the percentage of opto-tagged cells that have been correctly or incorrectly identified. Only 40% and 80% of opto-tagged dopaminergic and glutamatergic neurons, respectively, were correctly identified using the heuristic. (I) Distribution of firing rates and spike widths across opto-tagged and non-opto-tagged neurons. The occurrence of optogenetically identified cell-types in the distribution is indicated with vertical bars below the distribution (blue: glutamate, brown: dopamine).

3.5 Firing relationship of both dopaminergic and glutamatergic neurons to behavioural task events

Having established a method to attribute a neurotransmitter identity to VTA single units, I next wondered whether the two cell types responded differently to various task elements. To this end, I went back to the clustering analysis conducted in Fig. 3 with the aim to determine groups of neurons that respond similarly to various task elements. I mapped glutamatergic and dopaminergic neurons onto the clusters identified in Fig. 11 and determined the frequency at which they occur in any of the 5 response-type clusters (Fig. 14). If the different cell types are randomly distributed across the different clusters, then one would expect the number of cells of a given neurotransmitter type in a given cluster to be proportional to the size of the clusters. I found that the percentage of expected dopaminergic/glutamatergic neurons was close

to their expected prevalence with the exception of two clusters: one smaller cluster (#4, 11.8% of classified VTA cells) contains only neurons that were labeled as dopaminergic. This cluster exhibits pronounced transient responses in response to the onset of the sucrose-paired LED and the consumption of the sucrose drop, which is consistent with commonly accepted temporal response-dynamics of reward-related dopaminergic cell firing in the VTA (Schultz 1998). The largest cluster (#1, 73.6% of clustered cells) appears to have a lower than expected frequency of glutamatergic cells while the same does not hold for dopaminergic neurons. Interestingly, cluster #1 does not respond to the task events. This may suggest a potentially stronger overall recruitment of glutamatergic VTA neurons in our behavioural task.

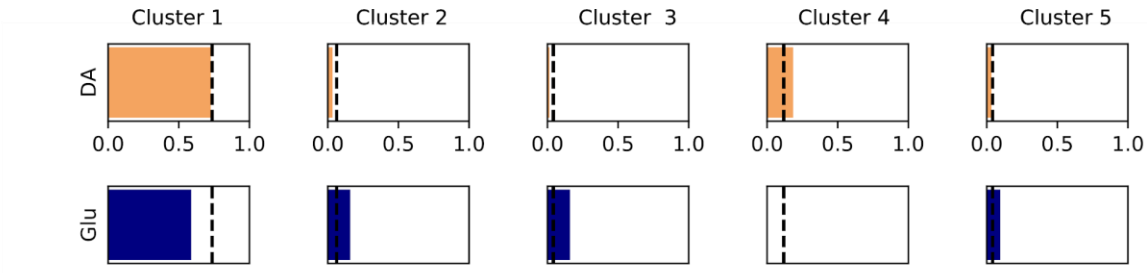

Fig. 14 Mapping of predicted dopaminergic and glutamatergic clusters onto response profile clusters

The width of the bars represents the proportion of the identified dopaminergic / glutamatergic neurons of their respective optogenetically identified group in the given cluster (see section 3.4 of this chapter). The dashed line indicates the expected proportion of dopaminergic and glutamatergic neurons in the cluster based on the cluster size. Notably, cluster 1 appears to contain less glutamatergic neurons than would be expected by chance, while the same is not true for dopaminergic cells. Cluster 4 contains exclusively as dopaminergic classified cells.

To investigate this hypothesis, I determined how well firing activity of the two different cell types could distinguish between the different task sets (sucrose versus quinine) for each individual task event. (Fig. 14 A). To this end, I trained a Naive Bayes classifier to discriminate between the two task sets based on the time course of the response for every single cell separately (see chapter 2.12 for methodological details). The

prediction accuracy of the classifier is indicative of how well a given cell discriminates between the two conditions (Fig. 14 B). I found that glutamatergic neurons discriminate between the two task sets significantly better than dopaminergic neurons in response to the LED, tone and decision point, but not the drop identity (p=3.5e-6, 1.4e-5, 4.9e-3, 0.46, respectively, independent t-tests). This further suggests that glutamatergic VTA cells are more closely related to behavioural events in our task. As the ISI-distributions reveal, glutamatergic VTA cells have higher firing rates compared to dopaminergic neurons. This suggests that glutamatergic neurons have more degrees of freedom when it comes to encoding information by reducing the firing rate compared to dopaminergic neurons. To test for this possibility, I also trained Naive Bayes classifiers to the same z-scored spike trains, but all negative deflections were set to zero. In contrast to non-thresholded spike trains, I found that a difference in encoding between the two neuron types does not reach significance for the LED (p=5.9e-2, independent t-test) and the tone (p=0.61, independent t-test). The result for liquid delivery remains the same (p=0.37, independent t-test). Only positive deflections of spike trains of glutamatergic VTA neurons remain more informative when decoding during the tone period compared to dopaminergic neurons (p=6.3e-3, independent t-test). This confirms that glutamatergic neurons have more degrees of freedom to encode information due to their higher firing rates.

Furthermore, I noticed that the time course of the response to the drop identity during the quinine versus sucrose contingency is strikingly different between the dopaminergic and glutamatergic cell populations (Fig. 14 A, bottom row). While the response of the glutamatergic population seems to decrease over a longer period of time, dopaminergic neurons exhibit a clear, phasic increase in firing rate directly following the delivery of sucrose, but not quinine. Strikingly, in contrast to

dopaminergic neurons the activity of glutamatergic cells is negatively modulated upon receiving the reward. This is consistent with the landmark study from Cohen et al. investigating response differences of different VTA cell types using opto-tagging (Cohen et al. 2012). Notably, Cohen et al. described a non-dopaminergic and likely non-GABAergic group of neurons, which responded with a decrease in firing rate upon the receipt of a reward without assigning a definite molecular identity to it. In our experimental paradigm, glutamatergic neurons responded with a decreased firing rate upon the receipt of the reward. This would suggest the following cell type-to-response mapping in the VTA: first, a classical dopaminergic response predicting rewards and reporting the outcome (Cohen et al. 2012), GABAergic cells that increase in firing rate following reward receipt (Cohen et al. 2012), and a third glutamatergic cluster, that decreases in firing rate following reward receipt, as identified in this study. It is tempting to imagine a local microcircuitry where GABAergic neurons control the firing of glutamatergic VTA cells during the receipt of a reward.

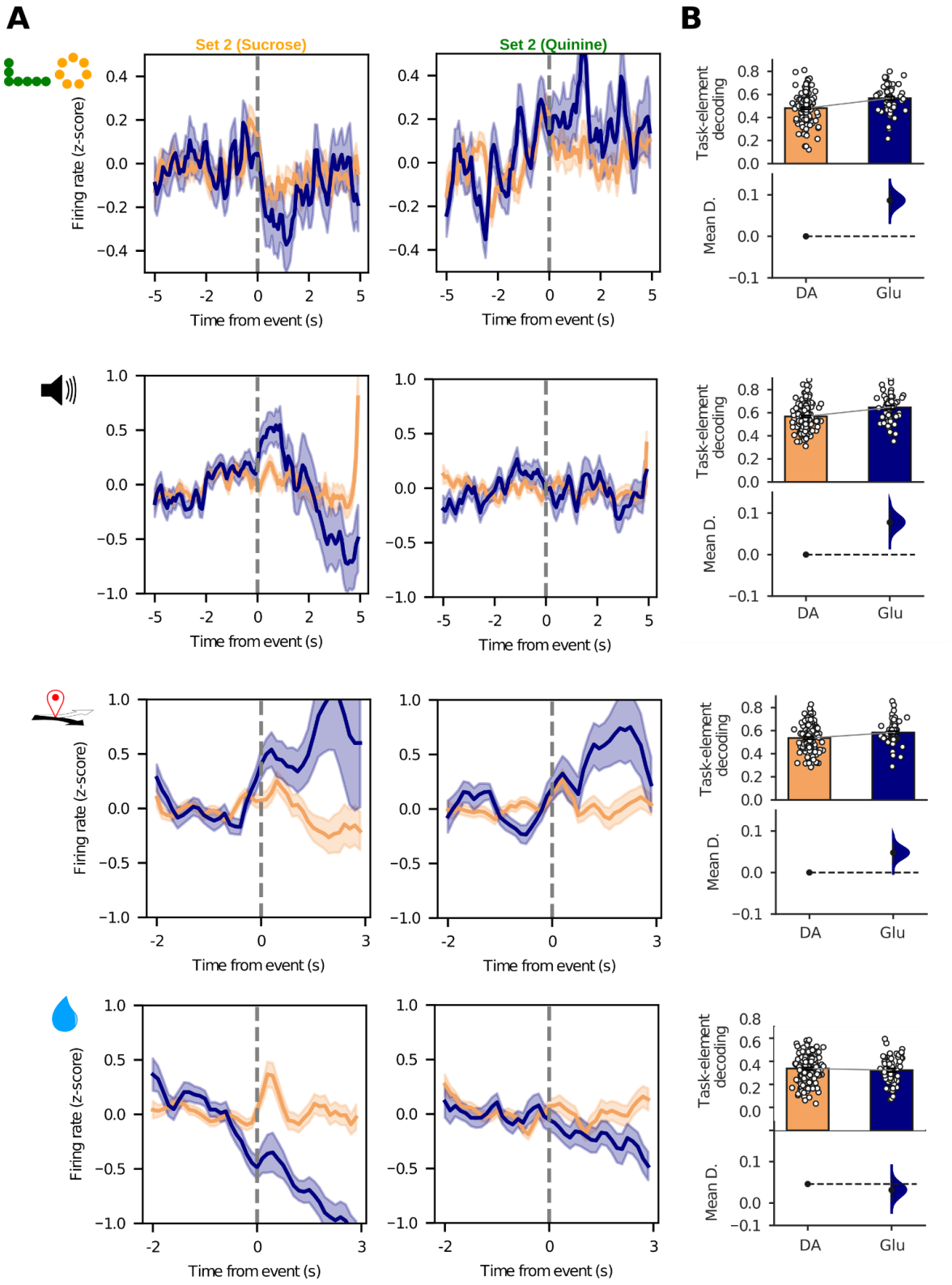

Fig. 15 Mapping of predicted dopaminergic and glutamatergic clusters onto response profile clusters

(A) Average z-scored firing rate responses to behavioural task events (rows in this order: LED, tone, decision point, drop consumption) during the different task sets columns right to left: quinine, sucrose). Dopaminergic neurons are in brown, and glutamatergic cells are in blue.

(B) Task set decoding based on the firing rate responses for glutamatergic (blue) versus dopaminergic neurons (brown). Each data point in (B) represents one cell.

3.6 VTA single units are grouped to behaviourally relevant cell assemblies

After having investigated task-relevant representations at the single cell level, I went on to ask whether there is evidence for a holistic integration of single cell activity in the form of local VTA co-firing patterns. To detect co-activity patterns, I used the PCA/ICA method (see chapter 2.10). In short, co-firing patterns are isolated by performing independent component analysis (ICA) on the simultaneously recorded spike trains of individual cells. The co-firing patterns are expressed as vectors of weights with the same length as cells used for the detection (all VTA cells recorded in that session). Each weight corresponds to the extent to which an individual neuron's spiking activity contributes to a particular co-firing pattern. This way, I identified 39 VTA assemblies, 24.5±2.1 cells per assembly.

I was first interested in how the organisation of co-firing patterns relates to the representation of individual task variables by single VTA neurons. In other words, are cells with similar task-event related response profiles more or less likely to be grouped into an assembly? To address this question, I developed a metric that accounts for both, the magnitude of contribution of an individual neuron to an assembly and its response profile to behavioural task events (see chapter 2.11 for methodological details). Briefly, every neuron was assigned a vector describing its firing rate responses to the different task events. For each assembly, this vector was weighted by the neuron's weight in the PCA/ICA assembly vector. I then computed the cosine similarity between the neurons of all co-firing patterns, which were then compared to

a shuffled null-distribution. Using this method, I found that individual cells of VTA co-firing patterns are grouped together based on the similarity of their firing response properties to behaviourally task events more than would be expected by chance (Fig. 16 A, n=39, U=-8.1, p<1e-6, Wilcoxon ranksums). It is important to note that assemblies have been detected outside the task trial periods (i.e. outside the tone and drop availability). Hence, co-activity during the tone, decision point or drop delivery does not cause the PCA/ICA algorithm to group the neurons into a co-firing assembly. I conclude that the more similar the task-event response profiles are, the more likely cells are to fire together. Notably, cosine similarity for neurons within assemblies is below 1, the boundary for complete similarity.

Next, I sought to determine the relevance of VTA co-firing patterns during ongoing behaviour. To this end, I tracked the expression strength of co-firing patterns over time (see chapter 2.5 for mouse tracking procedure) while the animal was left to explore a task-unrelated familiar enclosure and the task arena. I further split the time spent in the task arena into different ‘pre task’ and ‘task’ epochs. The ‘task’ epoch is defined by the onset of the tone and ends with the removal of the liquid from the dispenser while the ‘pre task’ period is defined as the time interval of equal length directly preceding the ‘task’ epoch. To evaluate whether these assembly patterns carried task relevant information, I tracked their coactivity strength over time. To disambiguate the methodology: I was not detecting new assemblies during different time periods, but rather determined how often cells defining an assembly fire together during a certain period of time. The time periods of trials would be too short to reliably detect statistically robust co-firing patterns. Coactivity pattern strength was different during the familiar, pre-task and task periods (Fig. 16 B, D; p=2.6e-3, F=6.41, ANOVA). Post hoc analysis revealed that VTA assembly strength is stronger during the task

compared to the other task-unrelated arena that mice also explored each day (p=1.32e-2, Tukey HSD adjusted p-value). Moreover, pattern strength increased more during tone-initiated trials than during periods before tone presentation ('off-trial') (Fig. 16 B; change in pattern strength relative to task-unrelated arena: 'off-trials'=11.1±8.4% versus 'on-trials'=31.5±10.4%, p=2.5e-2, Tukey HSD adjusted p-value). Consistently, Naive Bayes models trained on pattern strength time courses to discriminate between the task sets (see chapter 2.12 for methods; similar to analysis in Fig. 14) further showed that decoding performance increases from the 'pre task' to the 'task' epoch, indicating the recruitment of task relevant representations in the form of co-activity assembly patterns (p=3.4e-3, paired t-test).

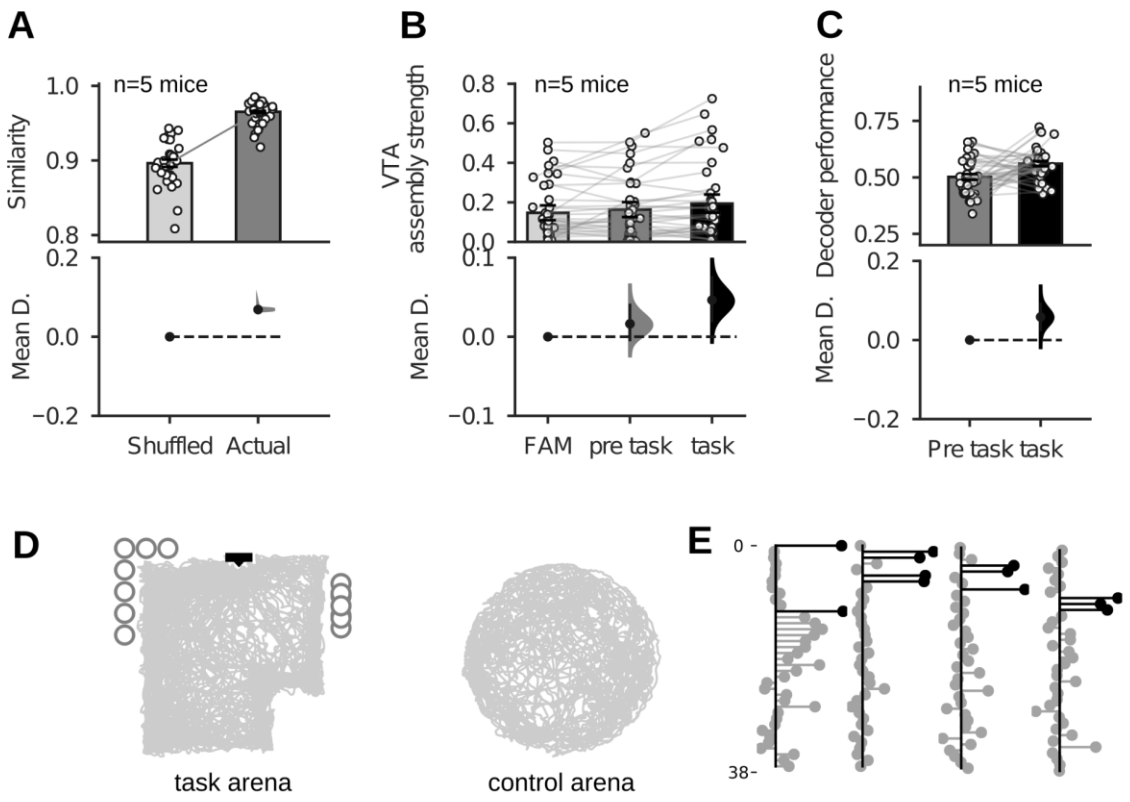

Fig. 16 Recruitment of VTA co-firing patterns during ongoing behaviour.

(A) Average cosine similarity of VTA cell-assembly members with respect to their responses to different behavioural task events. The contribution of individual cells has

been weighted based on their weights in the assembly vector and compared to a shuffled distribution of firing rate responses (see main text). (B) Average coactivity pattern strength was stronger in the task arena before tone presentation (pre-task) than in another control enclosure (FAM), further increasing during task trials (task). (C) Task-cue contingencies were better reported by coactivity pattern time course during tone trials compared to pre-task trials. (D) The task arena (dispenser: black rectangle) and the other (control) enclosure that mice also explored on each day. (E) Examples of assemblies detected during one recording day from the same mouse. For visualisation purposes, neurons with strong contribution to the assembly vector are grouped together and coloured in black.

3.7 Discussion

In this chapter, I introduce our behavioural task, which requires the animal to distinguish two sets of sensory cues in order to inform appetitive versus aversive behavioural responses. I utilise this design to explore the representation of task variables and report that single VTA cells have a rich repertoire of task-related responses, which is subject to strong variability between different VTA cells. Then I set out to establish a method to electrophysiologically separate dopaminergic from glutamatergic neurons using opto-tagging and find that a classification based on the ISI-distribution performs better than traditionally applied heuristics. With this method, I found that glutamatergic cells encode behavioural task events more reliably than dopaminergic neurons. Finally, I report the existence of VTA co-firing assembly patterns and establish that their expression is linked to ongoing behaviour. In these assemblies, single cells with similar responses to behavioural task variables are grouped together. In the following pages, I will discuss these findings and highlight methodological, mechanistic and functional considerations.

Behavioural task: our aim was to use a task that would require the animal to process and integrate multiple behaviourally relevant sensory modalities and would allow us to

monitor neural correlates alongside with behavioural readouts. To this end, I decided to develop a task in which stimuli are controlled externally via TTLs or easily heuristically estimated (i.e. decision point via position tracking). With this in mind, I used a spatio-visual context discrimination task which has events of a classical go-nogo task. The animal was required to integrate spatio-visual (LED), auditory (tone) and gustatory (delivered liquid) information in order to make a decision about an appetitive or aversive outcome. On the one hand, this design bears the question whether a rapid and repeated contextual switch is ethologically relevant. On the other hand, I reasoned that an open field design where the animal can move freely would be preferable over spatially confined (linear track) or physically restrained (headfixed) designs and accepted this as a trade-off between external control of stimuli and natural exploration behaviour. I observed that animals returned to near chance-level performance in the beginning of every new session, but rapidly improved over time. It is possible that mice required several trials to reinstate the memory of task rules based on the sensory context. Over time, however, mice expressed progressively more approach behaviour during the sucrose condition. Importantly, this intra-session learning may have implications for the analysis of neural signals. For instance, reward prediction errors signatures may change as a course of learning (Amo et al. 2020) or different patterns of cross-structural co-activation might emerge as the animal remembers. I found that animals did not switch to a block-based strategy to solve the task, since mice solved the task contingencies correctly already during the first trial of any given block. Furthermore, as I quantified approach and not drop consumption behaviour, it is unlikely that behavioural performance is explained by the usage of olfactory cues to determine the drop identity. Lastly, it is important to note that although a total of 29 behaviour-sessions were used for these behavioural experiments these

came from only 5 mice and hence, more animals are required to add statistical robustness to the results.

(i) Characterisation of the diversity of single unit responses to behavioural and sensory variables in the VTA.

Methodological considerations: in this analysis, I used average firing rates during ongoing behaviour to obtain single-cell responses to various behavioural task events. Since task events often overlap in time, there is a chance that the response of one task event will be contaminated by another concurrently happening task event (e.g. decision point and tone, i.e. in trials when the mouse starts running towards the dispenser while the tone is still playing). To circumvent this issue, I applied a z-scoring procedure relative to the baseline prior to any given event onset yielding successfully separated response estimates (e.g. the first two cells in Fig. 8, which have distinct firing rate increases during the tone and decision point). I then used those z-scored responses to classify cells into separate groups based on which task event they respond to. However, the definition of task events is arbitrary and subject to categories imposed by the human experimenter. Undoubtedly, the VTA is involved in processing more environmental and internal variables (Ilango et al. 2012; Gomperts, Kloosterman, and Wilson 2015) than I tested for here. Therefore, the cluster architecture might well have been biased by our selection of task events. This also likely influenced the separability of the data and, hence, the decision on the cluster number. However, the advantage of using the parameters I chose for this investigation is that they are temporally precisely defined, and they cover a spectrum of different modalities (visual, auditory, cognitive and gustatory). This, hence, serves as a simplified method to sample responses from the multidimensional representational space of the VTA. A further parameter influencing the detected single cell responses may be the

anatomical site of the tetrode recordings. Different regions in the VTA receive not qualitatively, yet quantitatively different inputs from other brain regions. VTA cells may, thus, be biased towards some modalities over others in accordance to the origin of the presynaptic input (Watabe-Uchida et al. 2012; Beier et al. 2015; Ogawa et al. 2014; Faget et al. 2016). Therefore, it is possible that the same experimental setup could yield different clustering results based on the exact position of recordings within the VTA. Furthermore, different response profiles do not necessarily imply different cell types but may instead reflect the proficiency of the animal. For instance, a response to the LED but not the tone could simply reflect a gradual backwards shift of the conditioned response in some cells but not others (Amo et al. 2020).

Mechanistic and functional considerations: I observed variability in the response to behavioural task events at the single-cell level across three dimensions: (i) which task event a cell responds to, (ii) if it responds with an increase or decrease in firing rate and (iii) how many such task events a cell responds to. Variables within and across those dimensions appear to be flexibly combinable giving rise to highly multidimensional representational properties of single VTA neurons. Three different mechanisms may underlie such high dimensionality: first, the response pattern of any given neuron may be inherited entirely from the pre-integrated presynaptic input it receives from other brain areas. For instance, the VTA has been shown to receive input from highly integrative brain structures such as the PFC (Beier et al. 2015) and hence, could inherit such high dimensional response properties. Second, the same authors showed that single VTA cells receive convergent input from different brain areas (Beier et al. 2015) and hence, may act as integrators for different behaviourally relevant parameters themselves. Third, as VTA cells are heavily interconnected, neurons may be sharing information locally between each other (Johnson and North

1992a; Tan et al. 2012; van Zessen et al. 2012; H.-L. Wang et al. 2015; Dobi et al. 2010). Ultimately, those mechanisms are not mutually exclusive and may contribute to certain degrees to the representational richness of single VTA neurons.

Whilst neurons exhibiting similar response patterns can be classified into separate clusters the borders between clusters as well as the optimal cluster number appears to be not clearly defined. This indicates that single-neuron response variability lies on a continuum. Why would it make sense to equip individual VTA cells with the ability to represent such complex and gradual combinations of behaviourally relevant parameters? One possibility is that this complexity allows for a fine-grained representation of the external and internal world and provides a way to modify behaviour in accordance with current environmental requirements. Furthermore, the brain may leverage the axonal infrastructure of single VTA cells to send a complex multimodal message via the same cell at the same time to different target cells, which can even be located in different brain regions (Aransay et al. 2015).

(ii) Do glutamatergic and dopaminergic VTA neurons respond differently to behavioural and sensory variables?

Methodological considerations. In order to classify cells electrophysiologically into glutamatergic or dopaminergic neurons, I first needed to find suitable metrics. I clustered VTA cells based on these electrophysiological metrics in an unsupervised manner and subsequently mapped opto-tagged neurons onto the previously identified clusters to assign a molecular profile. I chose this approach since this would allow us to build our model based on a comparatively large number of recorded neurons from the non-optotagged dataset. The reverse approach would be to train a classifier on the opto-tagged ground truth data and then predict the identity of non-opto-tagged

cells. However, this would render the model more vulnerable to potential to sample biases in the small opto-tagged populations. One limitation of our clustering framework is the lack of opto-tagged GABAergic neurons and so it is unclear which clusters these neurons correspond to. However, it is estimated that the proportion of GABAergic cells in the medial VTA (our recording site) is 12%, which is significantly lower than in other VTA nuclei, where prevalence can be up to 45% (Nair-Roberts et al. 2008). Whilst acknowledging the potentially drastic effects of individual interneurons on the local network, for the purposes of establishing a clustering framework based on extracellular signals, I consider this number negligible. Furthermore, a physiologically meaningful separation into glutamatergic versus dopaminergic clusters is supported by pronounced differences in the decoder performances as well as different temporal response profiles to the consumption of the sucrose drop (Fig. 14; bottom row) consistent with previously reported response phenotypes (Cohen et. al, 2012). Moreover, I noticed that two glutamatergic cells are located at the border of a dopaminergic cluster and one dopaminergic neuron is on the outskirts of the glutamatergic cluster. It is possible that these are misclassifications due to imprecisions in our model or alternatively, these neurons could be combinatorial neurons co-releasing glutamate and dopamine (Yamaguchi et al. 2015; Kawano et al. 2006). In fact, in this study I deliberately imposed a categorical framework on a biological phenomenon that might in reality be a continuum. Lastly, it is important to note that optogenetic ground truth data was obtained from only 2 DAT-Cre and 2 VGlut-Cre. In this sense, the validation of clusters obtained using unsupervised clustering using the ISI-distribution is subject to variability in tetrode placement. Similarly, despite the relatively high number of 318 VTA cells recorded in the non-optogenetic dataset, these clusters may be subject to variability in tetrode placement.

For instance, the electrophysiological signature in different regions of the VTA could be different for the same cell type; and conversely the features could be similar for different cell types depending on the locus of electrode placement. This could lead to different cell types being grouped together and erroneously validated as belonging to the same cluster. In connection with this, a post hoc histological verification of the electrode tracks is required.

In our dataset, methods previously used to identify dopaminergic neurons based on spike width, firing frequency and spike shape (Ungless, Magill, and Bolam 2004; Ungless and Grace 2012; Anstrom and Woodward 2005; Dahan et al. 2007; Hyland et al. 2002) did not yield satisfactory separation between glutamatergic and dopaminergic cells. Consistent with our findings, previous studies have questioned the validity of such heuristics (Lammel et al. 2008; Margolis, Lock, Hjelmstad, et al. 2006). At the time these electrophysiological heuristics were developed no cell-type specific optogenetic interrogation was available and hence, parameters were inherited from the study of substantia nigra dopaminergic neurons, where the cell population is much more electrophysiologically homogenous (Ungless and Grace 2012) and hence, possibly not readily applicable to the diversity of VTA neurons (Morales and Margolis 2017). It is worth noting that dopaminergic substantia nigra neurons are biochemically heterogeneous (Poulin et al. 2020). Furthermore, classification approaches are sensitive the specific anatomical locus within the VTA, which determines molecular make up, presynaptic input and hence, the electrophysiological properties of single cells (Lammel et al. 2008, 2011; Margolis et al. 2008; Ford, Mark, and Williams 2006).

In order to investigate the relationship of neurotransmitter identity to the representational diversity of single VTA cells, I investigated the proportion of

dopaminergic and glutamatergic cells in the clusters. I noticed that in one large cluster, the proportion of glutamatergic cells was lower than would be expected by chance, but the same was not true for dopaminergic cells. Interestingly, neurons grouped in this cluster did not exhibit any notable responses to the behavioural task events. One possible explanation would be a genuinely stronger involvement of glutamatergic cells in the task at hand. Alternatively, it is possible that I simply did not test for the relevant task parameters the dopaminergic cells in this cluster respond to. However, decoding analysis confirmed that glutamatergic cells spiking is more closely related to behavioural task events.

Mechanistic and functional considerations. This decoder-based approach revealed that glutamatergic VTA neurons encode three of the four task variables more reliably than dopaminergic cells (i.e. LED, tone, decision point but not drop consumption). I found that controlling for positive and negative modulation of the firing rate reduces the decoding accuracy of glutamatergic cells towards the level of dopaminergic neurons for the LED and the decision point. This suggests that the brain leverages the higher firing rate of glutamatergic VTA neurons to increase their information encoding capacity. From a mechanistic perspective, this could either be achieved by more glutamatergic cells being tuned to task relevant variables. Alternatively, glutamatergic neurons could exhibit a higher inter-trial reproducibility of spike trains during the same task contingency. Both options are not mutually exclusive and are subject to the input from presynaptic regions. Consistently, glutamatergic cells receive quantitatively different input from other brain regions compared to dopaminergic neurons (Watabe-Uchida et al. 2012; Beier et al. 2015; Faget et al. 2016; Ogawa et al. 2014). Additionally, spike train reliability is subject to differences in the molecular makeup of different cell types and their presynaptic inputs influencing stochastic noise processes

such as stochastic neurotransmitter release and opening/closing of ion channels (Deco, Rolls, and Romo 2009).

From a functional perspective, the precision of spike timing plays an important role for the downstream reader neurons. While glutamate acts on a millisecond timescale at ligand-gated ion channels on axo-dendritic synapses, dopamine is widely considered to act on a slower timescale via volume conduction on (slower) metabotropic dopamine receptors (Tritsch and Sabatini 2012). Therefore, the encoding time window for dopaminergic neurons allows for more variability spike timing precision. The fact that glutamatergic VTA neuron spiking is better at encoding environmental contingencies may also reflect differences in the function of those neurons on a circuit level. Glutamatergic neurons may specialise more in broadcasting specific information content relying on precise spike timing and fast postsynaptic responses, dopaminergic cells may instead transmit more general, slightly less content specific and time-sensitive signals such as motivational states (Bromberg-Martin, Matsumoto, and Hikosaka 2010) or general learning signals (Glimcher 2011). Importantly, our data do not support the idea that glutamatergic and dopaminergic VTA cells represent qualitatively different aspects of the internal or external world. Representational differences between the two cell types appear to be rather quantitative. Nonetheless the cell types may have functionally strikingly different roles from the perspective of downstream reader neurons given the temporal dynamics and metabotropic impact of glutamatergic versus dopaminergic neurotransmission. Ultimately, both cell-types in synergy could promote content-specific acute learning with glutamatergic cells selecting the right downstream neurons for ongoing behaviour whilst dopamine modulates their synaptic connectivity.

(iii) Are there behaviourally relevant co-firing assembly patterns within the VTA?

Methodological considerations. To our knowledge, this analysis reports for the first time the existence of co-firing assemblies in the VTA. Strikingly, despite the relatively low number of VTA cells recorded simultaneously, VTA cell co-firing patterns were successfully identified using the PCA/ICA method, which suggests a tight and reliable coupling of single unit activity in the VTA. In order to sample sufficient neural co-firing events I decided to integrate across the entire task period for the assembly analysis as opposed to focusing on single behavioural task events as done for single cell spiketrain-decoding analysis. The downside of this approach is that the assembly activation time course will co-vary with the onset of non-static behavioural events such as the start of the decision point or the time of drop consumption. This variability reduces the ability of classifiers to learn the relationship between assembly activation and the identity of the decoded task set.

Furthermore, I investigated whether cells representing similar task events are more likely to co-fire together in an assembly. To this end, I weighted the cell's responses by their weights in the assembly vector. Since most weights in an assembly vector are close to zero, most weighted feature vectors for each cell will be close to zero too, resulting in an inflated similarity score for both the shuffled and non-shuffled feature vectors. Nonetheless, despite this bias I measured a difference between the shuffled and original distributions hinting towards a real biological organisational principle. Lastly, the analysis suffers from sparsity of biological replicates (5 mice). This could be particularly impactful in the face of sparsity in the expression of neuronal co-activation strength over time and amplified by the low number of simultaneously recorded VTA neurons (15.4±1.7 per session). This could introduce noise in both, the

detection of assembly patterns as well as the usage of assembly strength traces for decoding of task contingencies.

Mechanistic and functional considerations. The representational cosine similarity of neurons grouped to co-firing assemblies was above chance and below the possible limit of 1. I suggest that the imperfect similarity of neurons grouped to an assembly is indicative of a partial overlap in the representational space covered by single neurons. This could allow for a minimally necessary degree of response similarity to enable co-activity whilst leaving room to flexibly integrate other neurons with partially dissimilar representational content. This finding is in line with recent research on distributional reinforcement learning in the brain suggesting that combinations of VTA neurons encode the spectrum of expected rewards (Lowet et al. 2020; Dabney et al. 2020). One could imagine a scenario in which cells responding to different sensory or behavioural variables jointly encode different quantiles of such a value distribution. This could provide a mechanism for the expansion and flexible adaptation of the behavioural repertoire driven by coordinated VTA single unit activity. In fact, I observed inter-regional variability of this property indicating that different brain structures apply degrees of similarity for grouping cells into assembly and hence support behavioural versatility to different degrees (results on other brain regions are presented in chapter 4). I found that assembly patterns increase in expression strength in a task-relevant manner and are predictive of behaviourally relevant parameters. Such increases in VTA unit co-activity may help activate relevant downstream reader neurons through the simultaneous convergence of different inputs (Buzsáki 2010) and broadcast information in a coordinated manner via different VTA cells projecting to different regions (Aransay et al. 2015). Ultimately, the VTA might act as both an integration and broadcasting hub. In this scenario, information is inherited from other circuits, further

integrated locally and finally passed on to wide-reaching glutamatergic and dopaminergic projection neurons which send messages to the VTA's downstream regions in a temporally and representationally coordinated fashion.

4. CHAPTER 4: BRAIN-WIDE TASK RELEVANT REPRESENTATIONS AND DISTRIBUTED CELL ASSEMBLIES

4.1. Introduction

It is currently thought that information in the sensory, motor, and cognitive domains is processed within specific brain circuits. Notably, individual neurons in the dorsal CA1 hippocampus (CA1) represent spatio-visual surroundings (O'Keefe and Dostrovsky 1971b; Wilson and McNaughton 1993; Leutgeb et al. 2005); amygdala (Amy) and ventral tegmental area (VTA) neurons process negative and positive stimuli (e.g., conditioned auditory cues) (Ambroggi et al. 2008; Beyeler et al. 2016; Herry et al. 2008; Cohen et al. 2012; Kyriazi, Headley, and Paré 2020); medial prefrontal cortex (PFC) neurons underpin decision- making (Sul et al. 2010; Narayanan and Laubach 2006; Passecker et al. 2019) and nucleus accumbens (NAc) neurons process cue-predicted reward outcomes (Lansink et al. 2012; van der Meer and Redish 2009; Lavoie and Mizumori 1994; Setlow, Schoenbaum, and Gallagher 2003; Roitman, Wheeler, and Carelli 2005). Furthermore, some neurons appear to encode more than one stimulus. For instance, some hippocampal cells respond to both, place and reward (Bittner et al. 2015), or auditory cortex neurons simultaneously encode pitch and timbre (Walker et al. 2011), thus forming conjunctive codes between two external variables. It is unknown whether neurons in different brain areas specialise in different stimulus conjunctions. However, the idea of pure functional specialisation of different brain areas has progressively been subject of criticism (Fox and Friston 2012) and is

rivalled by models based on the concept of distributed processing (Rumelhart and McClelland 1987; Rissman and Wagner 2012). According to the parallel distributed processing (PDP) framework (Rumelhart and McClelland 1987), brain areas do not have a single psychologically defined function. Instead, information is computed in a distributed manner across different parts of the system. This raises the following question: if different events of the same percept are processed separately, how could the brain compute one single coherent percept? Donald Hebb's idea of cell assemblies posits that neurons representing different items could be bound together through coincident firing and thus, form a rich and coherent representation (Hebb 1949b), 1949). Hence, I hypothesized that short-timescale neuronal coactivity forming co-firing assemblies spanning multiple brain regions could provide a 'platform' to bind different pieces of information together and this way form behaviourally relevant representations. Here, I performed simultaneous tetrode recordings from CA1, Amy, NAc, VTA and PFC whilst the animal was engaging in our two-contingency behavioural task. Using this framework, I addressed the following questions:

(i) Do different brain areas specialise in different behavioural task representations?

(ii) Are there behaviourally relevant co-firing assemblies across multiple structures?

4.2. Neuronal representations of task variables across five brain regions

I performed simultaneous tetrode recordings from PFC, NAc, CA1, Amy and VTA in the right hemisphere (Fig. 17) while the animal was performing our task. This enabled us to probe for potential differences and similarities in task representation in different brain regions. I recorded 1241 neurons in 9 mice (CA1: 344, Amy: 161, NAc: 176, PFC: 242, VTA: 318). The cell yield for every region was CA1: 11-20, Amy: 3-25, NAc: 11-14, PFC: 5-25, VTA: 6-43 (the range expresses minima and maxima across average cell yields by mouse). This variability may have an impact on population analyses conducted further below and is treated in the discussion.

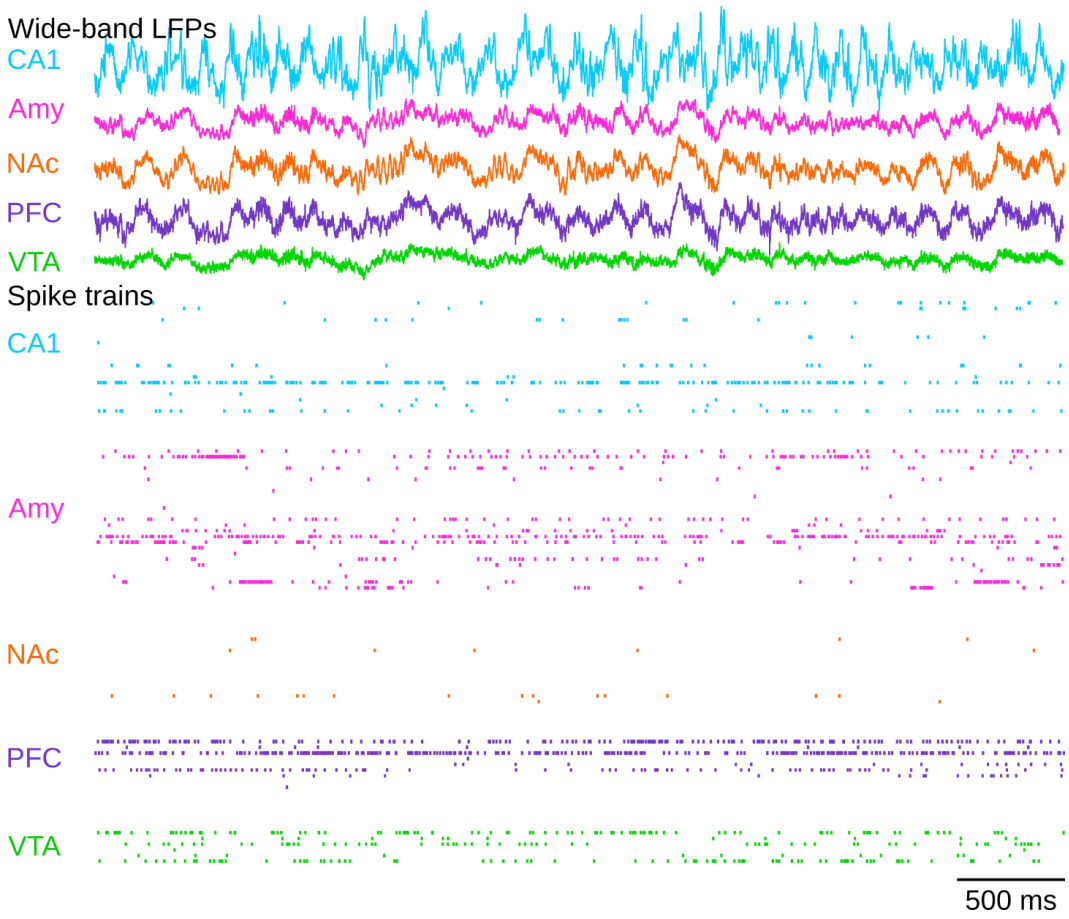

Fig. 17 Quintuple-brain-region tetrode recording from the right hemisphere.

Example wide-band signals (top; color-coded raw traces of local field potentials) simultaneously recorded in the PFC, NAc, CA1, Amy and VTA along with spike times of

neurons (bottom raster plot; one cell per row; color-coded spike trains according to brain region) from a mouse performing the task. All tetrodes were positioned in the right hemisphere.

I computed average PSTHs and standardise them with respect to the mean and standard deviation of the baseline directly prior to the onset of the event onset (LED, tone, decision point and drop consumption). Each region exhibited firing modulation to all the task variables, from LED to tone to outcome (Fig. 17-23). No differences in the mean response magnitude after event onset were observed between the regions for the LED and the Tone (p=0.27 and p=0.82, respectively; ANOVA). However, there were differences in the response magnitude between the regions during the decision point and the drop consumption (p=1.6e-7 and p=1.2e-5, ANOVA). Post hoc analyses revealed that CA1 responded significantly more strongly to the decision point compared to Amy, NAc and PFC (p=5.4e-3, p=1e-3 and p=1.7e-2, respectively; Tuckey HSD adjusted p-values). Furthermore, VTA responded more strongly than Amy, NAc and PFC (p=1.7e-3, p=1e-3 and p=4.6e-3, respectively; Tuckey HSD adjusted p-values). During drop consumption, CA1, Amy, responded more strongly than the VTA (p=6.1e-3 and p=2.7e-3, respectively; Tuckey HSD adjusted p-values) but the VTA responded more strongly compared to NAc and PFC (p=1e-3 and p=9.3e-3, Tuckey HSD adjusted p-values). For these analyses, each cell's preferred condition was first determined based on which condition elicited the greater average firing response. Only trials from that respective trial were considered for this analysis. Please note that the temporal dynamics are not being taken into account when comparing the responses of the different regions. Also, for this analysis, positive and negative deflections of the response are averaged. At different points in time it may well be that one region responds more strongly than another, even if it does not show

when averaging across the entire response period. It remains questionable however, how biologically significant these rather small differences in amplitude changes are.

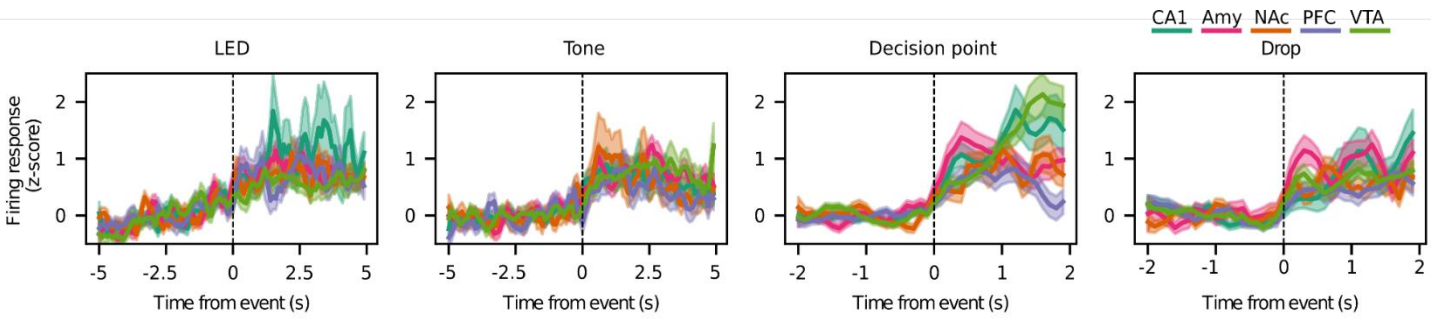

Fig. 18 Average responses of single neurons to task events in different brain regions.

From left to right: average firing rate responses to the LED, Tone, decision point and drop consumption split by region. For this analysis, I first determined which condition (sucrose or quinine) the cell responds more strongly to and calculated the PSTH only from those trials. The traces have been standardised with respect to the baseline preceding the event onset.

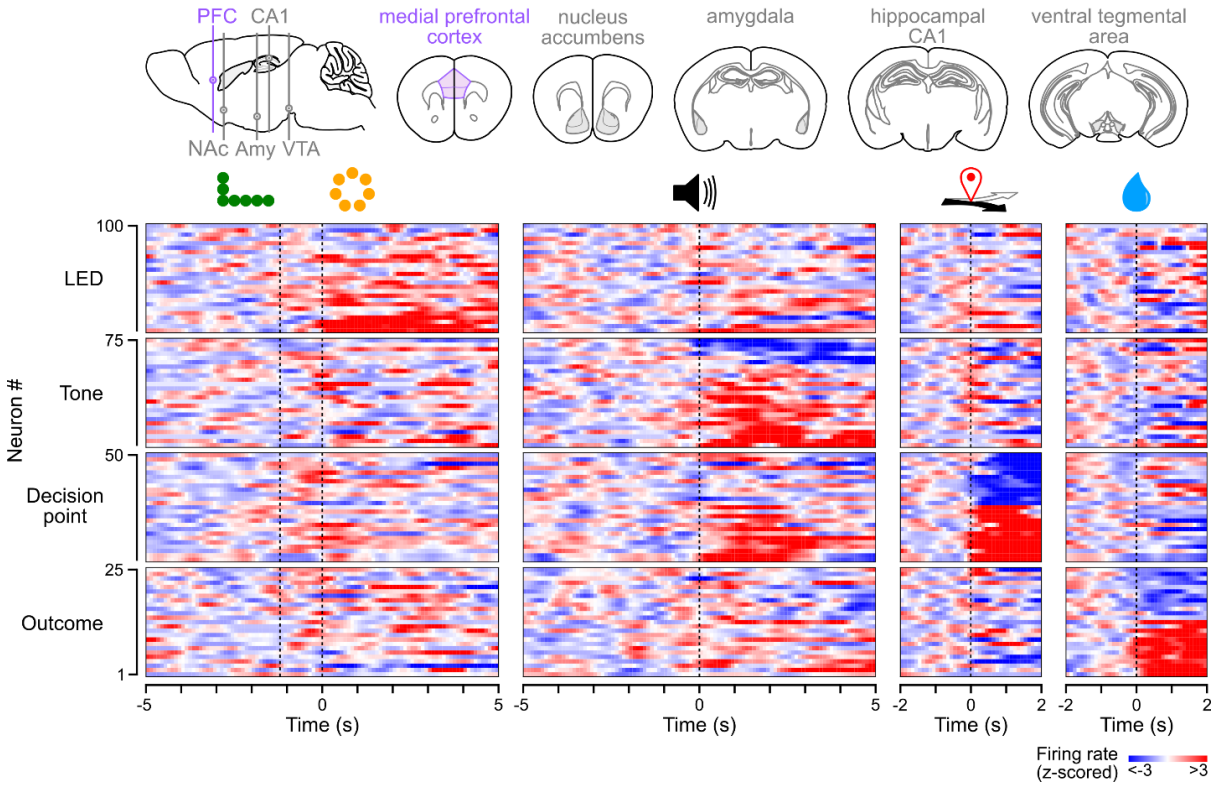

Fig. 19 Example single-neuron firing modulation to task variables in PFC.

Heatmap showing the average Z-scored firing rate (Hz) of example PFC neurons (one neuron per row) in response to each task variable. On the y-axis, neurons are organized according to their preferred task cue.

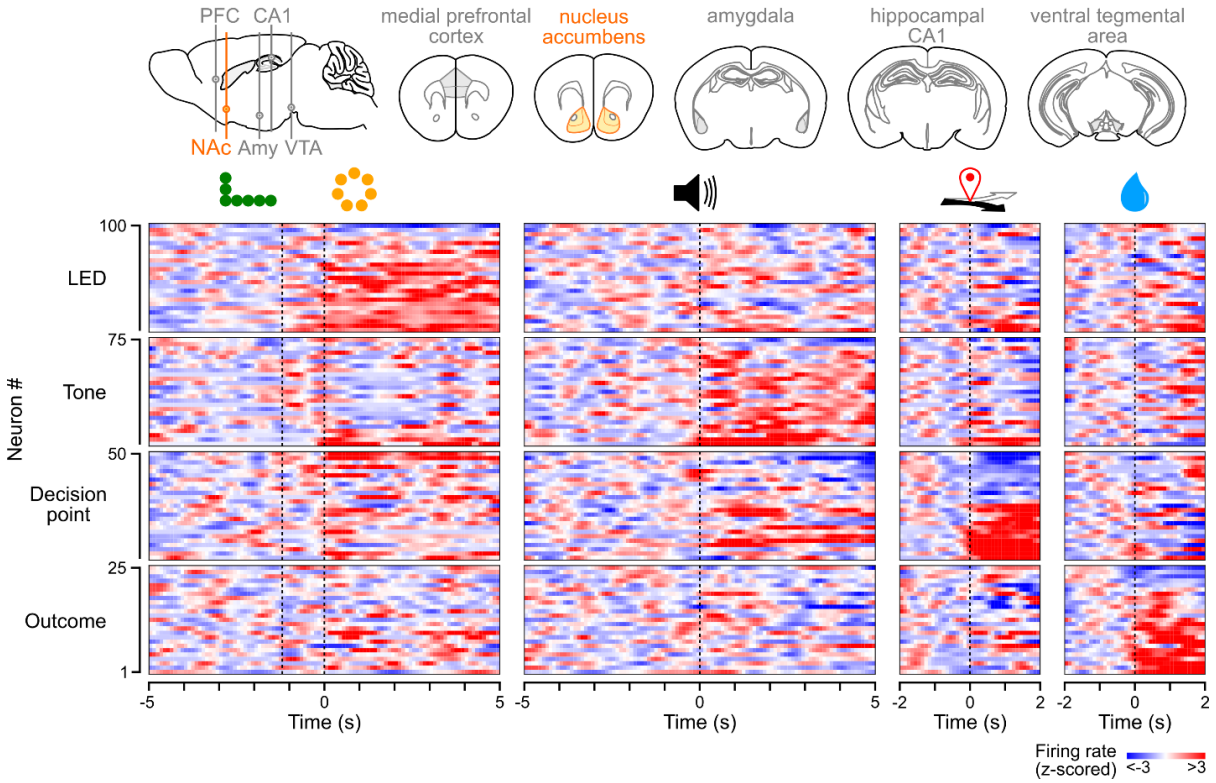

Fig. 20 Example single-neuron firing modulation to task variables in NAc.

Heatmap showing the average Z-scored firing rate (Hz) of example NAc neurons (one neuron per row) in response to each task variable. On the y-axis, neurons are organized according to their preferred task cue.

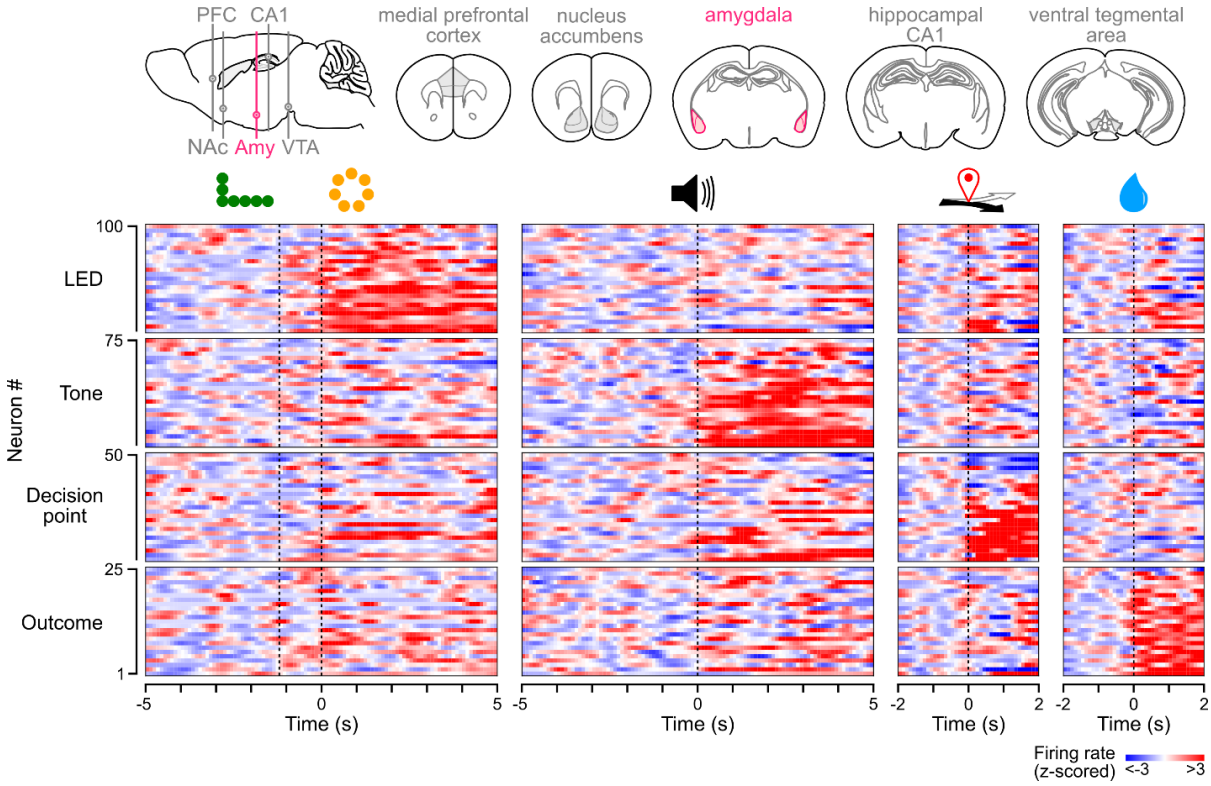

Fig. 21 Example single-neuron firing modulation to task variables in Amy.

Heatmap showing the average Z-scored firing rate (Hz) of example amygdala neurons (one neuron per row) in response to each task variable. On the y-axis, neurons are organized according to their preferred task cue.

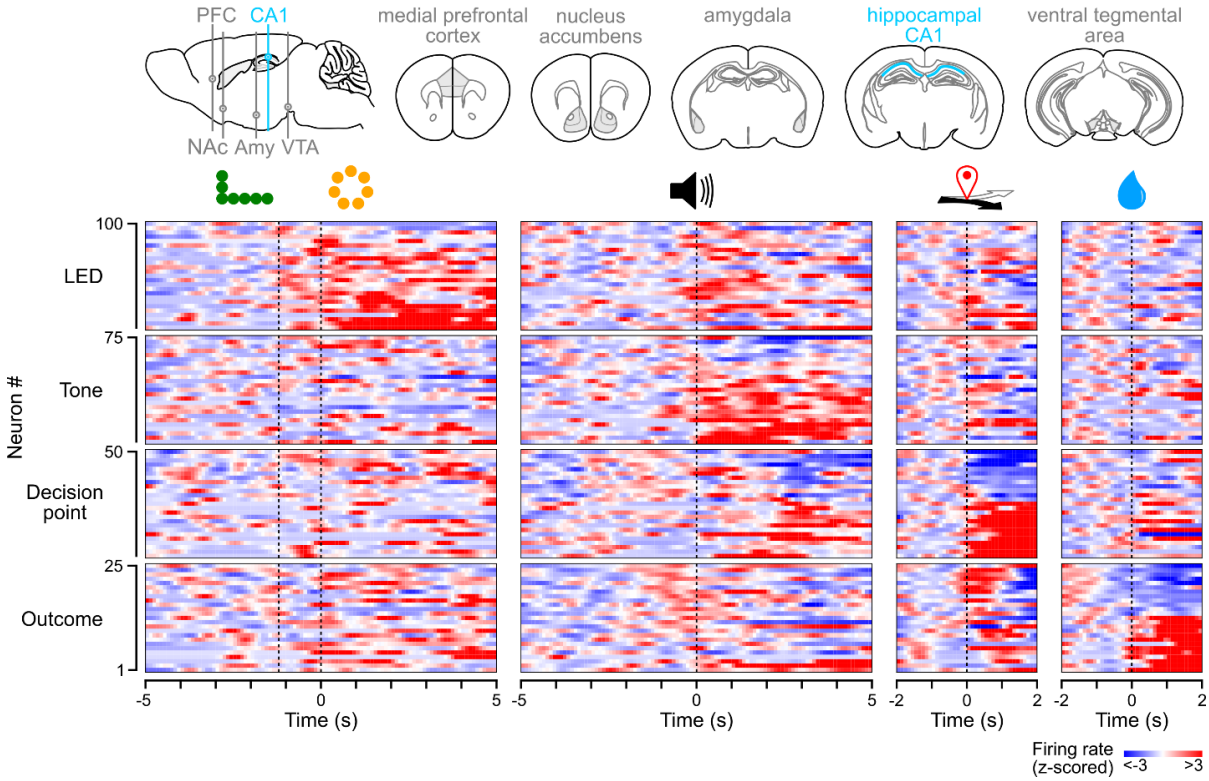

Fig. 22 Example single-neuron firing modulation to task variables in CA1.

Heatmap showing the average Z-scored firing rate (Hz) of example CA1 neurons (one neuron per row) in response to each task variable. On the y-axis, neurons are organized according to their preferred task cue.

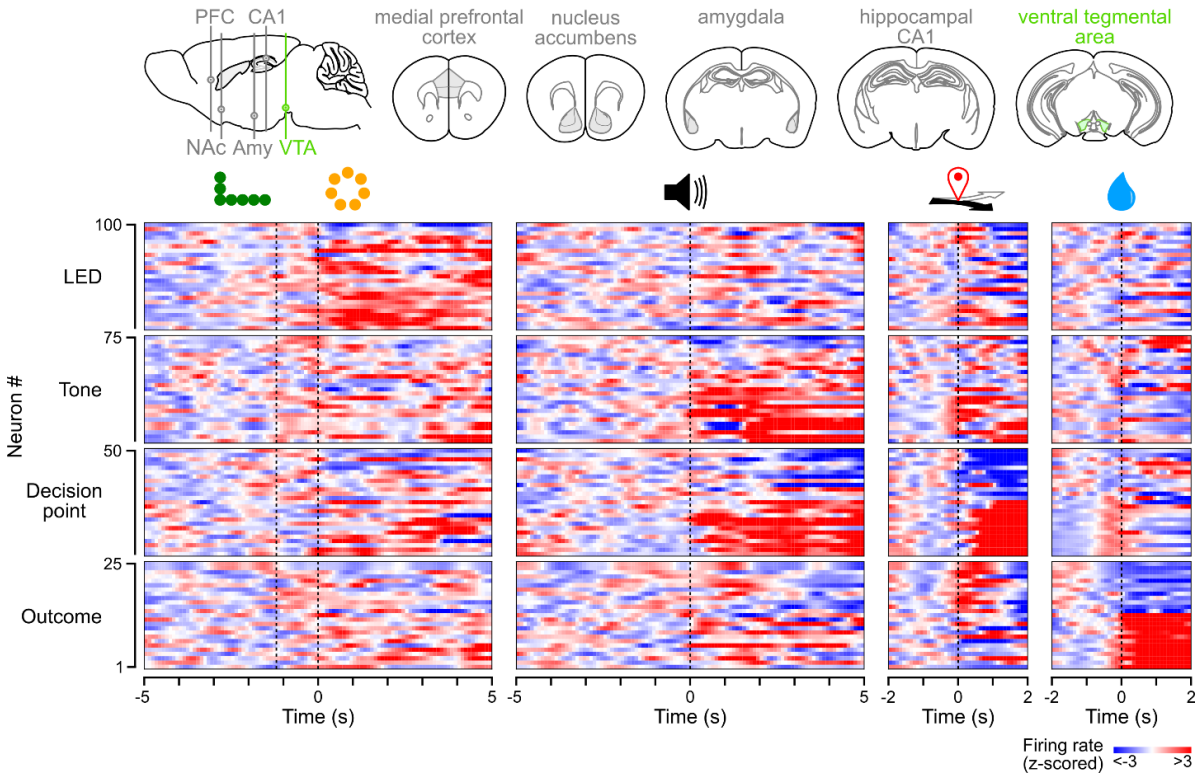

Fig. 23 Example single-neuron firing modulation to task variables in VTA.

Heatmap showing the average Z-scored firing rate (Hz) of example VTA neurons (one neuron per row) in response to each task variable. On the y-axis, neurons are organized according to their preferred task cue.

When expressing peak firing rates to a given task event as proportion of the sum of peak firing responses (of all behavioural task events), it becomes apparent that different brain regions exhibit a strong representational overlap. The proportions of represented task events are roughly similar across regions with the most strongly represented task event being the decision point in CA1, VTA, Amy and NAc (42.2, 42.1, 32.5 and 32.2%, respectively), and LED in PFC (30.1%) (Fig. 16). This indicated processing of multiple information streams in each brain region, yielding a substantial representational overlap between regions.

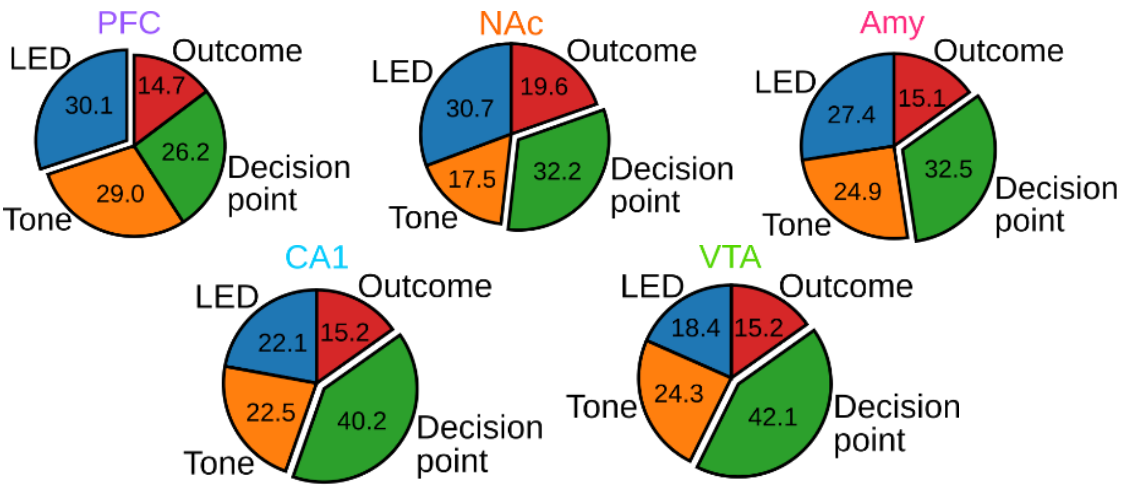

Fig. 24 Quantification of single-neuron representations of task variables within each brain region.

Each pie chart shows for one brain region the proportion of all task-event related z-scored firing rate changes attributed to a given task variable: LED, tone, “decision-making point” or outcome.

I next asked whether there were any differences with regards to conjunctive coding between the areas. To address this question, I created a ‘conjunction profile’ for each region consisting of conjunction scores for each possible stimulus pair in the following manner: for each given region I created separate population vectors for every stimulus. A population vector is composed of response scores to the given stimulus with the length equal to the number of neurons of the given region (i.e. one population vector each for LED, tone, decision point and drop consumption). Response scores were calculated as explained above as the maximum firing response standardised with respect to the baseline. Within each individual region I then computed the Pearson correlations between all possible combinations of the four population vectors. The resulting correlation coefficient is a measure of how correlated the responses of the neural population between different stimulus events are. I corrected the Pearson

correlation for each stimulus pair by subtracting the average of the null distribution, which was obtained by randomly shuffling response scores across neurons within the same region and same recording day. Only statistically significant Pearson correlations ($p<0.05$) were considered. Briefly, I created a firing-rate modulation score for each neuron based on the z-scored firing rate change from the baseline prior to the onset of the behavioural task event. Responses were binned in 100 ms bins windows and the largest positive or negative (whichever has the larger absolute value) value was taken as a response score. Across all regions, the strong correlations were obtained for the neural responses to the decision points during the sucrose and quinine conditions (Fig. 25). The VTA exhibited the most stimulus conjunctions. In addition, VTA, PFC and NAc but not CA1 and Amy showed strong stimulus conjunction between the decision point and tone during the sucrose condition. For VTA, PFC, Amy and CA1 the strongest negative correlations were between task events experienced during the two different contingencies. The only exception here was the negative correlation between quinine drop consumption and quinine-paired LED in CA1. This indicates that individual neurons in those regions responded with firing rate changes into opposite directions, i.e. inhibition versus excitation. Interestingly, the NAc did not follow this logic, and negative stimulus response correlations were both within the quinine condition indicating potentially less specialisation for contingency discrimination in the NAc compared to other regions. I observed positive correlations for stimulus events within and across the same contingency in all regions. Strikingly however, no two regions had the same conjunction profile. Instead, different regions exhibited unique combinations of conjunctions so that no single region but only several different regions together would

cover the entire space of possibilities. This indicates regional functional specialisation with respect to stimulus conjunction as opposed to single stimulus representation.

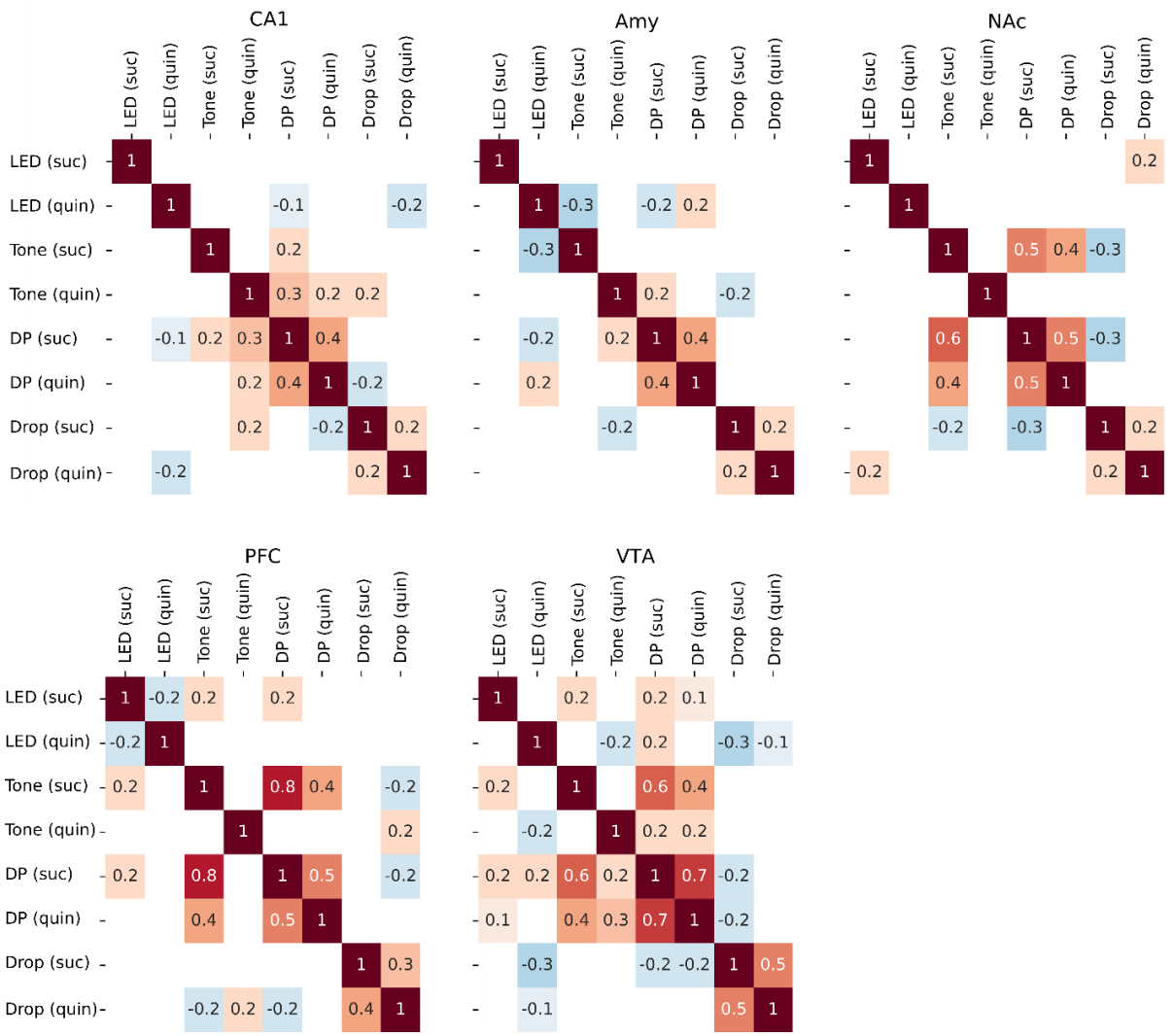

Fig. 25 Conjunctive stimulus coding by different brain regions.

Stimulus conjunction profiles for CA1, amygdala, NAc, PFC and VTA. The columns/rows of the matrix are organised as follows: LED (sucrose), LED (quinine), Tone (sucrose), Tone (quinine), decision point (sucrose), decision point (quinine), drop (sucrose), drop (quinine). DP stands for decision point. Each cell is the average Pearson correlation between the two stimulus representations. Numbers displayed in cells are the correlation coefficients of significant Pearson correlations ($p<0.05$).

4.3. Brain wide distributed cell assemblies

Next, I investigated whether I was able to detect behaviourally relevant representations at the population level across multiple brain structures, specifically in the form of co-firing assemblies. As in chapter 3 (Fig. 16), in order to detect such coactivity, I considered time intervals spanning off-trial epochs (i.e., time intervals before the tone and after the removal of the drop) when mice explored the task arena, using 25-ms windows as the timescale for cell assembly expression. A two-step statistical method estimated the number of coactivity patterns in the simultaneously recorded spike trains, and then extracted these patterns using the PCA/ICA assembly detection method (Fig. 26 A, see chapter 2.10 for methods). This approach yielded 78 co-activity patterns from 71.8±2.7 neurons recorded per day in 5 mice. Individual patterns exhibited sub-patterns (hereafter referred to as motifs) of local coactivity nested within CA1, PFC, NAc or Amy. Furthermore, consistent with our results from chapter 3 (Fig. 16), strong neuronal coactivity was further observed within the VTA (Fig. 26 B). Detected patterns further exhibited multiple within-region motifs of coincidental spiking, thus forming higher-order motifs of cross-structural coactivity (Fig. 26 A, B). Strikingly, VTA appeared to contribute the most to such distributed coactivity (Fig. 26 B, p=8.33e-8, Kruskal-Wallis). Between-region coactivity grouped neurons of anatomically directly connected structures (e.g., PFC and NAc) but would also group neurons of regions that are not directly connected (e.g., dorsal CA1 and Amy), thus opening the possibility that a common input functionally binds neurons distributed across regions at millisecond timescales.

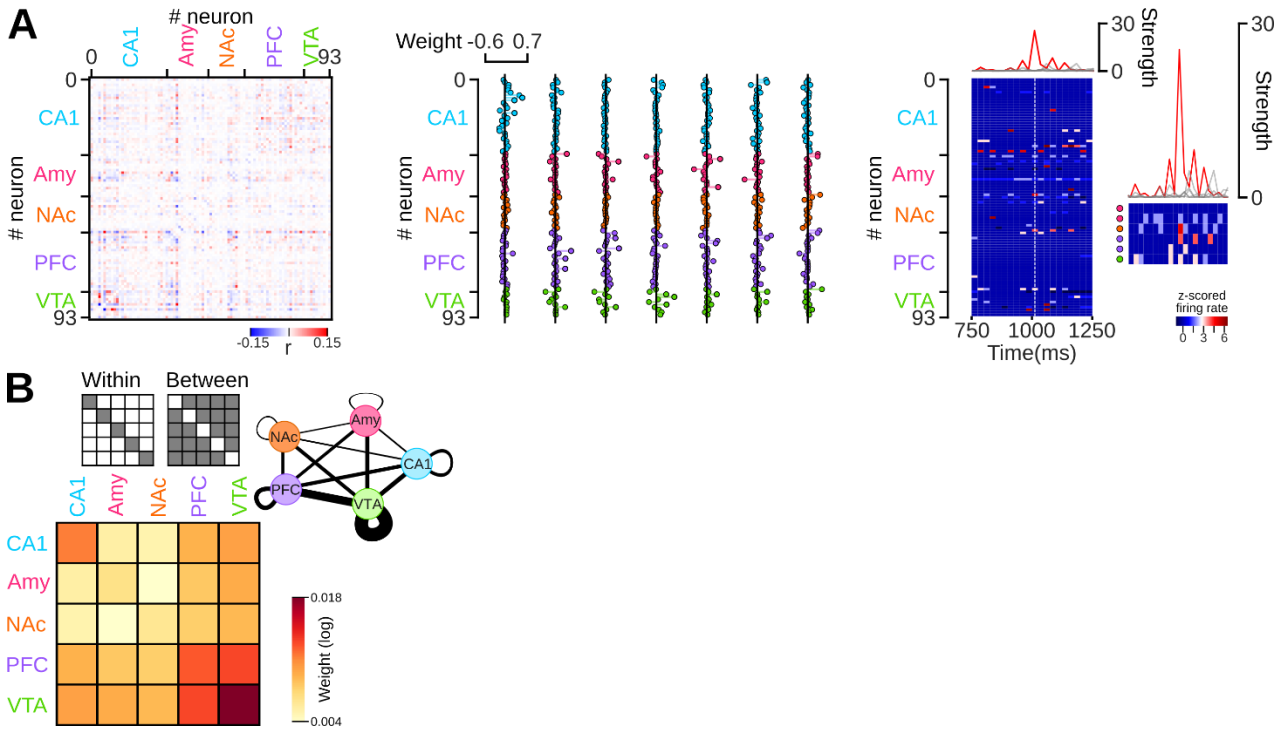

Fig. 26 Detection of cross-regional patterns of neuronal coactivity

(A) Detecting and tracking coactivity patterns. Shown for an example recording day, from left to right: correlation matrix for the spike trains of simultaneously recorded neurons, identified coactivity patterns (each of which is represented by a weight-vector indicating the contribution of each (color-coded) neuron to that pattern), and a 500-ms example z-scored spike trains with coactivity strength time course of the right-most weight-vector (red trace). Right inset: higher resolution showing, during the example (red) activation peak, the synchronized activity of the six (color-coded) neurons with the highest contribution to the right-most weight-vector. (B) Average contribution to coactivity patterns from neurons forming within-region (on-diagonal) versus between-region (off-diagonal) pairs. Coactivity strength represented using color-coded events in the (left) matrix and weighted edges in the corresponding (right) network graph.

Given the remarkably short timescale of co-firing across multiple brain structures, I sought to confirm the existence of the cross-structural co-firing patterns using other methods. To this end, I computed Pearson correlations between the spike trains of neurons with high contribution to detected patterns of coactivity (weight above/below two standard deviations of the mean assembly vector). I then formed pairs of such neurons with respect to the identity of both brain regions and coactivity patterns. That is, I considered neuron pairs of which the individual neurons were recorded in the

same brain region (within-region) or not (between-region), knowing whether these neurons had a high contribution to the same pattern (within-pattern) or to distinct patterns (between-pattern, Fig. 27 A). Consistently, neurons with high contribution to a given pattern's coactivity showed stronger temporal correlation with the spike trains of their co-members compared to neurons from other patterns (Fig. 27 A,B, p<1e-5, unpaired t-test). This confirms that the PCA/ICA method correctly identified cross-structural millisecond timescale synchronisation of single neurons.

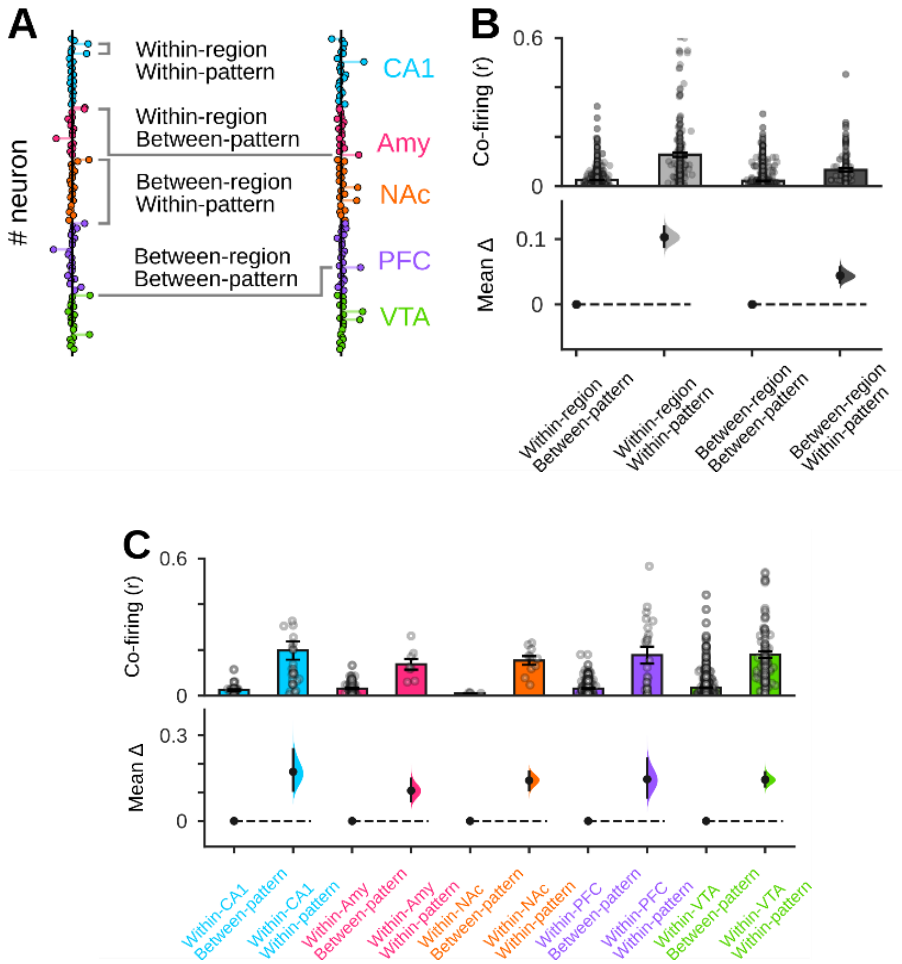

Fig. 27 Correlated spiking activity of neurons within and between brain regions.

(A) The Pearson correlation was computed between the spike trains of neurons with high contribution (assembly members, two standard deviations above the mean of the vector) to the detected patterns of coactivity. Pairs of such neurons were formed with respect to the identity of both brain regions and coactivity patterns. That is, I considered neuron pairs of which the individual neurons were recorded in the same brain region (within-region) or not (between-region), knowing whether these neurons had a high contribution to the same pattern (within-pattern) or to distinct patterns (between-pattern). (B) This distinction allowed to

compare co-firing of neurons, from left to right: (i) within the same region but not members of the same pattern (within-region between-pattern), (ii) within the same region and members of the same pattern (within-region within-pattern), (iii) from different regions and not members of the same pattern (between-region between-pattern), and (iv) from different regions and members of the same pattern (between-region within-pattern). Notably, the correlated activity between the neurons from different brain regions that are members of the same coactivity pattern, is substantially higher than the correlated activity of the neurons that are from the same region but belong to different patterns ($p<1e-5$, unpaired t-test). (C) This approach was leveraged to consider each brain region separately, by computing the Pearson correlation between the spike trains of the neurons within a given region and with high contribution to the same pattern (within-pattern) or not (between-pattern). Note the significant co-firing among VTA neurons members of the same pattern (within-VTA between-patterns versus within-VTA within-pattern: $p<1e-5$, unpaired t-test).

Additionally, I detected assembly patterns using tensor-component analysis (TCA) using the implementation provided in Python (Williams et al. 2018). This method relies on the construction of a tensor across the following dimensions: neuron identity, binned spike trains and trial number (but not trial identity). An unsupervised tensor decomposition method is then applied to extract lower dimensional patterns resulting in three vectors corresponding to the dimensions of neuron, time and trial for each TCA assembly (Fig. 28 B, C). As with the PCA/ICA method, I binned spike trains at 25 ms, which resulted in the detection of 51 TCA patterns. Since the contributions of neurons are expressed as weight vectors, I could analyse co-firing patterns in a similar fashion as the PCA/ICA method. Please note that the TCA method produces equivalent, but not necessarily the same assemblies, as inter-trial variability as a third dimension is taken into account with TCA. Using both methods, I assessed how much a given brain area would fire together with the other four brain regions. To address this question, I computed the average weight corresponding to such cross-regional interactions by applying a masking procedure (see chapter 2.10 for methodological details) to the ICA and TCA assemblies. For example, in order to assess the extent to which VTA neurons co-fire with the other brain regions, I selected only weights

corresponding to (VTA-CA1, VTA-Amy, VTA-NAc and VTA-PFC interactions). I found that regardless of which assembly detection method was used, co-firing activity between VTA and other brain areas was strongest (Fig. 28 A, B; ICA: p=8.3e-8; TCA: p=3.7e-25, Kruskal-Wallis). The next strongest cross-regional interaction was between PFC and other regions. Notably, for TCA assemblies, cross-regional interactions were markedly stronger for VTA than for PFC. Cross-regional interactions from CA1, NAc and Amy with other regions was equally strong. This point towards a central role of the VTA in organising cross-structural assembly activity. Furthermore, the similarity of characteristics obtained using the ICA and TCA methods further support the original results from the PCA/ICA method with regards to millisecond timescale cross-structural co-firing patterns. Lastly, I confirmed that the expression strength of cross-structural co-firing during ongoing behaviour is consistent with the co-firing weights of detected assemblies. To this end, I tracked assembly expression strength while the animal was in the task enclosure (Fig. 28 A). Indeed, the strength of cross-regional interactions is stronger when involving the VTA or PFC (Fig. 28 A, right panel, p=6.7e-7, ANOVA; all p<1e-3 for VTA and PFC compared to CA1, Amy and NAc, Tukey HSD adjusted p-values) mirroring the analysis of weight vectors. This highlights that cross-structural activity is recruited during ongoing behaviour and opens up the possibility of assembly activation in a task-relevant manner.

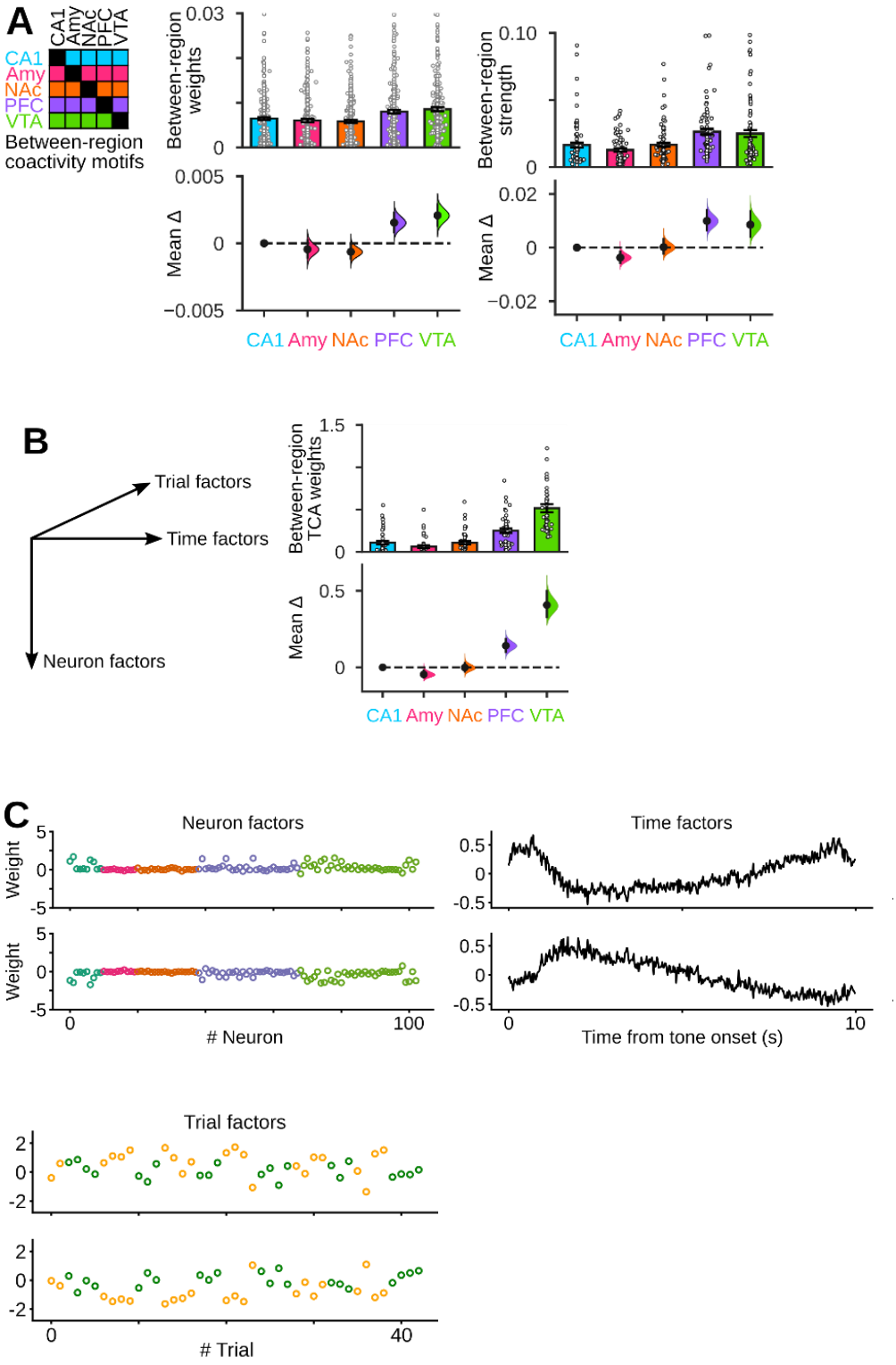

Fig. 28 Both PCA/ICA and TCA analyses highlight the central contribution of VTA neurons to cross-regional coactivity.

(A) Quantification of the contribution of each brain region to the coactivity motifs formed with the other four regions using the PCA/ICA analysis. Left: schematic matrix representing the selected (color-coded) pairs of brain regions used to calculate either the weight (middle) or the strength (right) contribution of each brain region to cross-regional co-firing. Middle: note that both VTA and PFC have the strongest weight contribution to cross-regional coactivity with

neurons of the other four regions (p=8.3e-8, Kruskal-Wallis). Right: Similarly, note that cross-regional coactivity strength during the task is stronger when involving either VTA or PFC neurons (p=6.7e-7, ANOVA). (B) Another analysis framework based on Tensor Component Analysis (TCA) allows exploring neuronal coactivity by extracting three low-dimensional descriptions of the data: neuron factors (reporting sets of coactive neurons), time factors (reporting time courses of coactivity) and trial factors (reporting trial-to-trial changes in coactivity). Note that when considering these three dimensions, VTA has the strongest contribution to coactivity involving neurons of the other four regions (p=3.7e-25, Kruskal-Wallis). (C) Shown for two example TCA-detected patterns (one per row) are the weight contribution of each neuron to detected coactivity, the time course of that coactivity pattern with respect to the onset of tone trials and the related trial-by-trial modulation of detected patterns. Please note that the TCA method is agnostic to the contingency of the trials and coloration was added for visualisation purposes afterwards (yellow: sucrose, green: quinine).

I next sought to explore the organisational principles of detected assemblies with respect to the task events represented by neurons forming the pattern. In other words: can I find evidence for Hebb's idea that rich perceptual representations are the result of co-firing neurons representing different mental items. To this end, I used the approach described previously (chapter 2.11) to assess representational similarity of neurons forming the assemblies. In short, single cells are assigned a vector describing the response magnitude to individual task events. This vector weighted by the contribution of the neuron to the assembly is then used to compute cosine similarity across the neurons/weights of an assembly pattern. The resulting cosine similarity is then corrected by subtracting the average of the shuffled null distribution and reflects the degree of representational similarity of cells contributing to the assembly. To investigate differences in co-firing patterns between the regions I applied this method to assemblies separately detected in the five regions. The number of analysed co-firing patterns were CA1=38, Amy=25, NAc=18, PFC=42 and VTA=39. In addition, I also used the patterns detected from across the five brain regions (n=78) and isolated only cross-structural co-firing pairs of neurons. I observed that all brain regions seem to group co-firing neurons based on representational similarity more than would be

expected by chance (p<1e-6 for all regions, paired t-tests against the respective shuffle distributions). This suggests the existence of a lower bound of representational dissimilarity governing the contribution of individual neurons to assembly patterns. However, there is inter-regional variability in this tendency: CA1, Amy and NAc neurons contributing to the same assembly are representationally more dissimilar than neurons in PFC and VTA. Interestingly, also cross-regional co-activity appears to be related to representational similarity (Fig. 29, p=1.4e-8 ANOVA). Post hoc tests revealed that Amy, NAc, PFC and VTA group neurons more strongly based on similarity than CA1 (p=1e-3 for all comparisons, Tukey HSD adjusted p-values). Furthermore, the representational similarity was greater within PFC assemblies compared to cross-structural co-activity (p=2.8e-3, Tukey HSD adjusted p-values). This suggests that co-firing activity is strongly related to representational similarity of neurons contributing to an assembly. Furthermore, this principle is expressed to varying degrees in different brain regions. However, differences appear to be small and it is unclear how biologically relevant these differences are.

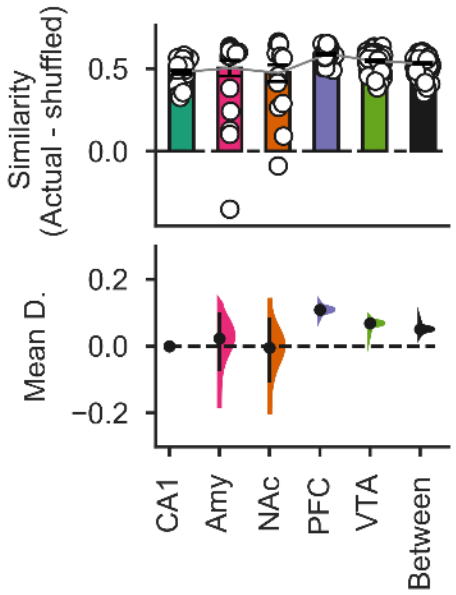

Fig. 29 Local and cross-structural assembly organisation with respect to behavioural task element representation.

Similarity scores of the firing rate responses to behavioural task events are weighted in proportion to the assembly vector weights of individual neurons. The resulting similarity scores are corrected by subtracting them from a shuffled distribution. All co-firing activity is related to representational similarity of neurons contributing to the pattern. Notably, co-firing of PFC, VTA and interregional neuron pairs ('Between') is more driven by representational similarity than co-firing activity in CA1, Amy and NAc.

Given the relationship of neurons forming assemblies to task variables, I next evaluated whether activation of cross-structural assembly patterns during the task carried task relevant information. To this end, I tracked their co-activity strength over time (Fig. 30 A). I found that coactivity patterns were stronger in the task arena compared to the task-unrelated arena that mice also explored each day (Fig. 30 C, p=1.26e-6, ANOVA). Moreover, pattern strength increased more during tone-initiated trials than during periods before tone presentation ('off-trial') (Fig. 30 C; change in pattern strength relative to task-unrelated arena: 'off-trials'=26.39±6.02% versus 'on-trials'=38.93±9.18%, p=1.2e-2, Tukey HSD adjusted p-value). Furthermore, I trained Naive Bayes classifiers to discriminate between the two task sets based on the pattern strength time courses. I found that assembly activity encodes the task sets more reliably during 'on trials' compared to 'off trials' (p<1e-5, paired t-test). This indicates that upon onset of a task-episode, as delineated by the onset of the tone, behaviourally meaningful co-activity of cross-structural assemblies is recruited. This prompted the question which regional motifs of co-firing this observation was driven by, specifically whether it is cross-structural or localised co-firing that drives the gain in behaviourally relevant assembly expression strength. To this end, I differentiated between weights describing local ('within' regions) or distributed co-activity ('between' regions) using the masking procedure (see chapter 2.10) and calculated the difference in decoder performance based on activity in 'on trials' versus 'off trials' ('decoder gain'). I found

that between-region coactivity motifs contributed more to decoding of task-cue contingencies once the trial was initiated compared to within-region motifs (Fig. 30 B, right; p=7.75e-3, paired t-test). These findings support task relevance of inter-regional coactivity.

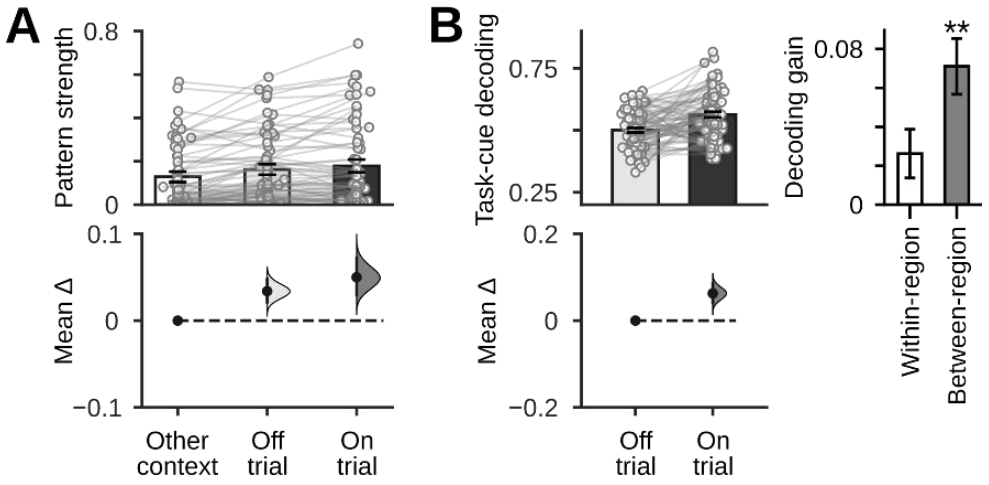

Fig. 30 Task-relevant activation of cross-structural assembly patterns.

(A) Average coactivity pattern strength was stronger in the task arena before tone presentation (Off-trial) than in another familiar control enclosure (Other context) and further increased during task trials (On-trial). (B) Task-cue contingencies were better reported by coactivity pattern time course during tone trials (left), a decoding gain explained by between-region coactivity motifs (right-inset).

4.4. Discussion

(i) Do different brain areas specialise in different behavioural task representations?

In this chapter I present evidence that firing rate modulation by behavioural task events is similar across different brain regions yielding a strong representational overlap. However, representational differences between brain regions become more apparent when investigating conjunctive coding of neurons of different areas. This leads us to ask the questions of how such representational similarity is achieved from a mechanistic perspective and why it makes sense for the brain to implement it.

Methodological considerations: Here, I report that firing rates of different brain regions are similarly modulated by different task events creating a strong representational overlap. However, single neurons of different brain regions appear to engage in different conjunctive codes. One limitation of our approach is the pre-selection of experimentally imposed and analytically investigated behavioural task events resulting in blind spots for potentially different responses to behavioural task events. Furthermore, it could be argued that a temporal overlap of behavioural events such as a tone and decision point might make it hard to distinguish between neuronal signatures belonging to separate events. However, since PSTHs are expressed as z-scores with respect to the baseline preceding the event onset, only additional increases on top of previous responses contribute to the scores. Furthermore, our approach of focusing on the magnitude of firing rate modulation is blind to temporal coding - as defined by sequential firing patterns or the relationship of spike timing to the LFP (Stefano Panzeri et al. 2010) - by single cells. However, at least sensory stimulus encoding by single neurons appears to be predominantly driven by the firing

rate while spike timing rather additionally boosts information content of single neuron spike trains (S. Panzeri et al. 2001; Kayser et al. 2009). Hence, I decided that I can reasonably accept this potential loss of information in favour of easier interpretability for the purpose of comparisons of inter-regional stimulus representations. Finally, within the chosen 25 ms time window of co-activity, not only direct monosynaptic connections, but also indirect polysynaptic between the regions may contribute to cross-structural co-activation. This means that it is not possible to make direct inferences from our sub-selected regions of interest whether co-activation is triggered via direct connections between the areas and which pieces of information (e.g. potential responses to task elements) have been transferred from one area to another purely based on co-activity.

Mechanistic and functional considerations: given the ascribed classical representational and behavioural roles of the brain regions under investigation (CA1: space, Amy and VTA: appetitive and aversive conditioned cues, NAc: cue-predicted reward outcomes, PFC: decision-making) (O'Keefe and Dostrovsky 1971a; Ambroggi et al. 2008; Sul et al. 2010; Lansink et al. 2012), I expected to find differences across the regions in the respective dimensions. However, I did not observe any striking functional specialisation of any region for a certain stimulus.

From a mechanistic perspective, such a representational overlap could be achieved anatomically by different but not mutually exclusive architectures. One extreme possibility is that all recorded regions inherit the same response properties from input originating from the same common upstream source. Such a source would need extensive anatomical connection to regions across the brain and receive inputs from areas covering a broad range of sensory modalities. For instance, the axonal arborisation of VTA projections could potentially provide a large part of the required

infrastructure. This is consistent with our findings showing the VTA has a very prominent role in co-firing patterns. In the other scenario, all regions are directly interconnected and share any processed information with each other, which inevitably leads to duplication of information across separate brain areas. For instance, recent graph-theoretical analyses of brain connectivity indicate that both solutions are utilised to some degree since the brain exhibits characteristics of a small world network (Bullmore and Sporns 2009). In such networks information is processed in local hubs consisting of multiple interconnected nodes and the output is then shared between interconnected hubs of the network. This idea has interesting implications in connection with our finding that different brain regions exhibit different stimulus conjunction profiles. In this scenario, single neurons in any given region or 'hub' specialise in certain combinations of stimulus conjunctions, which are then passed on to downstream target areas. Our findings suggest that it might be an oversimplification to ascribe unique functions to brain regions simply based on aggregate firing rate responses of single cells to individual stimuli. More refined approaches assessing multidimensional stimulus representations at the neuron level such as linear combinations of features (L. Chang and Tsao 2017), temporally multiplexed codes (Stefano Panzeri et al. 2010) or stimulus conjunction profiles might be more accurate at capturing representational differences between brain areas.

Our results provide new insights to the two-century-old debate on the localized versus distributed nature of brain function (Zola-Morgan 1995; Tizard 1959). In the functional localization framework, individual brain regions undertake specialized roles, reducing noise during information processing. Notably, the CA1, PFC, NAc, and Amy are thought to each use specific information streams for learned behaviours (O'Keefe and Dostrovsky 1971b; Kyriazi, Headley, and Paré 2020; Sul et al. 2010; Janak and Tye

2015; Peyrache et al. 2009). But here, neuronal correlates for sensory cues, behavioural actions and experienced outcomes all co-exist within each of these regions, in line with recent work showing that brain regions are less specialized than originally thought (Stringer et al. 2019; Steinmetz et al. 2019), and are also similar across regions. Understanding why the brain duplicates information across different brain regions to hold similar representations is an important challenge for neuroscientific research. One possible explanation might come from the redundancy versus degeneracy framework (Tononi, Sporns, and Edelman 1999): degeneracy refers to the ability of *structurally distinct events* to perform the same function. It is distinguished from redundancy because in the latter case, *similar events* perform the same function. Therefore, only from the perspective of the whole system it is possible to differentiate 'degenerate' events from 'redundant' ones. It is thought that like redundant components, degenerate events can contribute to the robustness to perturbation as they can functionally compensate for each other - provided the input into the system (i.e. environmental contingencies) remains constant. However, once the input to the system changes, degenerate events produce different output in response to changing conditions. This is not the case for systems built of redundant components. As a result, systems equipped with degeneracy are adaptable in addition to being resilient (Whitacre 2010). This concept is readily applicable to representational similarity across brain regions: while neurons of different brain regions represent similar behavioural events, their effect on the system and ultimately on the animal's behaviour is determined by their downstream projections. In line with this, I propose that the representational overlap across brain regions might not only support resilience but also adaptability of the brain and behaviour.

(ii) Are there behaviourally relevant co-firing assemblies across multiple structures?

Here I show that short timescale co-activation of neurons scattered across five brain regions exists by detecting co-firing assemblies using two unrelated and unsupervised methods. I further determine that the VTA appears to have a dominant role in the organisation of cross-structural assembly patterns. Our results suggest that assemblies are organised based on a certain degree of representational similarity of neurons forming the assembly. Finally, I show that cross-regional co-activity pattern strength is related to ongoing behaviour and bears information about behavioural task contingencies. These findings raise questions as to how such short timescale synchronisation spanning multiple brain regions is achieved mechanistically and what the benefits of the observed organisational principles could be.

Methodological considerations: In this study I report the successful detection of cross-regional co-firing patterns at a 25 ms timescale. As noted earlier (chapter 2.10), the PCA/ICA assembly detection method may have some inbuilt biases. First, there might be a firing rate bias in detection, which might skew cross-regional assembly detection towards regions with neurons that have higher average firing rates. However, this issue is addressed by z-scoring the spike trains relative to each neuron's own standard deviation and mean. If a neuron is particularly silent, this will lead to a very low standard deviation over time. This causes the z-score to rise and compensates for low firing frequencies by increasing variance that is picked up by the PCA/ICA assembly detection algorithm. Second, the variability in the number of neurons recorded from the different regions might bias the detected assemblies to be more dominated by one region over another. A possibility to counteract this would be to sub-sample the neurons that are used for assembly detection in a manner that equalises the number of cells from each region. However, this would severely reduce the number of pairwise interactions I could sample from and hence, introduce substantial noise in an already

challenging analytical paradigm (limited number of trials, short time windows of observation). Thus, I accept a potential bias towards regions with more neurons in exchange for a greater number of detected assemblies and noise reduction when tracking assembly strength over time. Importantly, this bias did not prevent the detection of cross-regional interactions.

Another important consideration is the low number of biological replicates. Variability electrode placement may result in very different pairwise co-activity strengths between regions depending on whether the recorded cells are directly connected with the other regions or not. As a result, in the Naive Bayes decoding analysis based on assemblies, not every assembly would encode the same aspect of the task and even if it did, the degree of encoding accuracy would vary. Furthermore, the assembly strength time course during the trials would also be expected to vary depending on the exact location of the electrodes. Post hoc confirmation of the recording sites is required and should be conducted in the future.

The remarkably short timescale for cross-structural co-firing activity of 25 ms prompted us to cross-validate detected assembly patterns using different methods. Both, the cross-correlation of assembly members and TCA method confirmed the existence of co-firing activity at this timescale. Interestingly, I noticed that for TCA assemblies, the VTA had by far the strongest weight contributions to cross-structural co-activity. This could be due to the fact that the TCA method detects patterns by taking into account the trial number. Hence, the resulting patterns might be more representative of inter-trial variability. This could indicate that cross-structural co-activity involving the VTA discriminates trials and possibly trial identity (Fig. 28 B ‘trial factors’) particularly well. This in turn suggests that the contribution of the VTA to cross-structural co-activity brings strong behavioural relevance into the assembly. Furthermore, I investigated

how behavioural task event representation by single neurons relates to assembly organisation in the different brain regions. To avoid contamination by other brain regions I detected assemblies only from cells of one single area at a time. The downside of doing so is that I was much more limited in the number of cells to sample from, especially in the case of Amy and NAc, which might explain the comparatively wide spread of similarity scores of those regions. I report co-activity within CA1, Amy, NAc and PFC in line with previous reports (Beyeler et al. 2016; Herry et al. 2008; Kyriazi, Headley, and Paré 2020; Peyrache et al. 2009)) and to our knowledge, for the first time in VTA.

Mechanistic and functional considerations: I observed a particularly strong average co-activation between CA1-PFC, VTA-CA1, VTA-NAc, VTA-Amy and VTA PFC. Consistent with previous literature, the CA1-PFC co-activation may serve memory retrieval that depends on contextual information (Schacter, Harbluk, and McLachlan 1984; K. A. Corcoran and Maren 2001). Co-activity between VTA-CA1 could support learning and modulate entry of new hippocampal dependent information into long-term memory through dopaminergic modulation of synaptic connectivity (John E. Lisman and Grace 2005). The VTA-PFC interaction may reflect either modulation of prefrontal decision-making via dopaminergic VTA fibers (Ellwood et al. 2017). VTA-NAc projections may be driving co-activity related to reward seeking as well as aversive behaviour (Ambroggi et al. 2008; Qi et al. 2016). Lastly, the projection from VTA to Amy may contribute to the salience of adverse events, such as quinine delivery in our task (Wei Tang et al. 2020). It should be noted that the absence of strong co-activity between regions on average does not mean that there are no individual cell pairs that there is no meaningful co-operation. There may simply be fewer of such connections, but these may not necessarily be functionally less important. One interesting question

to follow up on would be whether co-activity strength directly correlates with the strength of anatomical connectivity or with the impact it has on behaviour. One question is how the brain manages to synchronise neuronal firing across brain regions at such short time scales. One possible explanation is oscillatory activity which forms well defined periods of excitation and inhibition parsing neuronal firing into defined chunks of synchronicity (Buzsáki 2010). It has been shown that gamma oscillations support localised cell assembly formation, for instance in the hippocampus and the PFC (Kenneth D. Harris et al. 2003; Sirota et al. 2008). At the same time, it has been suggested that while local synchronisation is driven by fast oscillatory activity (e.g. in the gamma range), slower oscillations promote long range synchronisation (von Stein and Sarnthein 2000) at longer time scales, an idea that has been supported by more recent studies of PFC-Amy and PFC-hippocampus oscillatory coupling (Fanselow 2019; Roy et al. 2017). This suggests that while oscillations are likely to contribute to such short time scale brain wide synchronization (e.g. through nesting mechanisms (John E. Lisman and Jensen 2013) there might be other mechanisms to help synchronise neurons at millisecond timescales across different and possibly not even connected brain areas. Consistent with this notion I detected short timescale cross-regional co-activity between neurons of anatomically directly connected structures (e.g., PFC and NAc) but would also co-firing between regions that are not directly connected (e.g., dorsal CA1 and Amy). This opens up the possibility that a common input functionally binds neurons distributed across regions of not connected regions.

Another important question is why the brain synchronises firing activity of brain cells distributed across different brain regions in the first place. Generally, it is thought that the formation of assemblies is best understood from the perspective of a downstream reader neuron, which would only fire if a sufficient number of presynaptic neurons are

activated simultaneously, and hence, reflect the integration of the upstream neurons forming co-firing assembly (Buzsáki and Watson 2012). Consequently, neurons representing different pieces of information (e.g. from different modalities) can be bound in space and time to create rich representations. This makes sense as long as neurons that are bound together represent sufficiently different mental items. Interestingly, I observed that in assemblies, neurons with a strong degree of representational similarity are grouped together. Importantly, however, such representational similarity was not complete. This might reflect a balance between a need for a degree of representational flexibility on one side and the necessity to ensure a baseline representational similarity in order to ensure reliable co-activation on the other side. Hence, this may be reflective of a trade-off between flexibility at the behavioural level and reliability on the mechanistic level. One could imagine a scenario in which global synchronisation is driven by a certain degree of representational similarity across neurons of different brain regions. This similarity driven co-activation across regions sparks task-relevant activity within different brain regions in a localised manner, which in turn triggers region-specific computations (e.g. region-specific stimulus conjunctions). The output of these computations can then be shared with other components of the network. This is reminiscent of the parallel distributed processing framework, which posits that the whole system's constraints are reduced by incorporating multiple sub-systems devoted to different tasks. Furthermore, the authors argue that partial activity patterns can trigger the retrieval of whole patterns in such systems (Rumelhart and McClelland 1987). However, the authors of this seminal work were not able to expand on the mechanistic details or the distribution of computation across different brain regions. I suggest that PDP in the brain might be

enabled through co-activation of neurons scattered across different regions based on a minimally necessary degree of representational similarity.

5. CHAPTER 5: ROLE OF GLUTAMATERGIC VTA CELLS IN BRAIN-WIDE ASSEMBLY ORGANISATION

5.1. Introduction

In the previous chapter I have shown that ongoing behavioural task performance is accompanied by cross-structural assembly activation at millisecond timescales. Furthermore, I observed that the VTA occupied a privileged role in the organisation of cross-structural co-firing activity. This prompted us to investigate what the mechanisms behind such precisely timed synchronisation would be. Such mechanisms would have to be temporally precise, acting globally (or at least across the five brain structures I recorded from) and behaviourally relevant. With this in mind I hypothesised that glutamatergic inputs from the VTA could broadcast the fast synaptic transmission latencies (Jonas 2000). Consistent with this idea, glutamatergic VTA neurons have previously been shown to provide excitatory inputs to the PFC, NAc, Amy and CA1: using electrical stimulation in the VTA, one early study demonstrated that it is possible to evoke electrophysiological responses which are indicative of monosynaptic connections in the rat frontal cortex (Mercuri et al. 1985). Subsequent research has shown that glutamatergic VTA neurons synapse onto GABAergic neurons in the PFC and only exert a modest effect on pyramidal cells (Lavin et al. 2005; Kabanova et al. 2015). Anatomical tract tracing studies confirmed that dual glutamate-dopamine and glutamate-only neurons innervate the PFC (Yamaguchi et al. 2011). The same authors demonstrated that this was also true for glutamatergic projections from the VTA to the NAc. Consistently, optogenetic stimulation of genetically identified dopaminergic neurons in the VTA using ChRh2 demonstrated that glutamate-mediated excitatory postsynaptic potentials could be induced in the NAc (Stuber et al. 2010). Furthermore, optogenetic activation of

glutamatergic fibers from the VTA triggered spiking in NAc-GABAergic interneurons, which inhibited neighbouring medium-spiny neurons, the excitatory output cells of the NAc (Qi et al. 2016). Moreover, anatomical studies confirmed the existence of glutamatergic projections from the VTA to the Amy (Hnasko et al. 2012). Lastly, one recent study showed that optogenetic stimulation of glutamatergic VTA inputs into CA1 reliably induces pyramidal cell spiking (Adeniyi, Shrestha, and Ogundele 2020). However, one criticism of this study has been that the supramammillary nucleus may have been transfected in these experiments and hence, projections may not be attributable to the VTA. In light of these anatomical and functional connectivity studies I formulated the following two questions addressed in this chapter:

(i) Can glutamatergic VTA neurons entrain simultaneous spiking activity in CA1, Amy, NAc and PFC?

(ii) Is glutamatergic VTA neuron spiking necessary for cross-structural assembly formation?

Several previous studies have investigated the role of glutamatergic VTA neurons in behaviour. Optogenetic activation of glutamatergic VTA cell bodies produces appetitive behaviour (H.-L. Wang et al. 2015) in a dopamine dependent manner indicating excitation of neighbouring dopaminergic neurons or co-release of dopamine by VGlut2-expressing cells. Other studies demonstrated that activation of glutamatergic VTA fibers to the NAc and the lateral habenula drives aversive conditioning (Qi et al. 2016; Root, Mejias-Aponte, Qi, et al. 2014; Lammel et al. 2015) pointing towards a role in negative memory formation and expression. In line with this, recent work demonstrated that cell-type specific permanent ablation of glutamatergic VTA neurons abolishes innate defensive behaviour (Barbano et al. 2020).

Consistently, the firing rate of the majority of glutamatergic VTA cells increased during an aversive stimulus (airpuff) while the remaining cells decreased firing rate (Root, Estrin, and Morales 2018). Interestingly, the same study reports that amongst the neurons which responded to an increase in firing rate were neurons that also responded to reward delivery leading to the conclusion that glutamatergic VTA cell function is heterogeneous: one part of the glutamatergic VTA population responds to aversion whereas the other one signals general salience (Root, Estrin, and Morales 2018). Furthermore, a recent study showed that chemogenic inactivation of glutamatergic VTA fibers to the dorsal hippocampus prevents the acquisition as well as expression of context-specific fear memory (Han et al. 2020). However, in this study supramammillary nucleus transfection may have led to the effects observed. Interestingly, this procedure also impaired the retrieval of conditioned place preference memories, confirming a more general role of glutamatergic VTA neurons in signaling salience in addition to simply negative memories as reported in earlier studies cited above (Han et al. 2020). Furthermore, another study suggested that the specific role of glutamatergic VTA neurons in aversive versus appetitive behaviour may depend on the VTA subpopulation as defined by their presynaptic inputs (Montardy et al. 2019). Here, our study shows the effects of optogenetic silencing of glutamatergic VTA neurons on behavioural performance when there are ambiguous sets of stimuli combining multiple, negative as well as positive task elements. With this in mind, the third question addressed in this chapter is:

(iii) Is glutamatergic VTA neuron spiking necessary for the performance of a behavioural task requiring the discrimination of ambiguous sets of stimuli?

5.2. Brain-wide single unit responses to optogenetic stimulation of glutamatergic VTA neurons

In order to investigate whether glutamatergic VTA neuron firing could elicit simultaneous spiking activity in CA1, Amy, PFC and VTA, I transduced neurons expressing the vesicular-glutamate transporter-2 (Vglut2) with the blue light (473 nm)-driven neural activator channelrhodopsin-2 (ChR2)-eYFP while performing quintuple-site recordings in two mice (Fig. 31 A, B). For the recordings, animals were placed in a familiar environment or in a sleep box (see chapter 2.14 for methods). I recorded the following number of cells: CA1= 282, Amy = 199, NAc = 161, PFC = 240, VTA = 68. During each recording session, a total of 700 laser pulses were delivered with one pulse every every 8±2 seconds. Light delivery elicited robust responses in VTA neurons at different latencies. For the following number of cells the firing rate increased by two standard deviations above the mean within a 20ms window following the delivery of the light pulse: CA1=167 (59.2%); Amy = 135 (67.8%), NAc = 55 (34.2%), PFC = 82 (34.2%), VTA = 33 (38.5%) (Fig. 31 D, E). I classified cells as VGlut2-positive based on a significant firing rate increase (two standard deviations above the mean of the baseline prior to laser delivery) within a 4ms window following light delivery. This way, I identified 10 glutamatergic VTA neurons (4 and 6 cells from two separate mice), which fired the first spike following optogenetic stimulation on average after 1.2±0.15ms and reached their peak firing rate after 2.3±0.1ms (Fig. 24 C, D). Following the activation of these glutamatergic VTA cells, I observed a wave of excitation within the VTA with neurons reaching peak firing rates at slower latencies of up to 25 ms and was on average 9.6±1.0 ms following laser delivery (Fig. 31 E). In this VTA cell population, the average latency to the first spike in this population was 2.8±0.32 (Fig. 24 C). The existence of a second, slower responding population of VTA

cells suggests that glutamatergic VTA cells form excitatory synapses onto neighbouring cells in the VTA, triggering a wave of excitation through the local VTA microcircuitry, which is consistent with previous reports (Dobi et al. 2010).

Strikingly, optogenetic stimulation triggered a similar wave of excitation in the other four regions at similar latencies observed in the population of the VTA cells that responded more slowly to optogenetic stimulation (Fig. 13 E). Latencies to the first spike following laser pulse delivery were PFC=2.6±0.18ms, NAc=4.0±0.27ms; Amy=3.8±0.18ms, CA1=3.6±0.15ms. These responses appear after the 1.2 ms response latency of opto-tagged glutamatergic VTA neurons and hence, are suitably within the range of monosynaptic glutamatergic transmission. Furthermore, it is important to keep in mind that the probability of efficiently entraining spikes in the postsynaptic targets of glutamatergic VTA cells is very high, since transfected neurons have been activated as a population by the optic fiber above the VTA. The latency from laser onset to the peak firing peak response was: PFC=12.6±0.6ms, NAc=11.9±0.8ms; Amy=12.3±0.4ms, CA1=16.0±0.3ms (Fig. 32 C, D). Our results are consistent with previous reports showing functional glutamatergic connections between VTA and NAc/PFC (Mercuri et al. 1985; Lavin et al. 2005; Yamaguchi et al. 2011; Stuber et al. 2010), CA1 (Adeniyi, Shrestha, and Ogundele 2020) and Amy (Hnasko et al. 2012). Additionally, I noticed that glutamatergic VTA neuron activation produced a prolonged activation increase in firing rates in downstream regions which is sustained beyond the point when the cell reaches its peak response (Fig. 31 E). Our findings demonstrate for the first time simultaneous firing rate increases across five brain regions in response to glutamatergic VTA neuron activation indicating that glutamatergic VTA neuron firing is sufficient to elicit cross-structural spiking co-activity within a 25 ms time window.

Building on this idea, I hypothesised that I could be able to identify glutamatergic VTA neurons that fire prior to assembly activation. In order to address this idea, I cross-correlated peak activation times of assemblies with spike timing of all VTA cells previously recorded during task performance. Similar to previous studies, to determine peak activation times of assemblies, I used timestamps where assembly activation exceeded five standard deviations above the mean (van de Ven et al. 2016). I found three VTA neurons that showed significantly increased firing prior to CA1-Amy-NAc-PFC assembly peak activation (e.g. example neuron in Fig. 31 C). Consistently, these neurons were classified as glutamatergic in the classification framework described in chapter 3 (Fig. 13). I did not find any VTA cells that increased their firing rate prior to assembly activation in the dopaminergic clusters opening up the possibility that this could be a specific characteristic of VGlut2-expressing VTA neurons.

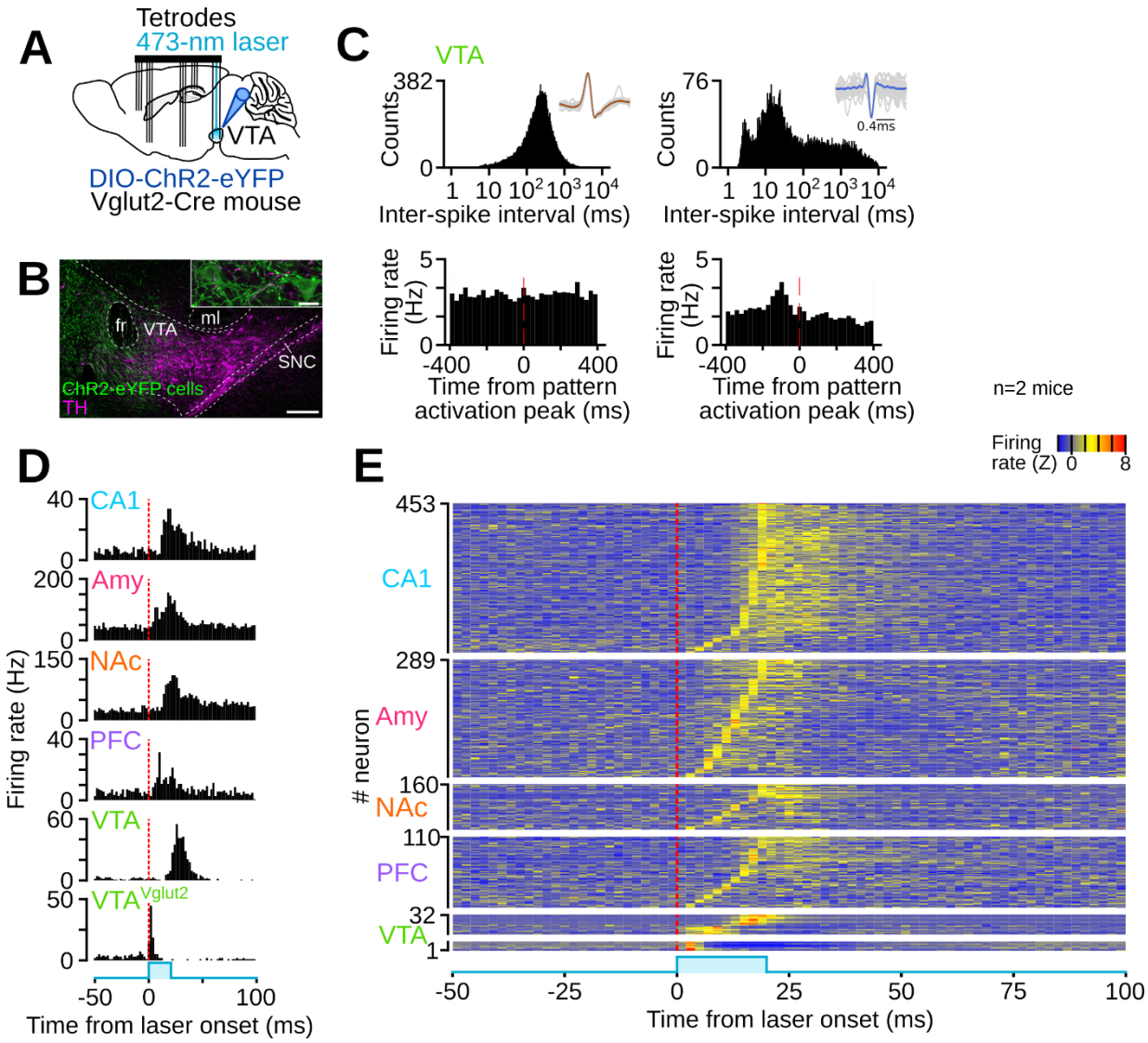

Fig. 31 Glutamatergic VTA neuron spiking entrains PFC-NAc-Amy-CA1 co-activity.

(A,B) Quintuple-brain-region recording layout with bilateral VTA optic fibers (B) targeting ChRh2-transduced glutamatergic Vglut2 VTA neurons (B scale bar=200 micron; inset: 20 micron). (C) Shown for two example VTA neurons (one per column) simultaneously recorded during the task: inter-spike interval (ISI) distribution, (color-coded) average spike waveform and firing rate with reference to activation peaks of cross-regional patterns detected using neurons from the other four regions. These two neurons were classified as putative dopaminergic (left) and glutamatergic (right) cells, respectively. Note the increased firing of the putative glutamatergic VTA neuron (with shorter ISIs) before neuronal co-activation distributed across PFC, NAc, CA1 and Amy. (D) Example single-neuron firing response to optogenetic stimulation of VTA Vglut2 neurons. (E) Optogenetic stimulation of VTA Vglut2 neurons entrains spiking activity spreading from VTA to PFC, NAc, Amy and CA1.

I next went on to investigate the fidelity of the temporal dynamics of the wave of excitation triggered by glutamatergic VTA cell stimulation. In other words, is the observed sequence of single-cell firing an artifact of temporally ordering cells by average response latency or is the sequence reliably reproducible across trials? To this end, I constructed a jitter score based on the following logic: I split the 700 laser pulse delivery trials 500 times randomly into two equally large sets and ranked the latency to peak firing for each cell for both sets independently. The difference between the position of the two cells hence is a measure of the trial-by-trial jitter of a cell's position in the sequence. Furthermore, with this approach I could leverage the advantage of maintaining a high number of sample trials to compute reliable PSTHs while destroying their chronological relationship. Jitter scores were computed as follows: I first ordered the cells based on their latency to reach peak firing rate (as shown in Fig. 31 E) so that the index of each cell would denote the ordered position of the cell in the sequence. I expressed the jitter of a given cell around its position in the sequence as the normalised absolute difference of the cell's position in one versus the other random set of trials. This procedure was repeated 500 times and for each cell I computed the average jitter from those repetitions. Normalisation was performed with respect to the number of cells to be ranked, which allowed us to compare jitter of cells from different brain regions. A value of 0.5 indicates a completely random position of a cell in the sequence, whereas 0 means no jitter at all. I found that the average jitter was: VTA-VGlut2=0.29±0.05, VTA-non-VGlut2=0.13±0.02, PFC=0.28±0.04, NAc=0.17±0.03, Amy=0.25±0.03, CA1=0.34±0.07. The results are visualised as the average position of each neuron during one laser trial set versus the other averaged over 500 trials. This resulted in a clear diagonal across the matrix (Fig. 32 E). Our findings show that glutamatergic VTA neuron firing elicits a wave of excitation across

downstream target regions and within each region the elicited sequence of neuronal firing follows a non-random order.

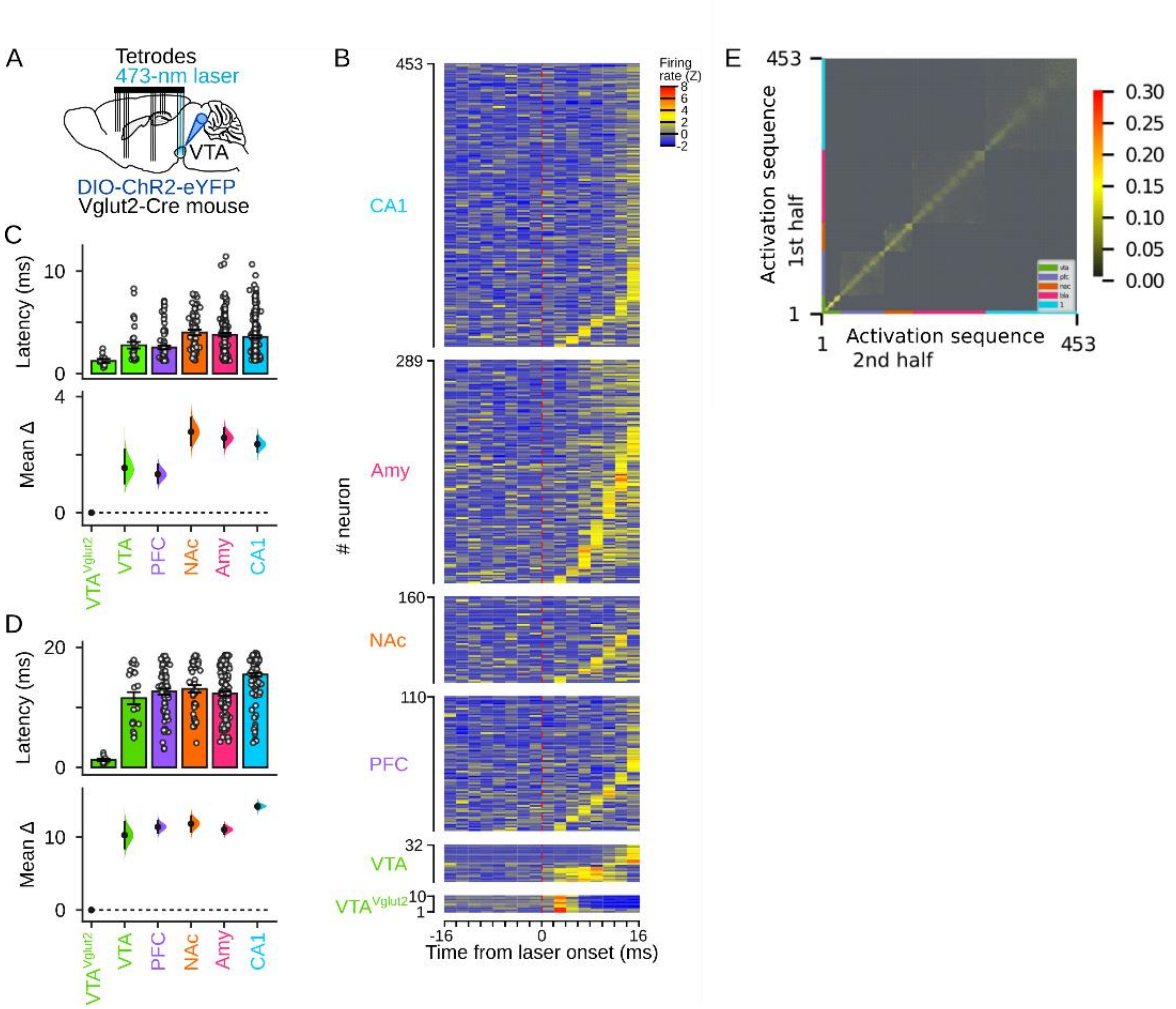

Fig. 32 Cross-regional effect of optogenetic activation of glutamatergic Vglut2 VTA neurons.

(A) Glutamatergic VTA neurons of Vglut2-Cre mice were transduced with DIO-ChR2-eYFP. Blue light was delivered using optic fibers targeting VTA while simultaneously monitoring neuronal spiking in VTA, PFC, NAc, CA1 and Amy with tetrodes. (B) Higher temporal resolution of the spike matrix shown in Fig. 31. Note that optogenetic VTA stimulation of glutamatergic VTA neurons entrains neuronal spiking in all recorded regions, from VTA to PFC, CA1, NAc and CA1. (C, D) Latency of spike response of non-opto-tagged VTA neurons and PFC, NAc, Amy and CA1 neurons following optogenetic activation of Vglut2 VTA neurons. Each data point represents one neuron. (C) Mean±SEM latency from laser onset to first spike response (D): Mean±SEM latency from laser onset to firing peak response. (E) Reliability of temporal dynamics response to optogenetic stimulation. Laser delivery trials were randomly split into two sets (i.e. the two axes) and neurons were ranked according to their latency to peak response following the laser delivery for both sets. Each row/column is one neuron and each pixel is the average of 0 or 1 for the position of the neuron in the 2D coordinate system over 500 randomly picked splits. Please note the clear

diagonal indicating little jitter of individual neurons around their position in the temporal activation sequence following laser pulse delivery.

5.3. Effects of optogenetic silencing of glutamatergic VTA neurons on distributed assemblies

To determine whether glutamatergic VTA projections form a diverging pathway that is required for distributed coactivity, I transduced Vglut2-expressing VTA neurons with the yellow light (561nm)-driven neural inhibitor Archaerhodopsin-T (ArchT; Fig. 33 A, B). Consistent with previous reports, Vglut2-expressing VTA axons densely innervated many brain regions including PFC, NAc, Amy and CA1 (Fig. 33 C) (Bariselli et al. 2016; Adeniyi, Shrestha, and Ogundele 2020; Morales and Margolis 2017). In our experimental design I considered the following potential behavioural confounds: first, if I were to lock the laser delivery to certain behavioural events such as the tone offset (i.e. drop delivery) the animal might get conditioned to the laser as opposed to sensory task cues. In order to avoid such optogenetic conditioning effects, I silenced glutamatergic VTA neurons for the time covering the entire task period, i.e. starting with the onset of the tone until the removal of the drop and added a temporal jitter of ±0.5-2.5 seconds prior and after the task period. Second, I considered the possibility that animals could unlearn the behavioural paradigm during the task if the stimulus-outcome (i.e. tone-liquid) contingencies would become unreliable. This scenario is contingent on optogenetic intervention influencing behavioural performance and optogenetic trials being mixed with non-optogenetic trials. To reduce such effects, I decided to apply optogenetic stimulation in a separate session. Accordingly, mice first experienced a non-optogenetic session followed by a 1h break. Subsequently mice were subjected to the task once again but with optogenetic intervention. Afterwards, I ensured that the animal was fit to perform the task on the next day by retraining mice

after a three-hour break at the end of the day. I found no significant difference in the performance between the session before laser delivery and the retraining session (p=0.89, paired t-test).

In these three Vglut2VTA::ArchT-GFP mice, I detected 81 co-firing patterns during 21 task-days and tracked their expression strength throughout the task period (using the assembly tracking procedure described in chapter 2.10). The task period encompassed the time from tone onset to the removal of the drop. Importantly, I focused on cross-structural assemblies formed by the four downstream regions only (PFC, NAc, CA1 and Amy) by applying the masking procedure (see chapter 2.10 for methods) to isolate only co-activation not involving the VTA. This way, our analysis would not be confounded by local optogenetic silencing of VTA neurons. Optogenetic silencing of glutamatergic VTA neurons during the tone-initiated trial periods (Fig. 33 D) prevented the dynamic strengthening of patterns distributed across the other four downstream structures compared to trials without optogenetic intervention. In fact, optogenetic silencing reduced cross-structural co-activity strength towards the non-specific strength levels seen in the control arena (Fig. 33 E; p=1e-4, ANOVA). This effect cannot be explained by a time-dependent change in assembly expression or laser pulse administration itself as light delivery did not affect assembly strength in Vglut2VTA::GFP-only control mice (Fig. 33 E; p=0.36, paired t-test, n=71 assemblies from 2 mice and 18 task-days). I cross-validated the reduction in co-activation strength in Vglut2VTA::ArchT-GFP mice by computing co-firing coefficients (Pearson r) between cell-pairs of significant members within a given assembly. Significant assembly members were defined as neurons with absolute weights of more than two standard deviations of the assembly vector. Co-firing coefficients for local and cross-regional co-activity was significantly reduced by light delivery (Fig. 33 G, p=3.7e-10

and p=4.1e-19, respectively, Mann-Whitney U-test). Finally, I tested for the ability of assemblies to encode the task sets by training Naive Bayes classifiers to discriminate between task-cue contingencies based on the assembly activation time course during the tone-initiated trials. As expected, decoding task-cue contingencies from PFC-NAc-CA1-Amy co-activity was impaired during VTA light delivery in Vglut2VTA::ArchT-GFP but preserved in Vglut2VTA:: GFP-only mice (Fig. 33 F; p=0.014, paired t-test). These results demonstrate that glutamatergic VTA neurons are necessary for cross-regional assembly activation.

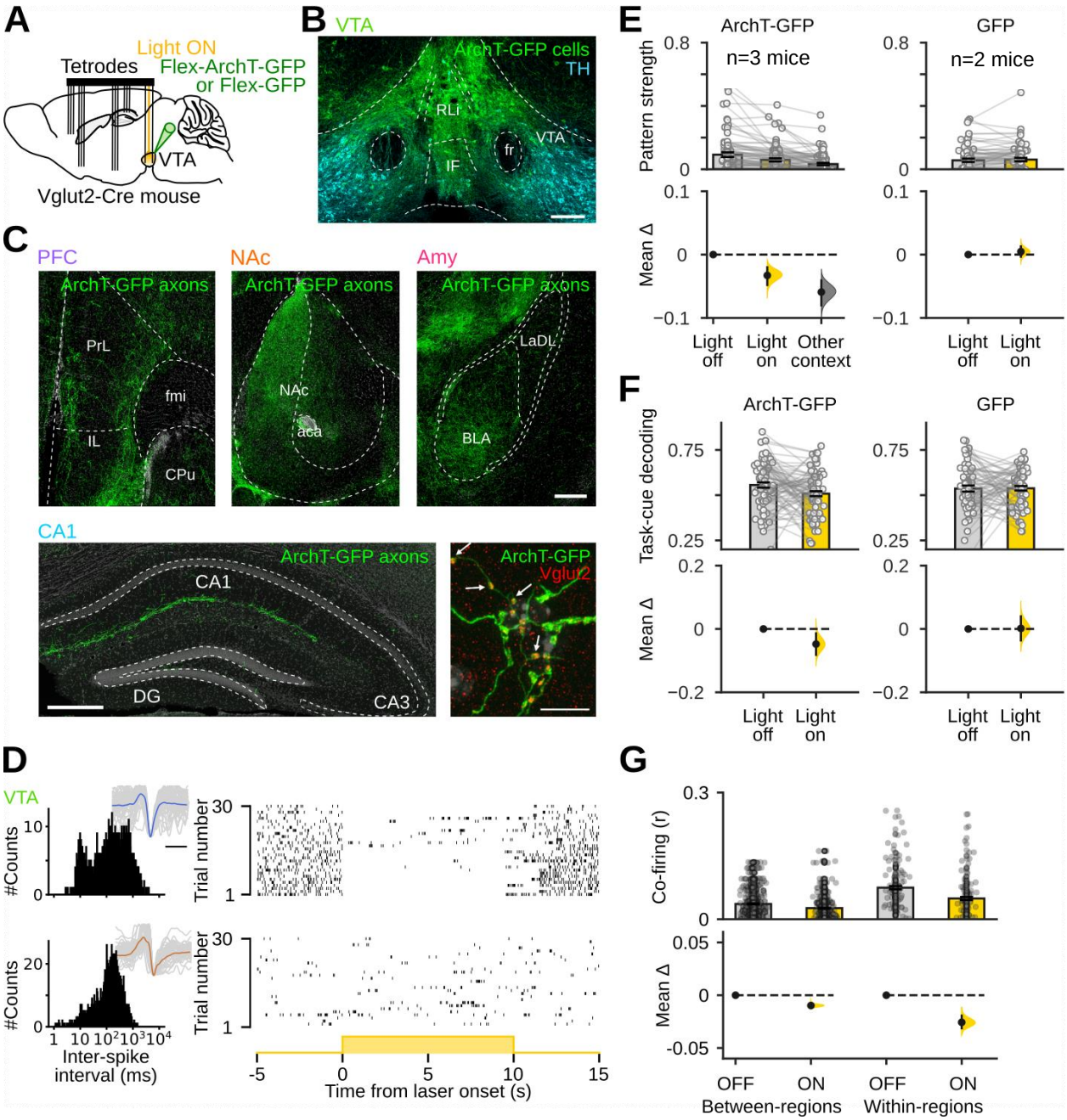

Fig. 33 Glutamatergic VTA neurons support cross-regional co-activity.

(A) Glutamatergic VTA neurons of Vglut2-Cre mice were transduced with either ArchT-GFP or GFP-only. Yellow light was delivered using optic fibers bilaterally targeting VTA while simultaneously monitoring VTA, PFC, NAc, CA1 and Amy neuronal spiking.(B, C) ArchT-GFP expression in VTA cell bodies (B; with tyrosine hydroxylase staining) and their axons observed in PFC, NAc, Amy and CA1 (C) of a Vglut2VTA::ArchT-GFP mouse. Cell nuclei stained with DAPI (grey). Bottom-right inset: high-magnification confocal picture of ArchT- and Vglut2-expressing axon terminals in CA1. (D) Shown for two example VTA neurons (one per row) simultaneously-recorded in a Vglut2VTA::ArchT-GFP mouse: example spikes (grey traces) with superimposed mean waveform (color-coded trace) above inter-spike interval distribution (left) and raster plots of spike discharge with respect to light delivery (right). Note the optogenetic suppression of the top cell indicating its Vglut2 profile. (E-F) VTA light-delivery in

Vglut2VTA::ArchT-GFP mice, but not control Vglut2VTA::GFP mice, disrupts cross-regional (PFC-NAc-Amy-CA1) co-activity towards non-specific levels seen in the control (task-unrelated) enclosure (E; each point represents one assembly from 3 ArchT-mice and 2 GFP-control animals), impairing co-activity pattern decoding of contingencies (F; each point represents one assembly from 3 ArchT-mice and 2 GFP-control animals). (G) Visualisation of changes in correlated spiking (co-firing) among neurons recorded across PFC, NAc, Amy and CA1 (between-region motifs of co-activity) or among neurons recorded within either PFC, NAc, Amy or CA1 (within-region motifs of co-activity) in Vglut2VTA::Arch-T mice during the two-contingency task. OFF: no VTA light delivery (gray); ON: 561-nm VTA light delivery during tone trials (yellow). Top panel shows the mean±SEM Pearson correlation coefficient for each condition (color-coded bar charts), with each data point representing the co-firing coefficient for a given cell pair. Bottom panel displays the mean change in co-firing caused by optogenetic silencing of Vglut2 VTA neurons for between-regions and within-region co-firing. Fluorescence microscopy and immunohistochemistry was conducted by Laura Lefevre and Ben Micklem.

5.4. Effects of optogenetic silencing of glutamatergic VTA neurons on behavioural performance

Silencing experiments were conducted in 3 ArchT animals and 2 GFP control mice. The number of behavioural recording days was 22 and 18, respectively. Since the recording days cannot be treated independently from each other, the statistics on behavioural experiments are underpowered and more behavioural experiments in separate mice will be required in the future. Nonetheless, I observed consistent trends across all animals. In line with our findings at the assembly level, silencing of Vglut2 VTA neurons during the task episode prevented successful behavioural performance of Vglut2VTA::ArchT-GFP mice as reflected by the complete abolishment of the preference score (Fig. 34 A; OFF: 0.6±0.09, ON: 0.1±0.06, n=3 mice, p=1.4e-2, paired t-test). This effect was not observed in GFP-control mice (Fig. 34 A; average sucrose preference score for first animal: OFF: 0.39±0.1, ON: 0.47± 0.1; second animal: OFF: 0.74±0.14, ON:0.74±2.4). This bears the question of what the reduction of the preference score was driven by; a change in preference for sucrose, quinine or both. I calculated the ratios of trials during which the mouse would approach the dispenser out of the total number of trials for each condition separately. I found that approach

behaviour towards the dispenser during the quinine condition was unaffected by laser delivery (Fig. 34 B; OFF: 0.54±0.01, ON: 0.54±0.04, n=3 mice, p=0.91, paired t-test). In contrast, mice approached the dispenser significantly less frequently during light delivery in the sucrose condition (OFF: 0.81±0.03, ON: 0.56±0.06, n=3 mice, p=0.02, paired t-test) and in fact approach ratios dropped to the levels of quinine trials without light delivery (n=3mice, p=0.78, paired t-test). This opens up two possibilities: first, the animal is unable to distinguish between the two task sets. Or second, the valence of or motivational drive to acquire sucrose is reduced upon silencing glutamatergic VTA cells. In order to test for this possibility, the same mice performed a simple pavlovian conditioning task whereby the same tone was paired with the delivery of sucrose at a dispenser. Importantly, mice learned and performed this task in a separate spatial enclosure in order to avoid any contextual cross-contamination from our main behavioural paradigm. The optogenetic silencing protocol was the same as during our main behavioural task. I discovered that simple silencing glutamatergic VTA neurons did not affect sucrose approach behaviour during a simple pavlovian conditioning task (Fig. 34 C; n=3 mice, p=0.12). Hence, I conclude that glutamatergic VTA neuron activity is necessary to perform a task in which conflicting task-related cues require disambiguation to decide on approach versus avoidance.

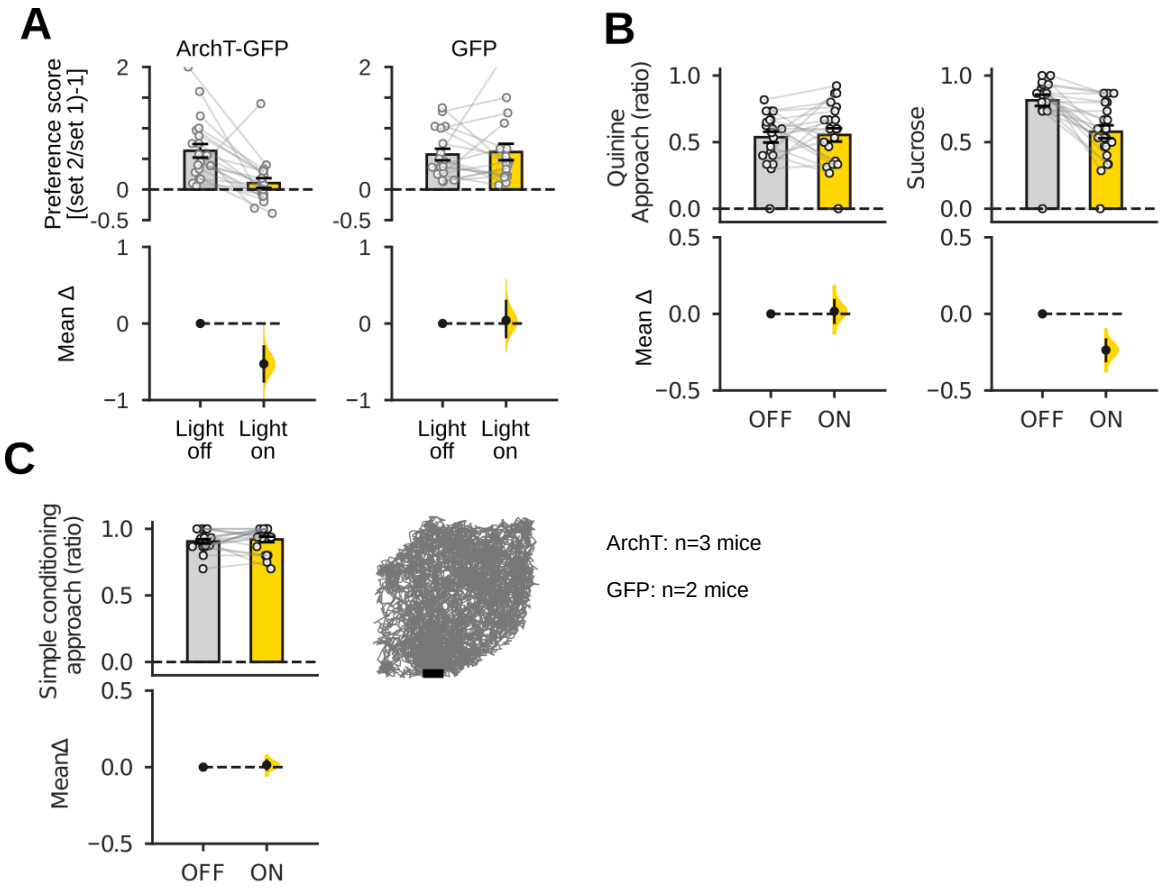

Fig. 34 Glutamatergic VTA neurons are required for successful task performance.

Individual recording days are shown as data points. Please note that statistics have been calculated from mouse-averages, not sessions (except for GFP controls, where individual mouse averages are listed).(A) Optogenetic silencing of glutamatergic VTA neurons in VGlut2VTA::Archt-GFP mice prevents the expression of a preference for sucrose over quinine. Light delivery had no impact on behavioural performance in VGlut2VTA::GFP-control animals. (B) Silencing of glutamatergic VTA neurons had no impact on the frequency of approach towards the dispenser during the quinine condition but reduced approach behaviour during the sucrose condition towards the levels seen in quinine trials. (C) Left: dispenser approach during a simple Pavlovian conditioning task in which the availability of a sucrose drop was signalled with the same tone remained unaffected by light delivery in VGlut2VTA::Archt-GFP animals. Right: enclosure in which the animal performed the simple conditioning task mapped out with animal positioning traces. The black rectangle shows the position of the liquid dispenser. This task was performed by the same animals in a different arena. (A-C) Every dot is one recording day.

5.5. Discussion

In this chapter I show that optogenetic activation of glutamatergic VTA neurons causes synchronous firing activity in downstream target regions, namely PFC, NAc, Amy and CA1. Using optogenetic silencing, I demonstrate that glutamatergic VTA neuron activity is not only sufficient but also necessary for the full expression of cross-structural co-activity. In chapter 4 I demonstrated that cross-structural assembly activation is linked to successful behavioural performance. Consistently, when assembly formation is impaired through silencing of glutamatergic VTA neurons the animal approaches the dispenser during the sucrose and quinine condition with equal frequency. In the following pages, I will discuss methodological, mechanistic and functional considerations of our findings.

(i) Can glutamatergic VTA neurons entrain simultaneous spiking activity in CA1, Amy, NAc and PFC?

Methodological considerations: I chose a 20ms laser pulse to closely match the timescale of the assembly detection window. One concern could be that the duration of the laser pulse would skew the response kinetics of VGlut2VTA-neurons and their postsynaptic targets. However, I found that opto-tagged VGlut2VTA-neurons were silent immediately following peak firing rate (Fig. 32 C) excluding the possibility of prolonged firing locked to the laser pulse. In fact, despite glutamatergic neurons being silent, excitation carried on locally suggesting a regional chain of excitation following glutamatergic VTA cell activation. Our results indicate that this temporal sequence of neuronal firing in this wave of excitation was non-random. The assessment of such temporal stability can be confounded by the following factors: first, are there enough laser-deliveries to obtain a sufficiently precise PSTH to calculate the time-to peak

latency? However, I found that 350 light pulses produced robust PSTHs in all five recorded regions. Second, plastic changes during light delivery might have influenced population response dynamics as a function of time. I sought to avoid such effects by leaving sufficiently long gaps with a random jitter between the laser deliveries (8±2sec). Third, are excitatory effects due to glutamatergic transmission alone or are they mixed with dopaminergic signaling? The sources of such a confound could be either due to the optogenetic activation of dual VGlut2VTA-positive neurons co-releasing dopamine and glutamate (Morales and Margolis 2017) or glutamatergic VTA neurons exciting neighbouring dopaminergic cells (H.-L. Wang et al. 2015). One possible concern is that spiking activity in other brain areas could be the result from antidromic stimulation of retrogradely transfected neurons. Another concern is the transfection of other target areas, such as the supramammillary nucleus located directly below the VTA. If this was the case, then cross-structural activity may have been driven by other regions and not glutamatergic VTA neurons. Although I used only 150 nl of viral injections via a glass pipette to enhance precision, transfection of other brain areas needs to be tested for in a formal histological analysis. Since dopamine acts on slower-scale metabotropic receptors modulating postsynaptic excitability (Tritsch and Sabatini 2012), it is unlikely that immediate responses at monosynaptic timescales are due to dopaminergic transmission. However, prolonged excitation in the target regions may have partly been caused or at least modulated by dopamine release.

Mechanistic and functional considerations: The short-timescales with response latencies of 2.6-4.0 ms indicate monosynaptic connections between glutamatergic VTA neurons and the PFC, NAc, Amy and CA1, which is consistent with previous functional and anatomical connectivity studies (Mercuri et al. 1985; Lavin et al. 2005;

Yamaguchi et al. 2011; Stuber et al. 2010; Adeniyi, Shrestha, and Ogundele 2020; Hnasko et al. 2012). I furthermore observed sustained activation in all of these regions, which could be explained by the following not mutually exclusive mechanisms. In the first scenario, glutamatergic inputs into a downstream region trigger a cascade of excitation propagating through the local microcircuitry. Previous studies have shown that glutamatergic VTA fibers synapse onto GABAergic interneurons in the NAc (Qi et al. 2016) and in the PFC (Kabanova et al. 2015). In light of this, it is possible that the first neurons to respond to the TTL pulse in our experiment are interneurons altering the excitation-inhibition balance of the local circuitry in such a way that triggers a wave of excitation. In chapter 3 I showed that glutamatergic VTA cell firing is related to behavioural task elements. In line with this observation, glutamatergic VTA inputs may serve as the initial behaviourally relevant impulse that triggers local task-related computations such as stimulus conjunctions (as described in chapter 4, Fig. 33) and possibly others such as pattern completion (Colgin, Moser, and Moser 2008) or pattern separation (Sahay, Wilson, and Hen 2011). This way the VTA may serve as a centralised hub that sparks downstream parallel computing processes in a coordinated fashion in other hubs of the network. The second possibility is that glutamatergic terminals cause excitation in other (not recorded) regions, which project to one or more of the five (recorded) regions causing a polysynaptic summation of response latencies in our target regions. The third option is that dopamine from co-releasing or polysynaptically activated dopaminergic neurons triggers slow changes in membrane conductance via metabotropic G-protein-coupled receptor signalling (Tritsch and Sabatini 2012) leading to spiking activity at later latencies. All these mechanisms likely contribute to some degree to the temporal dynamics of the wave of excitation spreading through the different brain regions following glutamatergic VTA cell spiking.

I observed that the wave of excitation exhibited a relatively stable sequence of single-cell activations. However, this sequence was not perfectly static and exhibited some degree of flexibility. Beyond the methodological factors discussed above, variability in the sequence could arise from biological determinants: for instance, the network state during which the laser pulse was delivered (Kelly et al. 2010), the probability of spike transmission following laser delivery, which is in turn dependent on synaptic properties such as quantal release probability, postsynaptic receptor density, identity and cellular geometry (Citri and Malenka 2008; Augustine and Kasai 2007; Freche et al. 2011) and presence of polysynaptic pathways accumulating probabilistic effects. In our experiments, CA1 exhibited the largest jitter, which may reflect the fact that glutamatergic VTA fibers largely target the stratum lacunosum moleculare and pyramidal neuron spiking is less reliably induced due to dendritic filtering (Dudman, Tsay, and Siegelbaum 2007). The relatively high jitter in the PFC might be a consequence of the fact that glutamatergic VTA axons tend to terminate preferentially on GABAergic interneurons and have only a modest effect on pyramidal cells (Kabanova et al. 2015). Ultimately, regardless of the mechanism, from the functional perspective, such jitter could be beneficial as it may support memory flexibility and updating and hence, behavioural adaptation (Mau, Hasselmo, and Cai 2020).

Another important question is whether the same glutamatergic VTA neuron can entrain spiking activity in different brain regions via a monosynaptic pathway or whether one cell projects to one region only. There is limited availability of single-cell tracing studies. While different multi-regional arborisation patterns have been confirmed for dopaminergic neurons (Aransay et al. 2015), there is no such data on specifically identified glutamatergic VTA neurons yet. However, one previous study identified TH-negative neurons projecting to the forebrain and brainstem in mice (Aransay et al.

2015). This opens up the possibility that one single glutamatergic neuron can send the same information and trigger behaviourally appropriate synchronised activity in different brain regions. However, generalizability of this idea across different rodent species might be put into question as another study in rats found that VTA neurons generally project only to one target region (Swanson 1982). Finally, multiple glutamatergic neurons with different downstream projection targets could be locally synchronised (as shown in chapter 3, Fig. 16) and thus, trigger co-activity in a broader range of downstream regions. One interesting future area of investigation would be to determine whether these glutamatergic inputs are subject to synaptic plasticity themselves. This would vastly expand the computational possibilities of a distributed processing network across different hubs and hence, support behavioural flexibility.

(ii) Is glutamatergic VTA neuron spiking necessary for cross-structural assembly formation?

Methodological considerations: In our study, I decided to silence the somata of glutamatergic VTA neurons. However, this approach makes it impossible to discern the effects of individual pathways on cross-structural assembly activity. For instance, it is possible that part of the assembly activity is driven by direct connections between VGlut2VTA cells and their downstream targets. The remainder would be attributable to indirect polysynaptic connections. Furthermore, our approach cannot distinguish between behavioural effects exerted by glutamate-only cells, dual glutamate-dopamine neurons (Zhang et al. 2015) and dopamine-only neurons that would normally receive excitatory input from neighbouring glutamatergic cells (H.-L. Wang et al. 2015). In fact, dopaminergic activity has been previously suggested to promote

striatal assembly formation in computational models (Humphries, Wood, and Gurney 2009).

Another concern is potential retrograde transfection of target areas. However, even if this is the case, laser exposure of the somata in target areas would be extremely limited, since the optic fibres were implanted above the VTA. However, this does not exclude antidromic stimulation. Additionally, during an initial visual inspection of target regions no transfected somata were detected (Fig. 33). Nonetheless, a formal histological quantification is required. Furthermore, it is possible that other regions, such as the supramammillary nucleus were transfected and hence, confounded effects on assemblies and behaviour, as it is implied in contextual memory formation and expression (Shim et al. 2018). Similarly, this needs to be shown histologically in the future.

Moreover, silencing experiments were conducted in only three animals. Hence, inter-animal variability in electrode placement may have impacted the composition of assemblies hence, the effect of silencing glutamatergic VTA cells on cross-structural assembly strength. Furthermore, different transfection rates across animals may result in variability affecting the effectiveness of perturbing cross-structural assembly formation. My colleague Laura Lefevre attempted to limit variability by using aliquots from the same batch for all mice and used glass pipettes for viral injections to enhance precision. Nonetheless, more mice will be required in the future to gain statistical robustness.

Another consideration is whether there was a time-dependent difference in assembly strength from sessions without optogenetic stimulation to sessions without light delivery. However, the fact that GFP-only control mice did not exhibit any changes in

assembly strength between the two sessions, this speaks to the stability of cross-structural co-activity patterns and hence, purely time dependent changes can be excluded. Finally, optogenetic silencing might trigger compensatory changes in the network that either act to re-establish learned co-firing patterns or alternatively, bypass previously established neural activity patterns. In the former case this would counteract the reduction of co-activity strength and in the latter case it would amplify the diminishing effect on assembly strength. While in our set up it is not possible to assess the contribution of those factors the necessity of glutamatergic VTA input for the expression of cross-structural co-activity remains evident.

Mechanistic and functional considerations: I noticed that without glutamatergic VTA input task related assembly activity was significantly reduced. However, a component of co-activation remained as assembly strength remained at levels above those seen when the animal was placed in another familiar enclosure. This shows that diverging glutamatergic input from the VTA is required for the full expression of the cross-structural co-activity but a component remains independent of it. Such remaining co-activity may then be supported by other means such as local oscillatory activity (Buzsáki and Watson 2012), cross-structural oscillations (Fujisawa and Buzsáki 2011) or other upstream diverging synchronising inputs (Allen et al. 2019).

One important question is how glutamatergic VTA inputs trigger co-activity in downstream regions from a mechanistic perspective. One component of cross-structural co-activity is likely to be driven by direct monosynaptic connections from VTA to cells in downstream target regions. Once this initial activity has been induced, it is up to local mechanisms to sustain it. One possibility is that glutamatergic VTA neurons directly synapse onto GABAergic interneurons (Mingote et al. 2015; Kabanova et al. 2015; Qi et al. 2016) which then inhibit neighbouring excitatory cells.

This could help select the right excitatory neurons for assembly formation. Consistently, glutamatergic VTA fiber activation preferentially excites interneurons, but only has modest effects on average pyramidal cell activity (Kabanova et al. 2015). Furthermore, the involvement of interneurons in the generation of oscillatory activity, as demonstrated for instance in the hippocampus (J. Csicsvari et al. 1999), opens up the possibility that glutamatergic inputs induce local oscillatory activity driving co-firing assemblies (Buzsáki and Watson 2012). In line with this, an interesting avenue for future research would be to investigate oscillatory coupling of glutamatergic VTA cells as well as LFP state dependence of the probability to elicit spikes in downstream target regions.

How could the brain benefit from using a central hub coordinating synchronisation across different brain structures as opposed to a fully decentralised mechanism? First, a centralised mechanism for distribution of information ensures that downstream regions are engaged towards processing a solution for the same behavioural demands. Second, a fully decentralised system could make it harder to synchronise neurons at a millisecond timescale as errors across regions would compound. On the other hand, a fully centralised system would make brain-wide synchronisation prone to errors or disruption of a central coordinator. Hence, I suggest that the brain might need to strike a balance between the resilience of a distributed coordination system and the benefits of a centralised coordinator. Alongside the VTA, other regions may exert large-scale synchronising effect, as has been demonstrated previously for the hypothalamus (Allen et al. 2019). Other potential candidate regions could be the locus coeruleus or the dorsal raphe nuclei both of which have widespread axonal projections capable of releasing glutamate (Liu et al. 1995; Fung et al. 1994; H.-L. Wang et al. 2019).

(iii) Is glutamatergic VTA neuron spiking necessary for the performance of a behavioural task requiring the discrimination of ambiguous sets of stimuli?

Methodological considerations: I chose to deliver trials with and without light stimulation in two separate sessions in order to avoid confusion effects from inconsistent reward/punishment associations and potential lag effects on the network from optogenetic perturbation within the same session. One possible criticism of this design is that in the first session, animals would be fed sufficient drops of sucrose to induce satiety effects and reduce the motivational drive for further approach behaviour. Another option is that after having performed the first session, mice might have been too tired for the second session, which I addressed by letting animals rest for 1h in the home cage between sessions. Ultimately, if either of these possibilities were true, approach behaviour to quinine should have been equally reduced in the laser session as sucrose approach behaviour. Furthermore and more strikingly, I did not observe any changes in dispenser approaches for either condition in VGlut2VTA:GFP-control mice.

I considered the possibility that animals switched to another strategy to circumvent optogenetic perturbation and obtain sucrose rewards. For instance, mice could choose to approach the dispenser with equal probabilities during both conditions whilst simply accepting the occasional quinine outcome. However, regardless of whether mice deliberately chose this strategy or simply could not discriminate between the conditions, the behavioural change was triggered by the lack of glutamatergic input from the VTA.

Previous reports showed that the locus of optogenetic activation of glutamatergic VTA neurons has different behavioural outcomes. Since generalised optogenetic activation

of glutamatergic VTA somata produces conditioned place preference and enhances instrumental behaviour by exciting dopaminergic projection neurons (H.-L. Wang et al. 2015), one possible criticism of our study would be that the observed reduction in approach behaviour towards the dispenser during the sucrose condition is due to a lack of dopaminergic tonus. However, this scenario is unlikely as dispenser approaches in the simple conditioning experiments remain unaffected, indicating that the effects I observe depend on the presence of multiple conflicting task elements.

Interestingly, previous pathway specific studies indicated that optogenetic activation of glutamatergic VTA fibers to the NAc or lateral habenula produced conditioned place aversion (Qi et al. 2016; Root, Mejias-Aponte, Qi, et al. 2014; Lammel et al. 2015). Hence, one might expect opposite results or 'reversal' of those optogenetic activation results in our optogenetic silencing study. However, I did not observe such a reversal. This could either be the result of the biological role of glutamatergic projections (discussed below in "mechanistic and functional considerations), methodological differences or a consequence of the recruitment of different compensatory mechanisms in the network in response to optogenetic stimulation compared to inhibition. From a methodological perspective there are two possible explanations: first, since our optogenetic stimulation protocol does not allow for a pathway specific analysis, our behavioural results represent the net consequence of a lack of generalised glutamatergic tonus from the VTA that is composed of several pathway dependent sub-effects. Second, differences in behavioural paradigms may explain the lack of a reversal of results. In a previous study mice were exposed to a black disc above the arena mimicking a predator. Animals which underwent glutamatergic VTA cell ablation showed a reduced innate escape response (Barbano et al. 2020). In our study, the animal was free to choose whether to approach the dispenser during the

quinine condition. Furthermore, quinine may not be an equally strong negative stimulus as the externally imposed threat. Furthermore, it is possible that permanent ablation of glutamatergic VTA cells produced more permanent network changes that contributed to the reduction of an escape response but might not have been evident upon short and reversible optogenetic intervention. Lastly, it is possible that the behavioural effects observed here are due to a reduction of dopaminergic tonus resulting either from silencing dopamine-glutamate co-releasing neurons or the lack of excitation onto dopaminergic VTA cells receiving local glutamatergic input (H.-L. Wang et al. 2015). For instance, manipulation of dopaminergic input to the PFC causes a deviation from previously learned rules (Ellwood et al. 2017)

Mechanistic and functional considerations: In light of a previous study showing that generalised glutamatergic VTA cell activation produces appetitive behaviour (H.-L. Wang et al. 2015), one might hypothesise that silencing would produce the reverse effect, namely aversive conditioning or at least a lack of appetitive behaviour. Whilst I observed a decline in sucrose preference in our experiment this is unlikely to be the result of this idea since I did not observe any optogenetically induced changes in dispenser approach behaviour during simple conditioning experiments.

Previous studies demonstrated that activation of glutamatergic VTA fibers to the NAc and the lateral habenula drives aversive conditioning (Qi et al. 2016; Root, Mejias-Aponte, Qi, et al. 2014; Lammel et al. 2015). It is tempting to hypothesise that silencing could produce a reversal of those results, i.e. appetitive behaviour, which is inconsistent with our results. However, as discussed above, differences in the behavioural and optogenetic stimulation protocol may account for the lack of such a reversal. However, I argue that glutamatergic neurons are not solely responsible for signaling negative events. A recent study showed that chemogenic inactivation of

glutamatergic VTA cells projecting to the dorsal hippocampus results in a reduction of both, appetitive and aversive memory retrieval (Han et al. 2020). Furthermore, previous authors suggested that part of glutamatergic VTA cells is involved in signalling general salience (Root, Estrin, and Morales 2018). I suggest that the loss of glutamatergic VTA signalling in downstream structures across the brain equips the system with the ability to retrieve salient memory elements scattered across the brain regardless of their positive or negative content. Hence, glutamatergic VTA cells could be required for the processing of tasks involving multiple contingencies by supporting the integration of all (positive and negative) relevant task elements. Taken together with our results at the assembly level, I suggest that glutamatergic VTA neurons are required to retrieve and synthesize behaviourally relevant information through the formation of behaviourally appropriate brainwide co-firing assembly patterns.

6. CONCLUSION AND PERSPECTIVES

6.1 Conclusions

In this thesis, I show the existence of co-firing assemblies composed of neurons distributed across CA1, Amy, NAc, PFC and VTA. Importantly, these assembly patterns carry behaviourally relevant information.

On an initially separate note, I describe strong variability in VTA single cell responses to task events. Single neurons respond with decreases and increases in firing rates to rewarding or aversive unconditioned stimuli as well as to their associated conditioned stimuli. To investigate differences in task variable representation between glutamatergic and dopaminergic VTA neurons, I establish a clustering framework

allowing us to separate the two cell types based on extracellular electrophysiological recordings. Using this method, I found that both cell types respond to the task stimuli. Notably, however, I found that spike trains of glutamatergic VTA neurons carry more information about behavioural task variables indicating an important role in behavioural control.

In the last chapter, I bring the above findings together and show that activation of glutamatergic VTA cells is sufficient to trigger simultaneous cross-structural spiking activity. Notably, I also demonstrate that glutamatergic VTA activity is necessary for the formation of brain-wide distributed assembly patterns as well as for the expression of appropriate behaviour. Interestingly, the expression of simple conditioning is not dependent on glutamatergic VTA cell input, but the animal's ability to discriminate between an aversive versus an appetitive condition based on predictive sensory cues is. This suggests a crucial role of glutamatergic VTA neurons in the formation of cross-structural co-firing assemblies ultimately enabling the brain to synthesise information to produce appropriate behaviour.

6.2 Perspectives

6.2.1 Future experiments

a) An anatomical validation of tetrode placement is required in order to interpret the emergence of cross-structural co-activity. It would help the functional interpretation of such connections based on the classical understanding of the function of brain regions investigated here. Additionally, it would help answer the question whether the observed co-activity is driven through direct monosynaptic connections or whether it could be attributed in full or in part to the diverging glutamatergic pathway.

b) A detailed analysis of tetrode placement within the VTA is required to discern ambiguity in the classification framework for glutamatergic versus dopaminergic VTA neurons. Depending on the tetrode location within the VTA, different cell types (as defined by their neurotransmitter) may appear electrophysiologically similar or similar cell types may appear different (Hnasko et al. 2012).

c) Additionally, it would be valuable to see the proportion of optogenetically transfected cells co-expressing VGlut2 and TH to estimate the degree to which optogenetic experiments were contaminated by dopamine release. Moreover, the same experiments could also be conducted while silencing dopaminergic VTA neurons. These investigations would reveal how specific the observations in this study are to glutamatergic transmission.

d) A formal histological analysis of ArchT and ChRh2 expression across the brain to exclude retrograde transfection and unintended leakage of the virus into other areas such as the supramammillary nucleus would be required to ensure that results here are not contaminated by direct stimulation or inhibition of other areas.

e) In order to account for methodological variability in tetrode placement, viral transfection and biological variability, such as animal behaviour, more biological replicates of the experiments need to be conducted in the future.

f) It would be interesting to see how specific the synchronising effect of glutamatergic projections is to the VTA. Other heavily interconnected regions such as the PFC, locus coeruleus or raphe nuclei may be equally important in cross-structural synchronisation and replicating our experiments while silencing those other regions could help shed light on this question.

g) It would be useful to apply other methods, such as a generalised linear model, to measure representational differences between the regions. While the approach I chose here is simple and easily interpretable, other methods may be more sensitive and uncover subtle representational differences between the regions in our task after all.

h) One could explore the change in cross-structural co-activation as the animal learns the task by relating co-firing motifs to different stages of learning. For instance, this could be done during simple conditioning, first exposure to the task and learning within the same session.

e) Similarly, it would be interesting to see whether VTA cells are related to ongoing learning. For instance, one could relate glutamatergic VTA neuron firing to intra-session learning curves and determine if their spiking activity changes as a function of learning. By extension, silencing experiments could be used to answer the question whether glutamatergic VTA neurons are necessary to learn (not perform) a simple conditioning paradigm or a more complex task, such as the one I employed here.

i) Lastly, I would be interested in seeing whether glutamatergic VTA cell inputs into downstream target regions are subject to synaptic plasticity. Mechanisms governing the induction of such plastic changes could be uncovered in vitro and possibly perturbed in vivo during learning.

6.2.2 Match/mismatch computations in CA1

The anatomical circuitry of the hippocampus has led to the suggestion that CA1 functions as a coincidence or mismatch detector (J. E. Lisman 1999). This is underpinned by the observation that CA1 pyramidal neurons receive convergent

inputs via the distal dendrites in the stratum lacunosum moleculare from the entorhinal cortex, while the Schaffer collaterals synapse onto apical dendrites in the stratum radiatum (Jarsky et al. 2005). It has been suggested that the hippocampus, thus, serves as a comparator between present environmental contingencies, as transmitted by entorhinal cortex inputs, and remembered states as encoded in the hippocampus. This ultimately allows for an update of internal models of the world (S.-H. Wang and Morris 2010). Similar to the entorhinal inputs into CA1, I observed a strikingly selective innervation of the stratum lacunosum moleculare by glutamatergic VTA fibers (Fig. 33 C). Given this anatomical resemblance, it is tempting to hypothesise that such match/mismatch computations in CA1 account for direct input from glutamatergic VTA neurons and, hence, expand the computational repertoire of CA1 as match/mismatch detector. As I have shown, such input could contain information on reward, punishment, associated conditioned stimuli (Fig. 11; 8) and brain-wide synchronisations signals (Fig. 33 E).

6.2.3 Disease

Schizophrenia is thought to result from the lack of functional integration in the brain and, therefore, depends on intact connectivity between different brain systems (Friston 2002). Our results demonstrate that such functional connectivity depends on synchronising glutamatergic input from the VTA and, hence, raise the possibility of its involvement in the pathogenesis of schizophrenia. Indeed, there has been much early interest in the involvement of glutamatergic hypofunction in schizophrenia (Kitzinger and Arnold 1949). However, more recent research has been inconclusive. While a large metanalysis showed significant benefits of treatment with NMDAR agonists (G. E. Tsai and Lin 2010), this could not be replicated in a subsequent study (Weiser et al. 2012). Recent evidence points to abnormalities in trafficking of specific NMDAR subunits as opposed to a generalised glutamatergic tonus (Howes, McCutcheon, and Stone 2015). These findings could potentially be reconciled by accounting for the source of glutamatergic innervation, such as the VTA, in animal models of schizophrenia (Jones, Watson, and Fone 2011).

6.2.4 Central coordination of distributed processing

Our findings add a new perspective to the debate on functional localisation versus distribution in the brain. I suggest that distributed processing may be supported—if not coordinated—from centralised hubs, such as the VTA and so the seat of distributed processing is localised. This property may be a function of downstream interconnectedness of the hub in question. One other strong candidate region to act as such a synchronising hub could be the PFC due to its widespread downstream connectivity (Gabbott et al. 2005). Consistently, I observed an almost equally prominent position of PFC neurons compared to VTA cells in brain wide distributed

co-activity patterns (Fig. 28 A, B). Similarly, other neuromodulatory systems with neurons co-releasing glutamate, such as in the raphe nuclei or locus coeruleus (Trudeau 2004), could potentially prove to be potent sources of brain wide assembly formation in the future.

6.2.5 Is representational redundancy a semantic artifact?

In this thesis, I show that there is a strong representational overlap across brain regions in the sense that different brain regions exhibit firing rate changes following the experience of the same stimuli. Such responses have traditionally been referred to as representations of a specific external stimulus or internal variable. However, recent philosophical work has brought the concept of representation into question by claiming that such responses are merely the result of the activity of 'detectors' (Ramsey 2007) and have no meaning in isolation. In line with connectionist views of the mind (Buckner and Garson 2019), I suggest that the representation carried by a single neuron's response is determined by the neuron's position within the network. The same stimulus can elicit firing rate changes in neurons scattered across the brain, but their responses do not necessarily represent the stimulus with a precise one-to-one mapping, but instead merely reflect the neuron's contribution to the network's ultimate output, i.e. behaviour. In this light, neural responses are only overlapping in the sense that they occur after the experience of a certain stimulus. Their meaning for the network and, hence, representational content is totally different. The traditional usage of the term 'representation' may in fact confound neuroscientific research. One possibility to attach representational meaning to single neuron responses could be to transfer recent research on the interpretability of the output of artificial neural networks (Montavon, Samek, and Müller 2018) to biological systems.

The main conclusions of my dissertation are: brain regions are less specialised than previously thought with regards to the representation of stimuli or behavioural variables. Spiking of individual neurons in multiple different brain areas is coordinated in brain-wide distributed assemblies. Such assemblies encode behavioural contingencies and group neurons together based on a minimally necessary degree of representational similarity, while leaving room for differences across neurons contributing to an assembly. Such an organisational principle may support adaptability of neural representations and behaviour. Finally, I discovered that glutamatergic VTA neuron firing causes cross-structural co-activity and is required for the expression of appropriate approach and avoidance behaviour when conflicting predictive sensory cues overlap. I conclude that glutamatergic VTA inputs to its target areas causes the formation of multisensory brain-wide distributed assemblies, which in turn are required to drive effective behaviour.

References

Adcock, R. Alison, R. Alison Adcock, Arul Thangavel, Susan Whitfield-Gabrieli, Brian Knutson, and John D. E. Gabrieli. 2006. “Reward-Motivated Learning: Mesolimbic Activation Precedes Memory Formation.” *Neuron*. https://doi.org/10.1016/j.neuron.2006.03.036.

Adeniyi, Philip A., Amita Shrestha, and Olalekan M. Ogundele. 2020. “Distribution of VTA Glutamate and Dopamine Terminals, and Their Significance in CA1 Neural Network Activity.” *Neuroscience* 446 (October): 171–98.

Aghajanian, George K., and Benjamin S. Bunney. 1974. “Central Dopaminergic Neurons: Neurophysiological Identification and Responses to Drugs.” *Biochemical Pharmacology*. https://doi.org/10.1016/0006-2952(74)90074-4.

Allen, William E., Michael Z. Chen, Nandini Pichamoorthy, Rebecca H. Tien, Marius Pachitariu, Liqun Luo, and Karl Deisseroth. 2019. “Thirst Regulates Motivated Behavior through Modulation of Brainwide Neural Population Dynamics.” *Science* 364 (6437): 253.

Ambroggi, Frederic, Ali Ghazizadeh, Saleem M. Nicola, and Howard L. Fields. 2011. “Roles of Nucleus Accumbens Core and Shell in Incentive-Cue Responding and Behavioral Inhibition.” *The Journal of Neuroscience: The Official Journal of the Society for Neuroscience* 31 (18): 6820–30.

Ambroggi, Frederic, Akinori Ishikawa, Howard L. Fields, and Saleem M. Nicola. 2008. “Basolateral Amygdala Neurons Facilitate Reward-Seeking Behavior by Exciting Nucleus Accumbens Neurons.” *Neuron* 59 (4): 648–61.

Amo, R., A. Yamanaka, K. F. Tanaka, and N. Uchida. 2020. “A Gradual Backward Shift of Dopamine Responses during Associative Learning.” *bioRxiv*. https://www.biorxiv.org/content/10.1101/2020.10.04.325324v1.abstract.

Andersen, Per, Richard Morris, David Amaral, John O’Keefe, Tim Bliss, and Division of Neurophysiology Tim Bliss. 2007. *The Hippocampus Book*. Oxford University Press, USA.

Anstrom, Kristin K., and Donald J. Woodward. 2005. “Restraint Increases Dopaminergic Burst Firing in Awake Rats.” *Neuropsychopharmacology: Official Publication of the American College of Neuropsychopharmacology* 30 (10): 1832–40.

Aransay, Ana, Claudia Rodríguez-López, María García-Amado, Francisco Clascá, and Lucía Prensa. 2015. “Long-Range Projection Neurons of the Mouse Ventral Tegmental Area: A Single-Cell Axon Tracing Analysis.” *Frontiers in Neuroanatomy* 9 (May): 59.

Aristotle. 2014. *De Sensu and De Memoria*. Cambridge University Press.

Aston-Jones, Gary, and David Moorman. 2009. “Faculty Opinions Recommendation of Phasic Excitation of Dopamine Neurons in Ventral VTA by Noxious Stimuli.” *Faculty Opinions – Post-Publication Peer Review of the Biomedical Literature*. https://doi.org/10.3410/f.1160133.620423.

Augustine, G. J., and H. Kasai. 2007. “Bernard Katz, Quantal Transmitter Release and the Foundations of Presynaptic Physiology.” *The Journal of Physiology*. https://www.ncbi.nlm.nih.gov/pmc/articles/pmc2151334/.

Babayan, Benedicte M., Naoshige Uchida, and Samuel J. Gershman. 2018. “Belief State Representation in the Dopamine System.” *Nature Communications* 9 (1): 1891.

Barbano, M. Flavia, Hui-Ling Wang, Shiliang Zhang, Jorge Miranda-Barrientos, David J. Estrin, Almaris Figueroa-González, Bing Liu, David J. Barker, and

Marisela Morales. 2020. “VTA Glutamatergic Neurons Mediate Innate Defensive Behaviors.” *Neuron* 107 (2): 368–82.e8.
Bariselli, Sebastiano, Christelle Glangetas, Stamatina Tzanoulinou, and Camilla Bellone. 2016. “Ventral Tegmental Area Subcircuits Process Rewarding and Aversive Experiences.” *Journal of Neurochemistry* 139 (6): 1071–80.
Barron, Helen C., Hayley M. Reeve, Renée S. Koolschijn, Pavel V. Perestenko, Anna Shpektor, Hamed Nili, Roman Rothaermel, et al. 2020. “Neuronal Computation Underlying Inferential Reasoning in Humans and Mice.” *Cell* 183 (1): 228–43.e21.
Bartlett, F. C., and Cyril Burt. 1933. “REMEMBERING: A STUDY IN EXPERIMENTAL AND SOCIAL PSYCHOLOGY.” *British Journal of Educational Psychology*. https://doi.org/10.1111/j.2044-8279.1933.tb02913.x.
Bauer, Elizabeth P., Glenn E. Schafe, and Joseph E. LeDoux. 2002. “NMDA Receptors and L-Type Voltage-Gated Calcium Channels Contribute to Long-Term Potentiation and Different Components of Fear Memory Formation in the Lateral Amygdala.” *The Journal of Neuroscience: The Official Journal of the Society for Neuroscience* 22 (12): 5239–49.
Baxter, Mark G., and Elisabeth A. Murray. 2002. “The Amygdala and Reward.” *Nature Reviews. Neuroscience* 3 (7): 563–73.
Bazelot, Michaël, Marco Bocchio, Yu Kasugai, David Fischer, Paul D. Dodson, Francesco Ferraguti, and Marco Capogna. 2015. “Hippocampal Theta Input to the Amygdala Shapes Feedforward Inhibition to Gate Heterosynaptic Plasticity.” *Neuron* 87 (6): 1290–1303.
Beckstead, R. M. 1979. “An Autoradiographic Examination of Corticocortical and Subcortical Projections of the Mediodorsal-Projection (prefrontal) Cortex in the Rat.” *The Journal of Comparative Neurology* 184 (1): 43–62.
Beier, Kevin T., Elizabeth E. Steinberg, Katherine E. DeLoach, Stanley Xie, Kazunari Miyamichi, Lindsay Schwarz, Xiaojing J. Gao, Eric J. Kremer, Robert C. Malenka, and Liqun Luo. 2015. “Circuit Architecture of VTA Dopamine Neurons Revealed by Systematic Input-Output Mapping.” *Cell* 162 (3): 622–34.
Belova, Marina A., Joseph J. Paton, and C. Daniel Salzman. 2008. “Moment-to-Moment Tracking of State Value in the Amygdala.” *The Journal of Neuroscience: The Official Journal of the Society for Neuroscience* 28 (40): 10023–30.
Berendse, H. W., and H. J. Groenewegen. 1990. “Organization of the Thalamostriatal Projections in the Rat, with Special Emphasis on the Ventral Striatum.” *The Journal of Comparative Neurology* 299 (2): 187–228.
Berger, T. W., B. Alger, and R. F. Thompson. 1976. “Neuronal Substrate of Classical Conditioning in the Hippocampus.” *Science* 192 (4238): 483–85.
Berridge, Kent C. 2007. “The Debate over Dopamine’s Role in Reward: The Case for Incentive Salience.” *Psychopharmacology* 191 (3): 391–431.
Beyeler, Anna, Praneeth Namburi, Gordon F. Glober, Clémence Simonnet, Gwendolyn G. Calhoon, Garrett F. Conyers, Robert Luck, Craig P. Wildes, and Kay M. Tye. 2016. “Divergent Routing of Positive and Negative Information from the Amygdala during Memory Retrieval.” *Neuron* 90 (2): 348–61.
Bittner, Katie C., Christine Grienberger, Sachin P. Vaidya, Aaron D. Milstein, John J. Macklin, Junghyup Suh, Susumu Tonegawa, and Jeffrey C. Magee. 2015. “Conjunctive Input Processing Drives Feature Selectivity in Hippocampal CA1 Neurons.” *Nature Neuroscience* 18 (8): 1133–42.
Björklund, Anders, and Stephen B. Dunnett. 2007. “Dopamine Neuron Systems in

the Brain: An Update." *Trends in Neurosciences* 30 (5): 194–202.
Blanchard, D. Caroline, D. Caroline Blanchard, and Robert J. Blanchard. 1972. "Innate and Conditioned Reactions to Threat in Rats with Amygdaloid Lesions." *Journal of Comparative and Physiological Psychology*. https://doi.org/10.1037/h0033521.
Bontempi, B., C. Laurent-Demir, C. Destrade, and R. Jaffard. 1999. "Time-Dependent Reorganization of Brain Circuitry Underlying Long-Term Memory Storage." *Nature* 400 (6745): 671–75.
Bossert, Jennifer M., Sweta Adhikary, Robyn St Laurent, Nathan J. Marchant, Hui-Ling Wang, Marisela Morales, and Yavin Shaham. 2016. "Role of Projections from Ventral Subiculum to Nucleus Accumbens Shell in Context-Induced Reinstatement of Heroin Seeking in Rats." *Psychopharmacology* 233 (10): 1991.
Brady, Scott, George Siegel, R. Wayne Albers, and Donald Price. 2005. *Basic Neurochemistry: Molecular, Cellular and Medical Aspects*. Elsevier.
Brischoux, Frédéric, Subhojit Chakraborty, Daniel I. Brierley, and Mark A. Ungless. 2009. "Phasic Excitation of Dopamine Neurons in Ventral VTA by Noxious Stimuli." *Proceedings of the National Academy of Sciences of the United States of America* 106 (12): 4894–99.
Brog, J. S., A. Salyapongse, A. Y. Deutch, and D. S. Zahm. 1993. "The Patterns of Afferent Innervation of the Core and Shell in the 'Accumbens' Part of the Rat Ventral Striatum: Immunohistochemical Detection of Retrogradely Transported Fluoro-Gold." *The Journal of Comparative Neurology* 338 (2): 255–78.
Bromberg-Martin, Ethan S., Masayuki Matsumoto, and Okihide Hikosaka. 2010. "Dopamine in Motivational Control: Rewarding, Aversive, and Alerting." *Neuron* 68 (5): 815–34.
Brown, Matthew T. C., Kelly R. Tan, Eoin C. O'Connor, Irina Nikonenko, Dominique Muller, and Christian Lüscher. 2012. "Ventral Tegmental Area GABA Projections Pause Accumbal Cholinergic Interneurons to Enhance Associative Learning." *Nature* 492 (7429): 452–56.
Brown, Ritchie E., and James T. McKenna. 2015. "Turning a Negative into a Positive: Ascending GABAergic Control of Cortical Activation and Arousal." *Frontiers in Neurology* 6 (June): 135.
Brown, Sanger, and Edward Albert Sharpey-Schafer. 1888. "XI. An Investigation into the Functions of the Occipital and Temporal Lobes of the Monkey's Brain." *Philosophical Transactions of the Royal Society of London. (B.)* 179 (January): 303–27.
Buckner, Cameron, and James Garson. 2019. "Connectionism." In *The Stanford Encyclopedia of Philosophy*, edited by Edward N. Zalta, Fall 2019. Metaphysics Research Lab, Stanford University. https://plato.stanford.edu/archives/fall2019/entries/connectionism/.
Bullmore, Ed, and Olaf Sporns. 2009. "Complex Brain Networks: Graph Theoretical Analysis of Structural and Functional Systems." *Nature Reviews. Neuroscience* 10 (3): 186–98.
Buzsáki, György. 2010. "Neural Syntax: Cell Assemblies, Synapsembles, and Readers." *Neuron* 68 (3): 362–85.
Buzsáki, György, and Brendon O. Watson. 2012. "Brain Rhythms and Neural Syntax: Implications for Efficient Coding of Cognitive Content and Neuropsychiatric Disease." *Dialogues in Clinical Neuroscience* 14 (4): 345–67.
Cador, M., T. W. Robbins, and B. J. Everitt. 1989. "Involvement of the Amygdala in Stimulus-Reward Associations: Interaction with the Ventral Striatum."

Neuroscience 30 (1): 77–86.
Caliński, T., and J. Harabasz. 1974. “A Dendrite Method for Cluster Analysis.” *Communications in Statistics: Simulation and Computation* 3 (1): 1–27.
Cardinal, Rudolf N., and Timothy H. C. Cheung. 2005. “Nucleus Accumbens Core Lesions Retard Instrumental Learning and Performance with Delayed Reinforcement in the Rat.” *BMC Neuroscience* 6 (February): 9.
Carr, D. B., and S. R. Sesack. 2000. “Projections from the Rat Prefrontal Cortex to the Ventral Tegmental Area: Target Specificity in the Synaptic Associations with Mesoaccumbens and Mesocortical Neurons.” *The Journal of Neuroscience: The Official Journal of the Society for Neuroscience* 20 (10): 3864–73.
Castañé, Anna, David E. H. Theobald, and Trevor W. Robbins. 2010. “Selective Lesions of the Dorsomedial Striatum Impair Serial Spatial Reversal Learning in Rats.” *Behavioural Brain Research* 210 (1): 74–83.
Chang, A. J., L. Wang, F. Lucantonio, M. Adams, and A. Lemire. 2021. “Neuron-Type Specificity of Dorsal Raphe Projections to Ventral Tegmental Area.” *bioRxiv*. https://www.biorxiv.org/content/10.1101/2021.01.06.425641v1.abstract.
Chang, Le, and Doris Y. Tsao. 2017. “The Code for Facial Identity in the Primate Brain.” *Cell* 169 (6): 1013–28.e14.
Chaudhury, Dipesh, Jessica J. Walsh, Allyson K. Friedman, Barbara Juarez, Stacy M. Ku, Ja Wook Koo, Deveroux Ferguson, et al. 2013. “Rapid Regulation of Depression-Related Behaviours by Control of Midbrain Dopamine Neurons.” *Nature* 493 (7433): 532–36.
Ciano, Patricia Di, Patricia Di Ciano, Rudolf N. Cardinal, Rosie A. Cowell, Simon J. Little, and Barry J. Everitt. 2001. “Differential Involvement of NMDA, AMPA/Kainate, and Dopamine Receptors in the Nucleus Accumbens Core in the Acquisition and Performance of Pavlovian Approach Behavior.” *The Journal of Neuroscience*. https://doi.org/10.1523/jneurosci.21-23-09471.2001.
Ciliax, B. J., C. Heilman, L. L. Demchyshyn, Z. B. Pristupa, E. Ince, S. M. Hersch, H. B. Niznik, and A. I. Levey. 1995. “The Dopamine Transporter: Immunochemical Characterization and Localization in Brain.” *The Journal of Neuroscience: The Official Journal of the Society for Neuroscience* 15 (3 Pt 1): 1714–23.
Citri, Ami, and Robert C. Malenka. 2008. “Synaptic Plasticity: Multiple Forms, Functions, and Mechanisms.” *Neuropsychopharmacology: Official Publication of the American College of Neuropsychopharmacology* 33 (1): 18–41.
Cohen, Jeremiah Y., Sebastian Haesler, Linh Vong, Bradford B. Lowell, and Naoshige Uchida. 2012. “Neuron-Type-Specific Signals for Reward and Punishment in the Ventral Tegmental Area.” *Nature* 482 (7383): 85–88.
Colgin, Laura Lee, Edvard I. Moser, and May-Britt Moser. 2008. “Understanding Memory through Hippocampal Remapping.” *Trends in Neurosciences* 31 (9): 469–77.
Corbit, Laura H., and Bernard W. Balleine. 2011. “The General and Outcome-Specific Forms of Pavlovian-Instrumental Transfer Are Differentially Mediated by the Nucleus Accumbens Core and Shell.” *The Journal of Neuroscience: The Official Journal of the Society for Neuroscience* 31 (33): 11786–94.
Corcoran, K. A., and S. Maren. 2001. “Hippocampal Inactivation Disrupts Contextual Retrieval of Fear Memory after Extinction.” *The Journal of Neuroscience: The Official Journal of the Society for Neuroscience* 21 (5): 1720–26.
Corcoran, Kevin A., and Gregory J. Quirk. 2007. “Activity in Prelimbic Cortex Is Necessary for the Expression of Learned, but Not Innate, Fears.” *The Journal of Neuroscience: The Official Journal of the Society for Neuroscience* 27 (4): 840–

44.
Csicsvari, J., H. Hirase, A. Czurkó, A. Mamiya, and G. Buzsáki. 1999. “Oscillatory Coupling of Hippocampal Pyramidal Cells and Interneurons in the Behaving Rat.” *The Journal of Neuroscience: The Official Journal of the Society for Neuroscience* 19 (1): 274–87.
Csicsvari, Jozsef, Hajime Hirase, Andras Czurko, and György Buzsáki. 1998. “Reliability and State Dependence of Pyramidal Cell–Interneuron Synapses in the Hippocampus: An Ensemble Approach in the Behaving Rat.” *Neuron* 21 (1): 179–89.
Dabney, Will, Zeb Kurth-Nelson, Naoshige Uchida, Clara Kwon Starkweather, Demis Hassabis, Rémi Munos, and Matthew Botvinick. 2020. “A Distributional Code for Value in Dopamine-Based Reinforcement Learning.” *Nature* 577 (7792): 671–75.
Dahan, Lionel, Bernadette Astier, Nicolas Vautrelle, Nadia Urbain, Bernat Kocsis, and Guy Chouvet. 2007. “Prominent Burst Firing of Dopaminergic Neurons in the Ventral Tegmental Area during Paradoxical Sleep.” *Neuropsychopharmacology: Official Publication of the American College of Neuropsychopharmacology* 32 (6): 1232–41.
Dang, W., R. J. Jaffe, X. L. Qi, and C. Constantinidis. 2020. “Emergence of Non-Linear Mixed Selectivity in Prefrontal Cortex after Training.” *bioRxiv*. https://www.biorxiv.org/content/10.1101/2020.08.02.233247v2.abstract.
Daumas, Stéphanie, Hélène Halley, Bernard Francés, and Jean-Michel Lassalle. 2005. “Encoding, Consolidation, and Retrieval of Contextual Memory: Differential Involvement of Dorsal CA3 and CA1 Hippocampal Subregions.” *Learning & Memory* 12 (4): 375–82.
Deco, Gustavo, Edmund T. Rolls, and Ranulfo Romo. 2009. “Stochastic Dynamics as a Principle of Brain Function.” *Progress in Neurobiology* 88 (1): 1–16.
Deering, R., and J. F. Kaiser. 2005. “The Use of a Masking Signal to Improve Empirical Mode Decomposition.” In *Proceedings. (ICASSP ’05). IEEE International Conference on Acoustics, Speech, and Signal Processing, 2005.*, 4:iv/485 – iv/488 Vol. 4.
De No, Rafael Lorente. 1938. “ANALYSIS OF THE ACTIVITY OF THE CHAINS OF INTERNUNCIAL NEURONS.” *Journal of Neurophysiology* 1 (3): 207–44.
Deolindo, Camila S., Ana C. B. Kunicki, Maria I. da Silva, Fabrício Lima Brasil, and Renan C. Moioli. 2017. “Neuronal Assemblies Evidence Distributed Interactions within a Tactile Discrimination Task in Rats.” *Frontiers in Neural Circuits* 11: 114.
Dobi, Alice, Elyssa B. Margolis, Hui-Ling Wang, Brandon K. Harvey, and Marisela Morales. 2010. “Glutamatergic and Nonglutamatergic Neurons of the Ventral Tegmental Area Establish Local Synaptic Contacts with Dopaminergic and Nondopaminergic Neurons.” *The Journal of Neuroscience: The Official Journal of the Society for Neuroscience* 30 (1): 218–29.
Domenech, Philippe, and Etienne Koechlin. 2015. “Executive Control and Decision-Making in the Prefrontal Cortex.” *Current Opinion in Behavioral Sciences* 1 (February): 101–6.
Dudman, Joshua T., David Tsay, and Steven A. Siegelbaum. 2007. “A Role for Synaptic Inputs at Distal Dendrites: Instructive Signals for Hippocampal Long-Term Plasticity.” *Neuron* 56 (5): 866–79.
Eichenbaum, H. 1993. “Thinking about Brain Cell Assemblies.” *Science*.
Eichenbaum, H., P. Dudchenko, E. Wood, M. Shapiro, and H. Tanila. 1999. “The

Hippocampus, Memory, and Place Cells: Is It Spatial Memory or a Memory Space?" *Neuron* 23 (2): 209–26.
Eichenbaum, H., M. Kuperstein, A. Fagan, and J. Nagode. 1987. "Cue-Sampling and Goal-Approach Correlates of Hippocampal Unit Activity in Rats Performing an Odor-Discrimination Task." *The Journal of Neuroscience: The Official Journal of the Society for Neuroscience* 7 (3): 716–32.
Eichenbaum, Howard. 2017. "Memory: Organization and Control." *Annual Review of Psychology* 68 (January): 19–45.
Ellwood, Ian T., Tosha Patel, Varun Wadia, Anthony T. Lee, Alayna T. Liptak, Kevin J. Bender, and Vikaas S. Sohal. 2017. "Tonic or Phasic Stimulation of Dopaminergic Projections to Prefrontal Cortex Causes Mice to Maintain or Deviate from Previously Learned Behavioral Strategies." *The Journal of Neuroscience: The Official Journal of the Society for Neuroscience* 37 (35): 8315–29.
Elsworth, J. D., and R. H. Roth. 1997. "Dopamine Synthesis, Uptake, Metabolism, and Receptors: Relevance to Gene Therapy of Parkinson's Disease." *Experimental Neurology* 144 (1): 4–9.
Engelhard, Ben, Joel Finkelstein, Julia Cox, Weston Fleming, Hee Jae Jang, Sharon Ornelas, Sue Ann Koay, et al. 2019. "Specialized Coding of Sensory, Motor and Cognitive Variables in VTA Dopamine Neurons." *Nature* 570 (7762): 509–13.
———2019 "Specialized and Spatially Organized Coding of Sensory, Motor, and Cognitive Variables in Midbrain Dopamine Neurons." https://doi.org/10.1101/456194.
Euston, David R., Aaron J. Gruber, and Bruce L. McNaughton. 2012. "The Role of Medial Prefrontal Cortex in Memory and Decision Making." *Neuron* 76 (6): 1057–70.
Everitt, B. J., M. Cador, and T. W. Robbins. 1989. "Interactions between the Amygdala and Ventral Striatum in Stimulus-Reward Associations: Studies Using a Second-Order Schedule of Sexual Reinforcement." *Neuroscience* 30 (1): 63–75.
Faget, Lauren, Fumitaka Osakada, Jinyi Duan, Reed Ressler, Alexander B. Johnson, James A. Proudfoot, Ji Hoon Yoo, Edward M. Callaway, and Thomas S. Hnasko. 2016. "Afferent Inputs to Neurotransmitter-Defined Cell Types in the Ventral Tegmental Area." *Cell Reports* 15 (12): 2796–2808.
Fallon, J. H., and R. Y. Moore. 1978. "Catecholamine Innervation of the Basal Forebrain. IV. Topography of the Dopamine Projection to the Basal Forebrain and Neostriatum." *The Journal of Comparative Neurology* 180 (3): 545–80.
Fanselow, Michael. 2019. "Faculty Opinions Recommendation of 4-Hz Oscillations Synchronize Prefrontal-Amygdala Circuits during Fear Behavior." *Faculty Opinions – Post-Publication Peer Review of the Biomedical Literature*. https://doi.org/10.3410/f.726148073.793563086.
Fenno, Lief, Ofer Yizhar, and Karl Deisseroth. 2011. "The Development and Application of Optogenetics." *Annual Review of Neuroscience* 34: 389–412.
Fiorillo, Christopher D., Philippe N. Tobler, and Wolfram Schultz. 2003. "Discrete Coding of Reward Probability and Uncertainty by Dopamine Neurons." *Science* 299 (5614): 1898–1902.
Fisher, R. A. 1936. "The Use of Multiple Measurements in Taxonomic Problems." *Annals of Eugenics* 7 (2): 179–88.
Floresco, Stan B., Sarvin Ghods-Sharifi, Claudia Vexelman, and Orsolya Magyar. 2006. "Dissociable Roles for the Nucleus Accumbens Core and Shell in

Regulating Set Shifting." *The Journal of Neuroscience: The Official Journal of the Society for Neuroscience* 26 (9): 2449–57.
Foote, S. L., F. E. Bloom, and G. Aston-Jones. 1983. "Nucleus Locus Ceruleus: New Evidence of Anatomical and Physiological Specificity." *Physiological Reviews* 63 (3): 844–914.
Ford, Christopher P., Gregory P. Mark, and John T. Williams. 2006. "Properties and Opioid Inhibition of Mesolimbic Dopamine Neurons Vary according to Target Location." *The Journal of Neuroscience: The Official Journal of the Society for Neuroscience* 26 (10): 2788–97.
Fox, Peter T., and Karl J. Friston. 2012. "Distributed Processing; Distributed Functions?" *NeuroImage* 61 (2): 407–26.
Freche, Dominik, Ulrike Pannasch, Nathalie Rouach, and David Holcman. 2011. "Synapse Geometry and Receptor Dynamics Modulate Synaptic Strength." *PloS One* 6 (10): e25122.
Friston, Karl J. 2002. "Dysfunctional Connectivity in Schizophrenia." *World Psychiatry: Official Journal of the World Psychiatric Association* 1 (2): 66–71.
Fujisawa, Shigeyoshi, and György Buzsáki. 2011. "A 4 Hz Oscillation Adaptively Synchronizes Prefrontal, VTA, and Hippocampal Activities." *Neuron* 72 (1): 153–65.
Fung, S. J., V. K. Reddy, R. H. Liu, Z. Wang, and C. D. Barnes. 1994. "Existence of Glutamate in Noradrenergic Locus Coeruleus Neurons of Rodents." *Brain Research Bulletin* 35 (5-6): 505–12.
Gabbott, Paul L. A., Tracy A. Warner, Paul R. L. Jays, Phillip Salway, and Sarah J. Busby. 2005. "Prefrontal Cortex in the Rat: Projections to Subcortical Autonomic, Motor, and Limbic Centers." *The Journal of Comparative Neurology* 492 (2): 145–77.
Gaffan, D., and S. Harrison. 1987. "Amygdalectomy and Disconnection in Visual Learning for Auditory Secondary Reinforcement by Monkeys." *The Journal of Neuroscience: The Official Journal of the Society for Neuroscience* 7 (8): 2285–92.
Gardner, Matthew P. H., Geoffrey Schoenbaum, and Samuel J. Gershman., 2018. "Rethinking Dopamine as Generalized Prediction Error." https://doi.org/10.1101/239731.
Girardeau, Gabrielle, Ingrid Inema, and György Buzsáki. 2017. "Reactivations of Emotional Memory in the Hippocampus–amygdala System during Sleep." *Nature Neuroscience* 20 (11): 1634–42.
Giustino, Thomas F., and Stephen Maren. 2015. "The Role of the Medial Prefrontal Cortex in the Conditioning and Extinction of Fear." *Frontiers in Behavioral Neuroscience* 9 (November): 298.
Glimcher, Paul W. 2011. "Understanding Dopamine and Reinforcement Learning: The Dopamine Reward Prediction Error Hypothesis." *Proceedings of the National Academy of Sciences of the United States of America* 108 Suppl 3 (September): 15647–54.
Gomperts, Stephen N., Fabian Kloosterman, and Matthew A. Wilson. 2015. "VTA Neurons Coordinate with the Hippocampal Reactivation of Spatial Experience." *eLife* 4 (October). https://doi.org/10.7554/eLife.05360.
Gore, Bryan B., Marta E. Soden, and Larry S. Zweifel. 2014. "Visualization of Plasticity in Fear-Evoked Calcium Signals in Midbrain Dopamine Neurons." *Learning & Memory* 21 (11): 575–79.
Goto, Yukiori, and Anthony A. Grace. 2005. "Dopaminergic Modulation of Limbic and

Cortical Drive of Nucleus Accumbens in Goal-Directed Behavior." *Nature Neuroscience* 8 (6): 805–12.
Grace, A. A., and B. S. Bunney. 1980. "Nigral Dopamine Neurons: Intracellular Recording and Identification with L-Dopa Injection and Histofluorescence." *Science* 210 (4470): 654–56.
———. 1983. "Intracellular and Extracellular Electrophysiology of Nigral Dopaminergic neurons—2. Action Potential Generating Mechanisms and Morphological Correlates." *Neuroscience* 10 (2): 317–31.
Grace, A. A., and S. P. Onn. 1989. "Morphology and Electrophysiological Properties of Immunocytochemically Identified Rat Dopamine Neurons Recorded in Vitro." *The Journal of Neuroscience: The Official Journal of the Society for Neuroscience* 9 (10): 3463–81.
Groenewegen, H. J., C. I. Wright, A. V. Beijer, and P. Voorn. 1999. "Convergence and Segregation of Ventral Striatal Inputs and Outputs." *Annals of the New York Academy of Sciences* 877 (June): 49–63.
Guarraci, F. A., and B. S. Kapp. 1999. "An Electrophysiological Characterization of Ventral Tegmental Area Dopaminergic Neurons during Differential Pavlovian Fear Conditioning in the Awake Rabbit." *Behavioural Brain Research* 99 (2): 169–79.
Guyenet, P. G., and G. K. Aghajanian. 1978. "Antidromic Identification of Dopaminergic and Other Output Neurons of the Rat Substantia Nigra." *Brain Research* 150 (1): 69–84.
Han, Yuan, Yi Zhang, Haram Kim, Viktoriya S. Grayson, Vladimir Jovasevic, Wenjie Ren, Maria V. Centeno, et al. 2020. "Excitatory VTA to DH Projections Provide a Valence Signal to Memory Circuits." *Nature Communications* 11 (1): 1466.
Haralambous, T., and R. F. Westbrook. 1999. "An Infusion of Bupivacaine into the Nucleus Accumbens Disrupts the Acquisition but Not the Expression of Contextual Fear Conditioning." *Behavioral Neuroscience* 113 (5): 925–40.
Harris, K. D., D. A. Henze, J. Csicsvari, H. Hirase, and G. Buzsáki. 2000. "Accuracy of Tetrode Spike Separation as Determined by Simultaneous Intracellular and Extracellular Measurements." *Journal of Neurophysiology* 84 (1): 401–14.
Harris, Kenneth D., Jozsef Csicsvari, Hajime Hirase, George Dragoi, and György Buzsáki. 2003. "Organization of Cell Assemblies in the Hippocampus." *Nature* 424 (6948): 552–56.
Hastie, T., R. Tibshirani, and J. Friedman. 2001. "The Elements of Statistical Learning. Springer Series in Statistics." : https://www.oeaw.ac.at/resources/Record/990003093550504498.
Hatfield, T., J. S. Han, M. Conley, M. Gallagher, and P. Holland. 1996. "Neurotoxic Lesions of Basolateral, but Not Central, Amygdala Interfere with Pavlovian Second-Order Conditioning and Reinforcer Devaluation Effects." *The Journal of Neuroscience: The Official Journal of the Society for Neuroscience* 16 (16): 5256–65.
Hebb, Donald Olding. 1949a. *The Organisation of Behaviour: A Neuropsychological Theory*. London.
———. 1949b. "The Organization of Behavior; a Neuropsycholocigal Theory." *A Wiley Book in Clinical Psychology* 62: 78.
Herry, Cyril, Stephane Ciocchi, Verena Senn, Lynda Demmou, Christian Müller, and Andreas Lüthi. 2008. "Switching on and off Fear by Distinct Neuronal Circuits." *Nature* 454 (7204): 600–606.
Hnasko, Thomas S., Gregory O. Hjelmstad, Howard L. Fields, and Robert H.

Edwards. 2012. “Ventral Tegmental Area Glutamate Neurons: Electrophysiological Properties and Projections.” *The Journal of Neuroscience: The Official Journal of the Society for Neuroscience* 32 (43): 15076–85.
Hobin, Jennifer A., Ki A. Goosens, and Stephen Maren. 2003. “Context-Dependent Neuronal Activity in the Lateral Amygdala Represents Fear Memories after Extinction.” *The Journal of Neuroscience: The Official Journal of the Society for Neuroscience* 23 (23): 8410–16.
Ho, Joses, Tayfun Tumkaya, Sameer Aryal, Hyungwon Choi, and Adam Claridge-Chang. 2019. “Moving beyond P Values: Data Analysis with Estimation Graphics.” *Nature Methods* 16 (7): 565–66.
Hoover, Walter B., and Robert P. Vertes. 2007. “Anatomical Analysis of Afferent Projections to the Medial Prefrontal Cortex in the Rat.” *Brain Structure & Function* 212 (2): 149–79.
Howes, Oliver, Rob McCutcheon, and James Stone. 2015. “Glutamate and Dopamine in Schizophrenia: An Update for the 21st Century.” *Journal of Psychopharmacology* 29 (2): 97–115.
Hume, David. 1874. *A Treatise on Human Nature*.
Humphries, Mark D., Ric Wood, and Kevin Gurney. 2009. “Dopamine-Modulated Dynamic Cell Assemblies Generated by the GABAergic Striatal Microcircuit.” *Neural Networks: The Official Journal of the International Neural Network Society* 22 (8): 1174–88.
Hyland, B. I., J. N. J. Reynolds, J. Hay, C. G. Perk, and R. Miller. 2002. “Firing Modes of Midbrain Dopamine Cells in the Freely Moving Rat.” *Neuroscience* 114 (2): 475–92.
Ilango, Anton, Jason Shumake, Wolfram Wetzel, Henning Scheich, and Frank W. Ohl. 2012. “The Role of Dopamine in the Context of Aversive Stimuli with Particular Reference to Acoustically Signaled Avoidance Learning.” *Frontiers in Neuroscience* 6 (September): 132.
Janak, Patricia H., and Kay M. Tye. 2015. “From Circuits to Behaviour in the Amygdala.” *Nature* 517 (7534): 284–92.
Jarsky, Tim, Alex Roxin, William L. Kath, and Nelson Spruston. 2005. “Conditional Dendritic Spike Propagation Following Distal Synaptic Activation of Hippocampal CA1 Pyramidal Neurons.” *Nature Neuroscience* 8 (12): 1667–76.
Jay, T. M., and M. P. Witter. 1991. “Distribution of Hippocampal CA1 and Subicular Efferents in the Prefrontal Cortex of the Rat Studied by Means of Anterograde Transport of Phaseolus Vulgaris-Leucoagglutinin.” *The Journal of Comparative Neurology* 313 (4): 574–86.
Johnson, S. W., and R. A. North. 1992a. “Opioids Excite Dopamine Neurons by Hyperpolarization of Local Interneurons.” *The Journal of Neuroscience: The Official Journal of the Society for Neuroscience* 12 (2): 483–88.
———. 1992b. “Two Types of Neurone in the Rat Ventral Tegmental Area and Their Synaptic Inputs.” *The Journal of Physiology* 450 (May): 455–68.
Jonas, Peter. 2000. “The Time Course of Signaling at Central Glutamatergic Synapses.” *News in Physiological Sciences: An International Journal of Physiology Produced Jointly by the International Union of Physiological Sciences and the American Physiological Society* 15 (April): 83–89.
Jones, C. A., D. J. G. Watson, and K. C. F. Fone. 2011. “Animal Models of Schizophrenia.” *British Journal of Pharmacology* 164 (4): 1162–94.
Kabanova, Anna, Milan Pabst, Markus Lorkowski, Oliver Braganza, Anne Boehlen, Negar Nikbakht, Leonie Pothmann, et al. 2015. “Function and Developmental

Origin of a Mesocortical Inhibitory Circuit." *Nature Neuroscience* 18 (6): 872–82.
Kadir, Shabnam N., Dan F. M. Goodman, and Kenneth D. Harris. 2014. "High-Dimensional Cluster Analysis with the Masked EM Algorithm." *Neural Computation* 26 (11): 2379–94.
Kawano, Michihiro, Akiko Kawasaki, Hiromi Sakata-Haga, Yoshihiro Fukui, Hitoshi Kawano, Haruo Nogami, and Setsuji Hisano. 2006. "Particular Subpopulations of Midbrain and Hypothalamic Dopamine Neurons Express Vesicular Glutamate Transporter 2 in the Rat Brain." *The Journal of Comparative Neurology*. https://doi.org/10.1002/cne.21054.
Kayser, Christoph, Marcelo A. Montemurro, Nikos K. Logothetis, and Stefano Panzeri. 2009. "Spike-Phase Coding Boosts and Stabilizes Information Carried by Spatial and Temporal Spike Patterns." *Neuron* 61 (4): 597–608.
Kelley, A. E., and V. B. Domesick. 1982. "The Distribution of the Projection from the Hippocampal Formation to the Nucleus Accumbens in the Rat: An Anterograde- and Retrograde-Horseradish Peroxidase Study." *Neuroscience* 7 (10): 2321–35.
Kelly, Ryan C., Matthew A. Smith, Robert E. Kass, and Tai Sing Lee. 2010. "Local Field Potentials Indicate Network State and Account for Neuronal Response Variability." *Journal of Computational Neuroscience* 29 (3): 567–79.
Kesner, Raymond P., and Michael E. Ragozzino. 2003. "The Role of the Prefrontal Cortex in Object–place Learning: A Test of the Attribute Specificity Model." *Behavioural Brain Research* 146 (1): 159–65.
Kim, Hyunggoo R., Athar N. Malik, John G. Mikhael, Pol Bech, Iku Tsutsui-Kimura, Fangmiao Sun, Yajun Zhang, et al. 2020. "A Unified Framework for Dopamine Signals across Timescales." *Cell* 183 (6): 1600–1616.e25.
Kitzinger, H., and D. G. Arnold. 1949. "A Preliminary Study of the Effects of Glutamic Acid on Catatonic Schizophrenics." *Rorschach Research Exchange and Journal of Projective Techniques* 13 (2): 210–18.
Klüver, Heinrich, and Paul C. Bucy. 1937. "' Psychic Blindness' and Other Symptoms Following Bilateral Temporal Lobectomy in Rhesus Monkeys." *The American Journal of Physiology*. https://psycnet.apa.org/record/1938-00651-001.
Koch, C., M. Rapp, and I. Segev. 1996. "A Brief History of Time (constants)." *Cerebral Cortex* 6 (2): 93–101.
Komorowski, R. W., and J. R. Manns. 2009. "Robust Conjunctive Item–place Coding by Hippocampal Neurons Parallels Learning What Happens Where." *Journal of*. https://www.jneurosci.org/content/29/31/9918.short.
Krettek, J. E., and J. L. Price. 1977. "Projections from the Amygdaloid Complex to the Cerebral Cortex and Thalamus in the Rat and Cat." *The Journal of Comparative Neurology* 172 (4): 687–722.
Kudrimoti, H. S., C. A. Barnes, and B. L. McNaughton. 1999. "Reactivation of Hippocampal Cell Assemblies: Effects of Behavioral State, Experience, and EEG Dynamics." *The Journal of Neuroscience: The Official Journal of the Society for Neuroscience* 19 (10): 4090–4101.
Kyriazi, Pinelopi, Drew B. Headley, and Denis Paré. 2020. "Different Multidimensional Representations across the Amygdalo-Prefrontal Network during an Approach-Avoidance Task." *Neuron* 107 (4): 717–30.e5.
Lammel, Stephan, Andrea Hetzel, Olga Häckel, Ian Jones, Birgit Liss, and Jochen Roeper. 2008. "Unique Properties of Mesoprefrontal Neurons within a Dual Mesocorticolimbic Dopamine System." *Neuron* 57 (5): 760–73.
Lammel, Stephan, Daniela I. Ion, Jochen Roeper, and Robert C. Malenka. 2011. "Projection-Specific Modulation of Dopamine Neuron Synapses by Aversive and

Rewarding Stimuli." *Neuron* 70 (5): 855–62.
Lammel, Stephan, Elizabeth E. Steinberg, Csaba Földy, Nicholas R. Wall, Kevin Beier, Liqun Luo, and Robert C. Malenka. 2015. "Diversity of Transgenic Mouse Models for Selective Targeting of Midbrain Dopamine Neurons." *Neuron* 85 (2): 429–38.
Lansink, Carien S., Jadin C. Jackson, Jan V. Lankelma, Rutsuko Ito, Trevor W. Robbins, Barry J. Everitt, and Cyriel M. A. Pennartz. 2012. "Reward Cues in Space: Commonalities and Differences in Neural Coding by Hippocampal and Ventral Striatal Ensembles." *The Journal of Neuroscience: The Official Journal of the Society for Neuroscience* 32 (36): 12444–59.
Lavin, Antonieta, Lourdes Nogueira, Christopher C. Lapish, R. Mark Wightman, Paul E. M. Phillips, and Jeremy K. Seamans. 2005. "Mesocortical Dopamine Neurons Operate in Distinct Temporal Domains Using Multimodal Signaling." *The Journal of Neuroscience: The Official Journal of the Society for Neuroscience* 25 (20): 5013–23.
Lavoie, A. M., and S. J. Y. Mizumori. 1994. "Spatial, Movement- and Reward-Sensitive Discharge by Medial Ventral Striatum Neurons of Rats." *Brain Research*. https://doi.org/10.1016/0006-8993(94)90645-9.
LeDoux, Joseph. 2003. "The Emotional Brain, Fear, and the Amygdala." *Cellular and Molecular Neurobiology* 23 (4-5): 727–38.
Leutgeb, Stefan, Jill K. Leutgeb, Carol A. Barnes, Edvard I. Moser, Bruce L. McNaughton, and May-Britt Moser. 2005. "Independent Codes for Spatial and Episodic Memory in Hippocampal Neuronal Ensembles." *Science* 309 (5734): 619–23.
Levita, Liat, Jeffrey W. Dalley, and Trevor W. Robbins. 2002. "Disruption of Pavlovian Contextual Conditioning by Excitotoxic Lesions of the Nucleus Accumbens Core." *Behavioral Neuroscience* 116 (4): 539–52.
Levy, Dana Rubi, Tal Tamir, Maya Kaufman, Ana Parabucki, Aharon Weissbrod, Elad Schneidman, and Ofer Yizhar. 2019. "Dynamics of Social Representation in the Mouse Prefrontal Cortex." *Nature Neuroscience* 22 (12): 2013–22.
Lisman, J. E. 1999. "Relating Hippocampal Circuitry to Function: Recall of Memory Sequences by Reciprocal Dentate-CA3 Interactions." *Neuron* 22 (2): 233–42.
Lisman, John E., and Anthony A. Grace. 2005. "The Hippocampal-VTA Loop: Controlling the Entry of Information into Long-Term Memory." *Neuron* 46 (5): 703–13.
Lisman, John E., and Ole Jensen. 2013. "The Theta-Gamma Neural Code." *Neuron* 77 (6): 1002–16.
Little, Justin P., and Adam G. Carter. 2012. "Subcellular Synaptic Connectivity of Layer 2 Pyramidal Neurons in the Medial Prefrontal Cortex." *The Journal of Neuroscience: The Official Journal of the Society for Neuroscience* 32 (37): 12808–19.
———. 2013. "Synaptic Mechanisms Underlying Strong Reciprocal Connectivity between the Medial Prefrontal Cortex and Basolateral Amygdala." *The Journal of Neuroscience: The Official Journal of the Society for Neuroscience* 33 (39): 15333–42.
Liu, R. H., S. J. Fung, V. K. Reddy, and C. D. Barnes. 1995. "Localization of Glutamatergic Neurons in the Dorsolateral Pontine Tegmentum Projecting to the Spinal Cord of the Cat with a Proposed Role of Glutamate on Lumbar Motoneuron Activity." *Neuroscience* 64 (1): 193–208.
Li, Xueping, Jia Qi, Tsuyoshi Yamaguchi, Hui-Ling Wang, and Marisela Morales.

2013. “Heterogeneous Composition of Dopamine Neurons of the Rat A10 Region: Molecular Evidence for Diverse Signaling Properties.” *Brain Structure & Function* 218 (5): 1159–76.
Ljungberg, T., P. Apicella, and W. Schultz. 1992. “Responses of Monkey Dopamine Neurons during Learning of Behavioral Reactions.” *Journal of Neurophysiology* 67 (1): 145–63.
Locke, John. 1847. *An Essay Concerning Human Understanding*. Kay & Troutman.
Lopes-dos-Santos, Vítor, Sidarta Ribeiro, and Adriano B. L. Tort. 2013. “Detecting Cell Assemblies in Large Neuronal Populations.” *Journal of Neuroscience Methods* 220 (2): 149–66.
Lowet, Adam S., Qiao Zheng, Sara Matias, Jan Drugowitsch, and Naoshige Uchida. 2020. “Distributional Reinforcement Learning in the Brain.” *Trends in Neurosciences* 43 (12): 980–97.
Loy, Rebekah, David A. Koziell, James D. Lindsey, and Robert Y. Moore. 1980. “Noradrenergic Innervation of the Adult Rat Hippocampal Formation.” *The Journal of Comparative Neurology*. https://doi.org/10.1002/cne.901890406.
Magland, Jeremy, James J. Jun, Elizabeth Lovero, Alexander J. Morley, Cole Lincoln Hurwitz, Alessio Paolo Buccino, Samuel Garcia, and Alex H. Barnett. 2020. “SpikeForest, Reproducible Web-Facing Ground-Truth Validation of Automated Neural Spike Sorters.” *eLife* 9 (May). https://doi.org/10.7554/eLife.55167.
Maldonado-Irizarry, Carmen S., and Ann E. Kelley. 1994. “Differential Behavioral Effects Following Microinjection of an NMDA Antagonist into Nucleus Accumbens Subregions.” *Psychopharmacology*. https://doi.org/10.1007/bf02244872.
Malvache, Arnaud, Susanne Reichinnek, Vincent Villette, Caroline Haimerl, and Rosa Cossart. 2016. “Awake Hippocampal Reactivations Project onto Orthogonal Neuronal Assemblies.” *Science* 353 (6305): 1280–83.
Mandler, George. 1979. “Organization, Memory, and Mental Structures.” *Memory Organization and Structure*, 303–19.
———. 2011. “From Association to Organization.” *Current Directions in Psychological Science* 20 (4): 232–35.
Manns, Joseph R., and Howard Eichenbaum. 2009. “A Cognitive Map for Object Memory in the Hippocampus.” *Learning & Memory* 16 (10): 616–24.
Maren, S., G. Aharonov, D. L. Stote, and M. S. Fanselow. 1996. “N-Methyl-D-Aspartate Receptors in the Basolateral Amygdala Are Required for Both Acquisition and Expression of Conditional Fear in Rats.” *Behavioral Neuroscience* 110 (6): 1365–74.
Margolis, Elyssa B., Hagar Lock, Vladimir I. Chefer, Toni S. Shippenberg, Gregory O. Hjelmstad, and Howard L. Fields. 2006. “Kappa Opioids Selectively Control Dopaminergic Neurons Projecting to the Prefrontal Cortex.” *Proceedings of the National Academy of Sciences of the United States of America* 103 (8): 2938–42.
Margolis, Elyssa B., Hagar Lock, Gregory O. Hjelmstad, and Howard L. Fields. 2006. “The Ventral Tegmental Area Revisited: Is There an Electrophysiological Marker for Dopaminergic Neurons?” *The Journal of Physiology* 577 (Pt 3): 907–24.
Margolis, Elyssa B., Jennifer M. Mitchell, Junko Ishikawa, Gregory O. Hjelmstad, and Howard L. Fields. 2008. “Midbrain Dopamine Neurons: Projection Target Determines Action Potential Duration and Dopamine D2 Receptor Inhibition.” *The Journal of Neuroscience: The Official Journal of the Society for Neuroscience* 28 (36): 8908–13.

Margolis, Elyssa B., Brian Toy, Patricia Himmels, Marisela Morales, and Howard L. Fields. 2012. “Identification of Rat Ventral Tegmental Area GABAergic Neurons.” *PLoS ONE*. https://doi.org/10.1371/journal.pone.0042365.
Matsumoto, Masayuki, and Okihide Hikosaka. 2009. “Two Types of Dopamine Neuron Distinctly Convey Positive and Negative Motivational Signals.” *Nature*. https://doi.org/10.1038/nature08028.
Mau, William, Michael E. Hasselmo, and Denise J. Cai. 2020. “The Brain in Motion: How Ensemble Fluidity Drives Memory-Updating and Flexibility.” *eLife* 9 (December). https://doi.org/10.7554/eLife.63550.
Mayford, Mark, Steven A. Siegelbaum, and Eric R. Kandel. 2012. “Synapses and Memory Storage.” *Cold Spring Harbor Perspectives in Biology* 4 (6). https://doi.org/10.1101/cshperspect.a005751.
McEchron, M. D., and J. F. Disterhoft. 1997. “Sequence of Single Neuron Changes in CA1 Hippocampus of Rabbits during Acquisition of Trace Eyeblink Conditioned Responses.” *Journal of Neurophysiology* 78 (2): 1030–44.
McGarry, Laura M., and Adam G. Carter. 2017. “Prefrontal Cortex Drives Distinct Projection Neurons in the Basolateral Amygdala.” *Cell Reports* 21 (6): 1426–33.
McGovern, Dillon J., Abigail M. Polter, and David H. Root. 2021. “Neurochemical Signaling of Reward and Aversion to Ventral Tegmental Area Glutamate Neurons.” *The Journal of Neuroscience: The Official Journal of the Society for Neuroscience* 41 (25): 5471–86.
McNamara, Colin G., Álvaro Tejero-Cantero, Stéphanie Trouche, Natalia Campo-Urriza, and David Dupret. 2014. “Dopaminergic Neurons Promote Hippocampal Reactivation and Spatial Memory Persistence.” *Nature Neuroscience* 17 (12): 1658–60.
Meer, Matthijs A. A. van der, and A. David Redish. 2009. “Covert Expectation-of-Reward in Rat Ventral Striatum at Decision Points.” *Frontiers in Integrative Neuroscience* 3 (February): 1.
Menegas, William, Korleki Akiti, Ryunosuke Amo, Naoshige Uchida, and Mitsuko Watabe-Uchida. 2018. “Dopamine Neurons Projecting to the Posterior Striatum Reinforce Avoidance of Threatening Stimuli.” *Nature Neuroscience* 21 (10): 1421–30.
Mercuri, N., P. Calabresi, P. Stanzione, and G. Bernardi. 1985. “Electrical Stimulation of Mesencephalic Cell Groups (A9-A10) Produces Monosynaptic Excitatory Potentials in Rat Frontal Cortex.” *Brain Research* 338 (1): 192–95.
Mesulam, M. M. 1998. “From Sensation to Cognition.” *Brain: A Journal of Neurology* 121 (Pt 6) (June): 1013–52.
Milad, Mohammed R., and Gregory J. Quirk. 2002. “Neurons in Medial Prefrontal Cortex Signal Memory for Fear Extinction.” *Nature* 420 (6911): 70–74.
Milivojevic, Branka, Alejandro Vicente-Grabovetsky, and Christian F. Doeller. 2015. “Insight Reconfigures Hippocampal-Prefrontal Memories.” *Current Biology: CB* 25 (7): 821–30.
Miller, Earl K., David J. Freedman, and Jonathan D. Wallis. 2002. “The Prefrontal Cortex: Categories, Concepts and Cognition.” *Philosophical Transactions of the Royal Society of London. Series B, Biological Sciences* 357 (1424): 1123–36.
Mingote, Susana, Nao Chuhma, Sheila V. Kusnoor, Bianca Field, Ariel Y. Deutch, and Stephen Rayport. 2015. “Functional Connectome Analysis of Dopamine Neuron Glutamatergic Connections in Forebrain Regions.” *The Journal of Neuroscience: The Official Journal of the Society for Neuroscience* 35 (49): 16259–71.

Mogenson, G. J. 1985. “From Motivation to Action: A Review of Dopaminergic Regulation of Limbic-> Nucleus Accumbens-> Ventral Pallidum-> Pedunculopontine Nucleus Circuitries Involved in Limbic-Motor Integration.” *Limbic Motor Circuits and Neuropsychiatry*, 193–236.

Mogenson, G. J., D. L. Jones, and C. Y. Yim. 1980. “From Motivation to Action: Functional Interface between the Limbic System and the Motor System.” *Progress in Neurobiology* 14 (2-3): 69–97.

Mohebi, Ali, Jeffrey R. Pettibone, Arif A. Hamid, Jenny-Marie T. Wong, Leah T. Vinson, Tommaso Patriarchi, Lin Tian, Robert T. Kennedy, and Joshua D. Berke. 2019. “Dissociable Dopamine Dynamics for Learning and Motivation.” *Nature* 570 (7759): 65–70.

Montardy, Quentin, Zheng Zhou, Zhuogui Lei, Xuemei Liu, Pengyu Zeng, Chen Chen, Yuanming Liu, Paula Sanz-Leon, Kang Huang, and Liping Wang. 2019. “Characterization of Glutamatergic VTA Neural Population Responses to Aversive and Rewarding Conditioning in Freely-Moving Mice.” *Science Bulletin of the Faculty of Agriculture, Kyushu University* 64 (16): 1167–78.

Montaron, M. F., J. M. Deniau, A. Menetrey, J. Glowinski, and A. M. Thierry. 1996. “Prefrontal Cortex Inputs of the Nucleus Accumbens-Nigro-Thalamic Circuit.” *Neuroscience* 71 (2): 371–82.

Montavon, Grégoire, Wojciech Samek, and Klaus-Robert Müller. 2018. “Methods for Interpreting and Understanding Deep Neural Networks.” *Digital Signal Processing* 73 (February): 1–15.

Morales, Marisela, and Elyssa B. Margolis. 2017. “Ventral Tegmental Area: Cellular Heterogeneity, Connectivity and Behaviour.” *Nature Reviews. Neuroscience* 18 (2): 73–85.

Murray, E. A., and M. Mishkin. 1984. “Severe Tactual as Well as Visual Memory Deficits Follow Combined Removal of the Amygdala and Hippocampus in Monkeys.” *The Journal of Neuroscience: The Official Journal of the Society for Neuroscience* 4 (10): 2565–80.

Nair-Roberts, R. G., S. D. Chatelain-Badie, E. Benson, H. White-Cooper, J. P. Bolam, and M. A. Ungless. 2008. “Stereological Estimates of Dopaminergic, GABAergic and Glutamatergic Neurons in the Ventral Tegmental Area, Substantia Nigra and Retrorubral Field in the Rat.” *Neuroscience* 152 (4): 1024–31.

Narayanan, Nandakumar S., and Mark Laubach. 2006. “Top-down Control of Motor Cortex Ensembles by Dorsomedial Prefrontal Cortex.” *Neuron* 52 (5): 921–31.

Neve, Kim A., Jeremy K. Seamans, and Heather Trantham-Davidson. 2004. “Dopamine Receptor Signaling.” *Journal of Receptors and Signal Transduction*. https://doi.org/10.1081/rrs-200029981.

Ogawa, Sachie K., Jeremiah Y. Cohen, Dabin Hwang, Naoshige Uchida, and Mitsuko Watabe-Uchida. 2014. “Organization of Monosynaptic Inputs to the Serotonin and Dopamine Neuromodulatory Systems.” *Cell Reports* 8 (4): 1105–18.

Ojala, Markus, and Gemma C. Garriga. 2009. “Permutation Tests for Studying Classifier Performance.” In *2009 Ninth IEEE International Conference on Data Mining*, 11:1833–63. IEEE.

O’Keefe, J., and J. Dostrovsky. 1971a. “The Hippocampus as a Spatial Map: Preliminary Evidence from Unit Activity in the Freely-Moving Rat.” *Brain Research*. https://psycnet.apa.org/record/1972-08318-001.

———. 1971b. “The Hippocampus as a Spatial Map. Preliminary Evidence from Unit

Activity in the Freely-Moving Rat." *Brain Research* 34 (1): 171–75.
O'keefe, John, and Lynn Nadel. 1978. *The Hippocampus as a Cognitive Map*. Oxford: Clarendon Press.
Olson, Valerie G., and Eric J. Nestler. 2007. "Topographical Organization of GABAergic Neurons within the Ventral Tegmental Area of the Rat." *Synapse* 61 (2): 87–95.
Omelchenko, Natalia, Roland Bell, and Susan R. Sesack. 2009. "Lateral Habenula Projections to Dopamine and GABA Neurons in the Rat Ventral Tegmental Area." *The European Journal of Neuroscience* 30 (7): 1239–50.
Pachitariu, Marius, Nicholas Steinmetz, Shabnam Kadir, Matteo Carandini, and Harris Kenneth D. 2016. "Kilosort: Realtime Spike-Sorting for Extracellular Electrophysiology with Hundreds of Channels." *bioRxiv*. https://doi.org/10.1101/061481.
Packard, Mark G., and Barbara J. Knowlton. 2002. "Learning and Memory Functions of the Basal Ganglia." *Annual Review of Neuroscience* 25 (March): 563–93.
Pan, Wei-Xing, Robert Schmidt, Jeffery R. Wickens, and Brian I. Hyland. 2005. "Dopamine Cells Respond to Predicted Events during Classical Conditioning: Evidence for Eligibility Traces in the Reward-Learning Network." *The Journal of Neuroscience: The Official Journal of the Society for Neuroscience* 25 (26): 6235–42.
Panzeri, S., R. S. Petersen, S. R. Schultz, M. Lebedev, and M. E. Diamond. 2001. "The Role of Spike Timing in the Coding of Stimulus Location in Rat Somatosensory Cortex." *Neuron* 29 (3): 769–77.
Panzeri, Stefano, Nicolas Brunel, Nikos K. Logothetis, and Christoph Kayser. 2010. "Sensory Neural Codes Using Multiplexed Temporal Scales." *Trends in Neurosciences* 33 (3): 111–20.
Parkinson, Dalley, Cardinal, Bamford, Fehnert, Lachenal, Rudarakanchana, Halkerston, Robbins, and Everitt. 2002. "Nucleus Accumbens Dopamine Depletion Impairs Both Acquisition and Performance of Appetitive Pavlovian Approach Behaviour: Implications for Mesoaccumbens Dopamine Function." *Behavioural Brain Research*. https://doi.org/10.1016/s0166-4328(02)00291-7.
Parkinson, Mary C. Olmstead, Lindsay H. Burns, Trevor W. Robbins, and Barry J. Everitt. 1999a. "Dissociation in Effects of Lesions of the Nucleus Accumbens Core and Shell on Appetitive Pavlovian Approach Behavior and the Potentiation of Conditioned Reinforcement and Locomotor Activity Byd-Amphetamine." *The Journal of Neuroscience*. https://doi.org/10.1523/jneurosci.19-06-02401.1999.
Parkinson, M. C. Olmstead, L. H. Burns, T. W. Robbins, and B. J. Everitt. 1999b. "Dissociation in Effects of Lesions of the Nucleus Accumbens Core and Shell on Appetitive Pavlovian Approach Behavior and the Potentiation of Conditioned Reinforcement and Locomotor Activity by D-Amphetamine." *The Journal of Neuroscience: The Official Journal of the Society for Neuroscience* 19 (6): 2401–11.
Parkinson, T. W. Robbins, and B. J. Everitt. 2000. "Dissociable Roles of the Central and Basolateral Amygdala in Appetitive Emotional Learning." *The European Journal of Neuroscience* 12 (1): 405–13.
Passecker, Johannes, Nace Mikus, Hugo Malagon-Vina, Philip Anner, Jordane Dimidschstein, Gordon Fishell, Georg Dorffner, and Thomas Klausberger. 2019. "Activity of Prefrontal Neurons Predict Future Choices during Gambling." *Neuron* 101 (1): 152–64.e7.
Paton, Joseph J., Marina A. Belova, Sara E. Morrison, and C. Daniel Salzman. 2006.

"The Primate Amygdala Represents the Positive and Negative Value of Visual Stimuli during Learning." *Nature* 439 (7078): 865–70.
Pavlov Ivan, P. 1927. "Conditioned Reflexes: An Investigation of the Physiological Activity of the Cerebral Cortex" Translated by GV Anrep." Oxford University Press LONDON.
Peyrache, Adrien, Mehdi Khamassi, Karim Benchenane, Sidney I. Wiener, and Francesco P. Battaglia. 2009. "Replay of Rule-Learning Related Neural Patterns in the Prefrontal Cortex during Sleep." *Nature Neuroscience* 12 (7): 919–26.
Phillipson, O. T., and A. C. Griffiths. 1985. "The Topographic Order of Inputs to Nucleus Accumbens in the Rat." *Neuroscience* 16 (2): 275–96.
Pickel, V. M., T. H. Joh, P. M. Field, C. G. Becker, and D. J. Reis. 1975. "Cellular Localization of Tyrosine Hydroxylase by Immunohistochemistry." *The Journal of Histochemistry and Cytochemistry: Official Journal of the Histochemistry Society* 23 (1): 1–12.
Pi, Guilin, Di Gao, Dongqin Wu, Yali Wang, Huiyang Lei, Wenbo Zeng, Yang Gao, et al. 2020. "Posterior Basolateral Amygdala to Ventral Hippocampal CA1 Drives Approach Behaviour to Exert an Anxiolytic Effect." *Nature Communications*. https://doi.org/10.1038/s41467-019-13919-3.
Pikkarainen, M., S. Rönkkö, V. Savander, R. Insausti, and A. Pitkänen. 1999. "Projections from the Lateral, Basal, and Accessory Basal Nuclei of the Amygdala to the Hippocampal Formation in Rat." *The Journal of Comparative Neurology* 403 (2): 229–60.
Plato. *Plato's Meno*. Vol. 82b9–84b1. Cambridge University Press.
Poulin, Jean-Francois, Zachary Gaertner, Oscar Andrés Moreno-Ramos, and Rajeshwar Awatramani. 2020. "Classification of Midbrain Dopamine Neurons Using Single-Cell Gene Expression Profiling Approaches." *Trends in Neurosciences* 43 (3): 155–69.
Puryear, Corey B., Min Jung Kim, and Sheri J. Y. Mizumori. 2010. "Conjunctive Encoding of Movement and Reward by Ventral Tegmental Area Neurons in the Freely Navigating Rodent." *Behavioral Neuroscience* 124 (2): 234–47.
Qi, Jia, Shiliang Zhang, Hui-Ling Wang, David J. Barker, Jorge Miranda-Barrientos, and Marisela Morales. 2016. "VTA Glutamatergic Inputs to Nucleus Accumbens Drive Aversion by Acting on GABAergic Interneurons." *Nature Neuroscience* 19 (5): 725–33.
Quirk, G. J., J. L. Armony, and J. E. LeDoux. 1997. "Fear Conditioning Enhances Different Temporal Components of Tone-Evoked Spike Trains in Auditory Cortex and Lateral Amygdala." *Neuron* 19 (3): 613–24.
Ramsey, William M. 2007. *Representation Reconsidered*. Cambridge University Press.
Reinert, Sandra, Mark Hübener, Tobias Bonhoeffer, and Pieter M. Goltstein. 2021. "Mouse Prefrontal Cortex Represents Learned Rules for Categorization." *Nature*, April. https://doi.org/10.1038/s41586-021-03452-z.
Rigotti, Mattia, Omri Barak, Melissa R. Warden, Xiao-Jing Wang, Nathaniel D. Daw, Earl K. Miller, and Stefano Fusi. 2013. "The Importance of Mixed Selectivity in Complex Cognitive Tasks." *Nature* 497 (7451): 585–90.
Rissman, Jesse, and Anthony D. Wagner. 2012. "Distributed Representations in Memory: Insights from Functional Brain Imaging." *Annual Review of Psychology* 63: 101–28.
Roitman, Mitchell F., Robert A. Wheeler, and Regina M. Carelli. 2005. "Nucleus Accumbens Neurons Are Innately Tuned for Rewarding and Aversive Taste

Stimuli, Encode Their Predictors, and Are Linked to Motor Output." *Neuron* 45 (4): 587–97.
Root, David H., David J. Estrin, and Marisela Morales. 2018. "Aversion or Salience Signaling by Ventral Tegmental Area Glutamate Neurons." *iScience*. https://doi.org/10.1016/j.isci.2018.03.008.
Root, David H., Carlos A. Mejias-Aponte, Jia Qi, and Marisela Morales. 2014. "Role of Glutamatergic Projections from Ventral Tegmental Area to Lateral Habenula in Aversive Conditioning." *The Journal of Neuroscience: The Official Journal of the Society for Neuroscience* 34 (42): 13906–10.
Root, David H., Carlos A. Mejias-Aponte, Shiliang Zhang, Hui-Ling Wang, Alexander F. Hoffman, Carl R. Lupica, and Marisela Morales. 2014. "Single Rodent Mesohabenular Axons Release Glutamate and GABA." *Nature Neuroscience* 17 (11): 1543–51.
Rousseeuw, Peter J. 1987. "Silhouettes: A Graphical Aid to the Interpretation and Validation of Cluster Analysis." *Journal of Computational and Applied Mathematics* 20 (November): 53–65.
Roy, Alexis, Frans Pettersson Svensson, Amna Mazeh, and Bernat Kocsis. 2017. "Prefrontal-Hippocampal Coupling by Theta Rhythm and by 2-5 Hz Oscillation in the Delta Band: The Role of the Nucleus Reuniens of the Thalamus." *Brain Structure & Function* 222 (6): 2819–30.
Rumelhart, David E., and James L. McClelland. 1987. *Parallel Distributed Processing : Explorations in the Microstructure of Cognition. 1. Foundations*. MIT Press.
Sahay, Amar, Donald A. Wilson, and René Hen. 2011. "Pattern Separation: A Common Function for New Neurons in Hippocampus and Olfactory Bulb." *Neuron* 70 (4): 582–88.
Sah, P., E. S. L. Faber, M. Lopez De Armentia, and J. Power. 2003. "The Amygdaloid Complex: Anatomy and Physiology." *Physiological Reviews* 83 (3): 803–34.
Sakurai, Yoshio. 1990. "Hippocampal Cells Have Behavioral Correlates during the Performance of an Auditory Working Memory Task in the Rat." *Behavioral Neuroscience*. https://doi.org/10.1037/0735-7044.104.2.253.
Salamone, John D., and Mercè Correa. 2012. "The Mysterious Motivational Functions of Mesolimbic Dopamine." *Neuron* 76 (3): 470–85.
Satoh, Takemasa, Sadamu Nakai, Tatsuo Sato, and Minoru Kimura. 2003. "Correlated Coding of Motivation and Outcome of Decision by Dopamine Neurons." *The Journal of Neuroscience: The Official Journal of the Society for Neuroscience* 23 (30): 9913–23.
Schacter, Daniel L., Joanne L. Harbluk, and Donald R. McLachlan. 1984. "Retrieval without Recollection: An Experimental Analysis of Source Amnesia." *Journal of Verbal Learning and Verbal Behavior* 23 (5): 593–611.
Schlichting, Margaret L., and Alison R. Preston. 2015. "Memory Integration: Neural Mechanisms and Implications for Behavior." *Current Opinion in Behavioral Sciences* 1 (February): 1–8.
Schultz. 2002. "Getting Formal with Dopamine and Reward." *Neuron* 36 (2): 241–63.
———. 2007. "Multiple Dopamine Functions at Different Time Courses." *Annual Review of Neuroscience* 30: 259–88.
Schultz, W. 1998. "Predictive Reward Signal of Dopamine Neurons." *Journal of Neurophysiology* 80 (1): 1–27.
Schultz, W., P. Dayan, and P. R. Montague. 1997. "A Neural Substrate of Prediction

and Reward." *Science* 275 (5306): 1593–99.
Schultz, W., and A. Dickinson. 2000. "Neuronal Coding of Prediction Errors." *Annual Review of Neuroscience* 23: 473–500.
Seo, Dong-Oh, Samuel C. Funderburk, Dionnet L. Bhatti, Laura E. Motard, Dillan Newbold, Kasey S. Girven, Jordan G. McCall, Michael Krashes, Dennis R. Sparta, and Michael R. Bruchas. 2016. "A GABAergic Projection from the Centromedial Nuclei of the Amygdala to Ventromedial Prefrontal Cortex Modulates Reward Behavior." *The Journal of Neuroscience: The Official Journal of the Society for Neuroscience* 36 (42): 10831–42.
Setlow, Barry, Geoffrey Schoenbaum, and Michela Gallagher. 2003. "Neural Encoding in Ventral Striatum during Olfactory Discrimination Learning." *Neuron* 38 (4): 625–36.
Sevelinges, Yannick, Rémi Gervais, Belkacem Messaoudi, Lionel Granjon, and Anne-Marie Mouly. 2004. "Olfactory Fear Conditioning Induces Field Potential Potentiation in Rat Olfactory Cortex and Amygdala." *Learning & Memory* 11 (6): 761–69.
Shim, Hyun Soo, Hyun-Jung Park, Mi-Sook Lee, Minsook Ye, and Insop Shim. 2018. "The Role of the Supramammillary Area of the Hypothalamus in Cognitive Functions." *Animal Cells and Systems* 22 (1): 37–44.
Shin, Justin D., Wenbo Tang, and Shantanu P. Jadhav. 2019. "Dynamics of Awake Hippocampal-Prefrontal Replay for Spatial Learning and Memory-Guided Decision Making." *Neuron* 104 (6): 1110–25.e7.
Sirota, Anton, Sean Montgomery, Shigeyoshi Fujisawa, Yoshikazu Isomura, Michael Zugaro, and György Buzsáki. 2008. "Entrainment of Neocortical Neurons and Gamma Oscillations by the Hippocampal Theta Rhythm." *Neuron* 60 (4): 683–97.
Sommer, Friedrich T., and Thomas Wennekers. 2003. "Models of Distributed Associative Memory Networks in the Brain." *Theory in Biosciences = Theorie in Den Biowissenschaften* 122 (1): 55–69.
Sotres-Bayon, Francisco, David E. A. Bush, and Joseph E. LeDoux. 2004. "Emotional Perseveration: An Update on Prefrontal-Amygdala Interactions in Fear Extinction." *Learning & Memory* 11 (5): 525–35.
Spence, K. W. 1950. "Cognitive versus Stimulus-Response Theories of Learning." *Psychological Review* 57 (3): 159–72.
Spiegler, B. J., and M. Mishkin. 1981. "Evidence for the Sequential Participation of Inferior Temporal Cortex and Amygdala in the Acquisition of Stimulus-Reward Associations." *Behavioural Brain Research* 3 (3): 303–17.
Spruston, N., and D. Johnston. 1992. "Perforated Patch-Clamp Analysis of the Passive Membrane Properties of Three Classes of Hippocampal Neurons." *Journal of Neurophysiology* 67 (3): 508–29.
Stalnaker, Thomas A., James D. Howard, Yuji K. Takahashi, Samuel J. Gershman, Thorsten Kahnt, and Geoffrey Schoenbaum. 2019. "Dopamine Neuron Ensembles Signal the Content of Sensory Prediction Errors." *eLife* 8 (November). https://doi.org/10.7554/eLife.49315.
Stamatakis, Alice M., Joshua H. Jennings, Randall L. Ung, Grace A. Blair, Richard J. Weinberg, Rachael L. Neve, Frederick Boyce, et al. 2013. "A Unique Population of Ventral Tegmental Area Neurons Inhibits the Lateral Habenula to Promote Reward." *Neuron*. https://doi.org/10.1016/j.neuron.2013.08.023.
Stein, Astrid von, and Johannes Sarnthein. 2000. "Different Frequencies for Different Scales of Cortical Integration: From Local Gamma to Long Range Alpha/theta

Synchronization.” *International Journal of Psychophysiology: Official Journal of the International Organization of Psychophysiology* 38 (3): 301–13.
Steinmetz, Nicholas A., Peter Zatka-Haas, Matteo Carandini, and Kenneth D. Harris. 2019. “Distributed Coding of Choice, Action and Engagement across the Mouse Brain.” *Nature*. https://doi.org/10.1038/s41586-019-1787-x.
Stringer, Carsen, Marius Pachitariu, Nicholas Steinmetz, Charu Bai Reddy, Matteo Carandini, and Kenneth D. Harris. 2019. “Spontaneous Behaviors Drive Multidimensional, Brainwide Activity.” *Science* 364 (6437): 255.
Stuber, Garret D., Thomas S. Hnasko, Jonathan P. Britt, Robert H. Edwards, and Antonello Bonci. 2010. “Dopaminergic Terminals in the Nucleus Accumbens but Not the Dorsal Striatum Corelease Glutamate.” *The Journal of Neuroscience: The Official Journal of the Society for Neuroscience* 30 (24): 8229–33.
Sul, Jung Hoon, Hoseok Kim, Namjung Huh, Daeyeol Lee, and Min Whan Jung. 2010. “Distinct Roles of Rodent Orbitofrontal and Medial Prefrontal Cortex in Decision Making.” *Neuron* 66 (3): 449–60.
Swanson, L. W. 1982. “The Projections of the Ventral Tegmental Area and Adjacent Regions: A Combined Fluorescent Retrograde Tracer and Immunofluorescence Study in the Rat.” *Brain Research Bulletin* 9 (1-6): 321–53.
Takahashi, D., Y. Asaoka, K. Kimura, and R. Hara. 2019. “Tonic Suppression of the Mesolimbic Dopaminergic System by Enhanced Corticotropin-Releasing Factor Signaling within the Bed Nucleus of the Stria Terminalis in Chronic ….” *Journal of*. https://www.jneurosci.org/content/39/42/8376.abstract.
Takahashi, Yuji K., Hannah M. Batchelor, Bing Liu, Akash Khanna, Marisela Morales, and Geoffrey Schoenbaum. 2017. “Dopamine Neurons Respond to Errors in the Prediction of Sensory Features of Expected Rewards.” *Neuron* 95 (6): 1395–1405.e3.
Tang, Wei, Olexiy Kochubey, Michael Kintscher, and Ralf Schneggenburger. 2020. “A VTA to Basal Amygdala Dopamine Projection Contributes to Signal Salient Somatosensory Events during Fear Learning.” *The Journal of Neuroscience: The Official Journal of the Society for Neuroscience* 40 (20): 3969–80.
Tang, Wenbo, Justin D. Shin, Loren M. Frank, and Shantanu P. Jadhav. 2017. “Hippocampal-Prefrontal Reactivation during Learning Is Stronger in Awake Compared with Sleep States.” *The Journal of Neuroscience: The Official Journal of the Society for Neuroscience* 37 (49): 11789–805.
Tan, Kelly R., Cédric Yvon, Marc Turiault, Julie J. Mirzabekov, Jana Doehner, Gwenaël Labouèbe, Karl Deisseroth, Kay M. Tye, and Christian Lüscher. 2012. “GABA Neurons of the VTA Drive Conditioned Place Aversion.” *Neuron* 73 (6): 1173–83.
Taylor, Janer, and Trevorw Robbins. 1986. “6-Hydroxydopamine Lesions of the Nucleus Accumbens, but Not of the Caudate Nucleus, Attenuate Enhanced Responding with Reward-Related Stimuli Produced by Intra-Accumbens D-Amphetamine.” *Psychopharmacology*. https://doi.org/10.1007/bf00179197.
Taylor, Seth R., Sylvia Badurek, Ralph J. Dileone, Raad Nashmi, Liliana Minichiello, and Marina R. Picciotto. 2014. “GABAergic and Glutamatergic Efferents of the Mouse Ventral Tegmental Area.” *Journal of Comparative Neurology*. https://doi.org/10.1002/cne.23603.
Tecuapetla, F., J. C. Patel, H. Xenias, D. English, I. Tadros, F. Shah, J. Berlin, et al. 2010. “Glutamatergic Signaling by Mesolimbic Dopamine Neurons in the Nucleus Accumbens.” *Journal of Neuroscience*. https://doi.org/10.1523/jneurosci.0265-10.2010.

Tizard, B. 1959. “Theories of Brain Localization from Flourens to Lashley.” *Medical History* 3 (2): 132–45.
Tolman, E. C. 1948. “Cognitive Maps in Rats and Men.” *Psychological Review* 55 (4): 189–208.
Tononi, G., O. Sporns, and G. M. Edelman. 1999. “Measures of Degeneracy and Redundancy in Biological Networks.” *Proceedings of the National Academy of Sciences of the United States of America* 96 (6): 3257–62.
Tritsch, Nicolas X., and Bernardo L. Sabatini. 2012. “Dopaminergic Modulation of Synaptic Transmission in Cortex and Striatum.” *Neuron* 76 (1): 33–50.
Trouche, Stéphanie, Vadim Koren, Natalie M. Doig, Tommas J. Ellender, Mohamady El-Gaby, Vítor Lopes-Dos-Santos, Hayley M. Reeve, et al. 2019. “A Hippocampus-Accumbens Tripartite Neuronal Motif Guides Appetitive Memory in Space.” *Cell* 176 (6): 1393–1406.e16.
Trudeau, Louis-Eric. 2004. “Glutamate Co-Transmission as an Emerging Concept in Monoamine Neuron Function.” *Journal of Psychiatry & Neuroscience: JPN* 29 (4): 296–310.
Tsai, Guochuan E., and Pao-Yen Lin. 2010. “Strategies to Enhance N-Methyl-D-Aspartate Receptor-Mediated Neurotransmission in Schizophrenia, a Critical Review and Meta-Analysis.” *Current Pharmaceutical Design* 16 (5): 522–37.
Tsai, Hsing-Chen, Feng Zhang, Antoine Adamantidis, Garret D. Stuber, Antonello Bonci, Luis de Lecea, and Karl Deisseroth. 2009. “Phasic Firing in Dopaminergic Neurons Is Sufficient for Behavioral Conditioning.” *Science* 324 (5930): 1080–84.
Ungless, Mark A., and Anthony A. Grace. 2012. “Are You or Aren’t You? Challenges Associated with Physiologically Identifying Dopamine Neurons.” *Trends in Neurosciences*. https://doi.org/10.1016/j.tins.2012.02.003.
Ungless, Mark A., Peter J. Magill, and J. Paul Bolam. 2004. “Uniform Inhibition of Dopamine Neurons in the Ventral Tegmental Area by Aversive Stimuli.” *Science* 303 (5666): 2040–42.
Usuda, Iwao, Koichi Tanaka, and Tanemichi Chiba. 1998. “Efferent Projections of the Nucleus Accumbens in the Rat with Special Reference to Subdivision of the Nucleus: Biotinylated Dextran Amine Study.” *Brain Research*. https://doi.org/10.1016/s0006-8993(98)00359-x.
Uwano, T., H. Nishijo, T. Ono, and R. Tamura. 1995. “Neuronal Responsiveness to Various Sensory Stimuli, and Associative Learning in the Rat Amygdala.” *Neuroscience* 68 (2): 339–61.
Van de Ven, Gido M., Stéphanie Trouche, Colin G. McNamara, Kevin Allen, and David Dupret. 2016. “Hippocampal Offline Reactivation Consolidates Recently Formed Cell Assembly Patterns during Sharp Wave-Ripples.” *Neuron*. https://doi.org/10.1016/j.neuron.2016.10.020.
Van De Werd, Henri J. J. M., and Harry B. M. Uylings. 2008. “The Rat Orbital and Agranular Insular Prefrontal Cortical Areas: A Cytoarchitectonic and Chemoarchitectonic Study.” *Brain Structure & Function* 212 (5): 387–401.
Ven, Gido M. van de, Stéphanie Trouche, Colin G. McNamara, Kevin Allen, and David Dupret. 2016. “Hippocampal Offline Reactivation Consolidates Recently Formed Cell Assembly Patterns during Sharp Wave-Ripples.” *Neuron* 92 (5): 968–74.
Voorn, Pieter, Louk J. M. J. Vanderschuren, Henk J. Groenewegen, Trevor W. Robbins, and Cyriel M. A. Pennartz. 2004. “Putting a Spin on the Dorsal–ventral Divide of the Striatum.” *Trends in Neurosciences* 27 (8): 468–74.

Walker, Kerry M. M., Jennifer K. Bizley, Andrew J. King, and Jan W. H. Schnupp. 2011. “Multiplexed and Robust Representations of Sound Features in Auditory Cortex.” *The Journal of Neuroscience: The Official Journal of the Society for Neuroscience* 31 (41): 14565–76.
Wallis, J. D., K. C. Anderson, and E. K. Miller. 2001. “Single Neurons in Prefrontal Cortex Encode Abstract Rules.” *Nature* 411 (6840): 953–56.
Wang, Hui-Ling, Jia Qi, Shiliang Zhang, Huikun Wang, and Marisela Morales. 2015. “Rewarding Effects of Optical Stimulation of Ventral Tegmental Area Glutamatergic Neurons.” *The Journal of Neuroscience: The Official Journal of the Society for Neuroscience* 35 (48): 15948–54.
Wang, Hui-Ling, Shiliang Zhang, Jia Qi, Huikun Wang, Roger Cachope, Carlos A. Mejias-Aponte, Jorge A. Gomez, et al. 2019. “Dorsal Raphe Dual Serotonin-Glutamate Neurons Drive Reward by Establishing Excitatory Synapses on VTA Mesoaccumbens Dopamine Neurons.” *Cell Reports* 26 (5): 1128–42.e7.
Wang, Szu-Han, and Richard G. M. Morris. 2010. “Hippocampal-Neocortical Interactions in Memory Formation, Consolidation, and Reconsolidation.” *Annual Review of Psychology* 61: 49–79, C1–4.
Ward, Joe H. 1963. “Hierarchical Grouping to Optimize an Objective Function.” *Journal of the American Statistical Association* 58 (301): 236–44.
Wassum, Kate M., and Alicia Izquierdo. 2015. “The Basolateral Amygdala in Reward Learning and Addiction.” *Neuroscience and Biobehavioral Reviews* 57 (October): 271–83.
Watabe-Uchida, Mitsuko, Lisa Zhu, Sachie K. Ogawa, Archana Vamanrao, and Naoshige Uchida. 2012. “Whole-Brain Mapping of Direct Inputs to Midbrain Dopamine Neurons.” *Neuron* 74 (5): 858–73.
Weiser, Mark, Uriel Heresco-Levy, Michael Davidson, Daniel C. Javitt, Nomi Werbeloff, Ari A. Gershon, Yehuda Abramovich, et al. 2012. “A Multicenter, Add-on Randomized Controlled Trial of Low-Dose D-Serine for Negative and Cognitive Symptoms of Schizophrenia.” *The Journal of Clinical Psychiatry* 73 (6): e728–34.
Wellman, Laurie L., Patrick A. Forcelli, Brittany L. Aguilar, and Ludise Malkova. 2016. “Bidirectional Control of Social Behavior by Activity within Basolateral and Central Amygdala of Primates.” *The Journal of Neuroscience: The Official Journal of the Society for Neuroscience* 36 (33): 8746–56.
Wheeler, M. E., S. E. Petersen, and R. L. Buckner. 2000. “Memory’s Echo: Vivid Remembering Reactivates Sensory-Specific Cortex.” *Proceedings of the National Academy of Sciences of the United States of America* 97 (20): 11125–29.
Whitacre, James M. 2010. “Degeneracy: A Link between Evolvability, Robustness and Complexity in Biological Systems.” *Theoretical Biology & Medical Modelling* 7 (February): 6.
Wible, C. G., R. L. Findling, M. Shapiro, E. J. Lang, S. Crane, and D. S. Olton. 1986. “Mnemonic Correlates of Unit Activity in the Hippocampus.” *Brain Research* 399 (1): 97–110.
Wickelgren, Wayne A. 1999. “Webs, Cell Assemblies, and Chunking in Neural Nets: Introduction.” *Canadian Journal of Experimental Psychology/Revue Canadienne de Psychologie Expérimentale*. https://doi.org/10.1037/h0087304.
Williams, Alex H., Tony Hyun Kim, Forea Wang, Saurabh Vyas, Stephen I. Ryu, Krishna V. Shenoy, Mark Schnitzer, Tamara G. Kolda, and Surya Ganguli. 2018. “Unsupervised Discovery of Demixed, Low-Dimensional Neural Dynamics

across Multiple Timescales through Tensor Component Analysis." *Neuron* 98 (6): 1099–1115.e8.
Wilson, M. A., and B. L. McNaughton. 1993. "Dynamics of the Hippocampal Ensemble Code for Space." *Science* 261 (5124): 1055–58.
Witten, Ilana B., Elizabeth E. Steinberg, Soo Yeun Lee, Thomas J. Davidson, Kelly A. Zalocusky, Matthew Brodsky, Ofer Yizhar, et al. 2011. "Recombinase-Driver Rat Lines: Tools, Techniques, and Optogenetic Application to Dopamine-Mediated Reinforcement." *Neuron* 72 (5): 721–33.
Wright, C. I., A. V. Beijer, and H. J. Groenewegen. 1996. "Basal Amygdaloid Complex Afferents to the Rat Nucleus Accumbens Are Compartmentally Organized." *The Journal of Neuroscience: The Official Journal of the Society for Neuroscience* 16 (5): 1877–93.
Wu, M., S. M. Brudzynski, and G. J. Mogenson. 1993. "Functional Interaction of Dopamine and Glutamate in the Nucleus Accumbens in the Regulation of Locomotion." *Canadian Journal of Physiology and Pharmacology* 71 (5-6): 407–13.
Wu, Michael, Stefan M. Brudzynski, and Gordon J. Mogenson. 1993. "Differential Effects of Quinpirole in the Nucleus Accumbens Depending on the Initial Level of Locomotor Activity." *Brain Research Bulletin*. https://doi.org/10.1016/0361-9230(93)90206-q.
Xiang, Jian-Zhong, and Malcolm W. Brown. 2004. "Neuronal Responses Related to Long-Term Recognition Memory Processes in Prefrontal Cortex." *Neuron* 42 (5): 817–29.
Xu, Z., Z. Feng, M. Zhao, Q. Sun, L. Deng, X. Jia, and T. Jiang. 2020. "Whole-Brain Connectivity Atlas of Glutamatergic and GABAergic Neurons in Mouse Dorsal and Median Raphe Nucleus." *bioRxiv*. https://www.biorxiv.org/content/10.1101/2020.12.15.422858v1.abstract.
Yamaguchi, Tsuyoshi, Jia Qi, Hui-Ling Wang, Shiliang Zhang, and Marisela Morales. 2015. "Glutamatergic and Dopaminergic Neurons in the Mouse Ventral Tegmental Area." *The European Journal of Neuroscience* 41 (6): 760–72.
Yamaguchi, Tsuyoshi, Whitney Sheen, and Marisela Morales. 2007. "Glutamatergic Neurons Are Present in the Rat Ventral Tegmental Area." *European Journal of Neuroscience*. https://doi.org/10.1111/j.1460-9568.2006.05263.x.
Yamaguchi, Tsuyoshi, Hui-Ling Wang, Xueping Li, Tsz H. Ng, and Marisela Morales. 2011. "Mesocorticolimbic Glutamatergic Pathway." *The Journal of Neuroscience: The Official Journal of the Society for Neuroscience* 31 (23): 8476–90.
Yang, Ying, and Jian-Zhi Wang. 2017. "From Structure to Behavior in Basolateral Amygdala-Hippocampus Circuits." *Frontiers in Neural Circuits* 11 (October): 86.
Yu, Jun, Masago Ishikawa, Junshi Wang, Oliver M. Schlüter, Susan R. Sesack, and Yan Dong. 2019. "Ventral Tegmental Area Projection Regulates Glutamatergic Transmission in Nucleus Accumbens." *Scientific Reports* 9 (1): 18451.
Zahm, D. S. 1999. "Functional-Anatomical Implications of the Nucleus Accumbens Core and Shell Subterritories." *Annals of the New York Academy of Sciences* 877 (1 ADVANCING FRO): 113–28.
———. 2000. "An Integrative Neuroanatomical Perspective on Some Subcortical Substrates of Adaptive Responding with Emphasis on the Nucleus Accumbens." *Neuroscience and Biobehavioral Reviews* 24 (1): 85–105.
Zahm, D. S., and L. Heimer. 1993. "Specificity in the Efferent Projections of the Nucleus Accumbens in the Rat: Comparison of the Rostral Pole Projection

Patterns with Those of the Core and Shell." *The Journal of Comparative Neurology* 327 (2): 220–32.
Zeithamova, Dagmar, April L. Dominick, and Alison R. Preston. 2012. "Hippocampal and Ventral Medial Prefrontal Activation during Retrieval-Mediated Learning Supports Novel Inference." *Neuron* 75 (1): 168–79.
Zell, Vivien, Thomas Steinkellner, Nick G. Hollon, Shelley M. Warlow, Elizabeth Souter, Lauren Faget, Avery C. Hunker, Xin Jin, Larry S. Zweifel, and Thomas S. Hnasko. 2020. "VTA Glutamate Neuron Activity Drives Positive Reinforcement Absent Dopamine Co-Release." *Neuron*. https://doi.org/10.1016/j.neuron.2020.06.011.
Zessen, Ruud van, Jana L. Phillips, Evgeny A. Budygin, and Garret D. Stuber. 2012. "Activation of VTA GABA Neurons Disrupts Reward Consumption." *Neuron* 73 (6): 1184–94.
Zhang, Shiliang, Jia Qi, Xueping Li, Hui-Ling Wang, Jonathan P. Britt, Alexander F. Hoffman, Antonello Bonci, Carl R. Lupica, and Marisela Morales. 2015. "Dopaminergic and Glutamatergic Microdomains in a Subset of Rodent Mesoaccumbens Axons." *Nature Neuroscience* 18 (3): 386–92.
Zhou, Y., and N. C. Danbolt. 2014. "Glutamate as a Neurotransmitter in the Healthy Brain." *Journal of Neural Transmission*. https://doi.org/10.1007/s00702-014-1180-8.
Zhou, Zheng, Xuemei Liu, Shanping Chen, Zhijian Zhang, Yu-Anming Liu, Quentin Montardy, Yongqiang Tang, et al. 2018 "A VTA GABAergic Neural Circuit Mediates Visually Evoked Innate Defensive Responses." https://doi.org/10.1101/493007.
Zola-Morgan, S. 1995. "Localization of Brain Function: The Legacy of Franz Joseph Gall (1758-1828)." *Annual Review of Neuroscience* 18: 359–83.